CRYSTAL ISOSTRUCTURALITY AND X-RAY DIFFRACTION STUDIES OF CYCLODEXTRIN INCLUSION COMPOUNDS

By

Siyanda Lubhelwana

Dissertation Presented for the Degree of MASTER OF SCIENCE in the Department of Chemistry, Faculty of Science, University of Cape Town

June 2005

TABLE OF CONTENTS

CHAPTER 2: EXPERIMENTAL MATERIALS AND METHODS

CHAPTER 3: AN UPDATE ON THE ISOSTRUCTURALITY OF CYCLODEXTRIN INCLUSION COMPOUNDS

CHAPTER 6: CONCLUSIONS, COMMENTS AND RECOMMENDATIONS

ACKNOWLEDGEMENTS

My sincere thanks go to the following incredible people, for it were not for them, this work would not have been possible:

- *Professor Mino R. Caira* for so many things he has done in making this possible. Once again Prof I thank you for not being tired of me throughout this adventure, and now here is the outcome;

- *Associate Professor Susan A. Bourne* for being the second commander in charge of this project. We all know what that entails, and I thank you a lot more, and more;

- *Professor Luigi R. Nassimbeni* for creating a good working atmosphere at all times. This is what makes research either interesting or boring, so please keep it up Prof.;

- *All members (past and present) and visitors of the UCT Supramolecular Chemistry Research group.* As these were the people I was sitting with most of the time, I had to consult them as my first point of reference. Thank you guys for being there for me at the times I needed you the most;

- *NRF, CSIR* and *the University of Cape Town* for their financial support, to make my dream come true;

- *Friends* and *Family,* especially *my mother,* for their understanding and support in the decision that I took, of coming back to varsity for this Masters degree;

- *My girlfriend* for her love and support throughout this adventure.

PUBLICATIONS AND PRESENTATIONS

Parts of this dissertation have been presented in the form of:

A poster entitled "INCLUSION OF SALTS OF DICLOFENAC IN CYCLODEXTRINS: X-ray Crystal Structure of the Potassium Diclofenac Complex in β-Cyclodextrin" at *The 37th National Convention of the South African Chemical Institute* at the CSIR International Convention Centre, in Pretoria, South Africa, 4–9 July 2004. Authors: S. Lubhelwana, M. R. Caira and S. A. Bourne.

A poster entitled "INCLUSION OF SALTS OF DICLOFENAC IN CYCLODEXTRINS: X-ray Crystal Structures of the Potassium and Caesium Diclofenac Complexes with β-Cyclodextrin" at *The 25th Annual Academy of Pharmaceutical Sciences Silver Jubilee Congress* at Rhodes University, Grahamstown, South Africa, 12–15 September 2004. Authors: S. Lubhelwana, M. R. Caira and S. A. Bourne.

An oral presentation titled "Definitive Characterization of Crystalline Cyclodextrin-Drug Inclusion Complexes by PXRD – An Update" at *The Seventh International Workshop on Physical Characterization of Pharmaceutical Solids (IWPCPS-7)* at Kona, Hawaii, 5–10 June 2005. Authors: M. R. Caira, S. Lubhelwana and S. A. Bourne.

ABBREVIATIONS AND SYMBOLS

Drugs

SALM	:	Salicylamide, 2-hydroxybenzamide
SSAL	:	Sufasalazine, 5-{4-[(2-pyridylamino)sulfonyl]phenyldiazenyl}-salicylic acid
MSSAL	:	Monoclinic crystal form of Sulfasalazine
TSSAL	:	Triclinic crystal form of Sulfasalazine
DNa	:	Diclofenac sodium, 2-[(2,6-dichlorophenyl)amino]benzene-acetate sodium salt

Cyclodextrins

CDs	:	Cycloamyloses, Cyclomaltoses, Cycloglucans, Schardinger's dextrins, Cyclodextrins
ACD, α-CD	:	An alpha cyclodextrin, cyclohexaamylose
DIMEA	:	(2,6-Di-O-methyl)-α-cyclodextrin
TRIMEA	:	(2,3,6-Tri-O-methyl)-α-cyclodextrin
RAMEA	:	A randomly methylated α-CD derivative
AcetylA	:	(2,3,6-Tri-O-acetyl)-α-cyclodextrin
BCD, β-CD	:	A beta cyclodextrin, cycloheptaamylose
MONOMEB	:	2-O-oligomethyl-β-cyclodextrin
DIMEB	:	(2,6-Di-O-methyl)-β-cyclodextrin
TRIMEB	:	(2,3,6-Tri-O-methyl)-β-cyclodextrin
MONOBrB	:	Perbromo-6-deoxy-β-cyclodextrin
GCD, γ-CD	:	A gamma cyclodextrin, cyclooctaamylose
TRIMEG	:	A trimethylated γ-CD derivative

Abbreviated Organic Solvents

THF	:	Tetrahydrofuran, Tatramethylene oxide
MEK	:	Methylethylketone, 2-butanone

Cyclodextrin-Drug Complexes

SALMBCD	:	Salicylamide•β-CD inclusion complex
MSSALBCD	:	Monoclinic sulfasalazine•β-CD inclusion complex
MSSALGCD	:	Monoclinic sulfasalazine•γ-CD inclusion complex
DNaBCD	:	Diclofenac sodium•β-CD inclusion complex
DKBCD	:	Diclofenac potassium•β-CD inclusion complex
DCsBCD	:	Diclofenac caesium•β-CD inclusion complex

Techniques

HSM	:	Hot Stage Microscopy
TGA	:	Thermal Gravimetric Analysis
DSC	:	Differential Scanning Calorimetry
PXRD	:	X-Ray Powder Diffraction
SCXRD	:	Single Crystal X-Ray Diffraction

Other Terms and Symbols

H	:	Host compound (or the hydrogen atom)
G	:	Guest compound
H:G	:	Host to guest ratio
G_n	:	The n^{th} glucose residue in a cyclodextrin
IUPAC	:	International Union of Pure and Applied Chemistry
IsoPXRD	:	Isostructural method of X-ray powder diffraction analysis
CSD	:	Cambridge Structural Database
NSAIDs	:	Non-steroidal anti-inflammatory drugs
I_{hkl}	:	Intensity of a reflection
θ	:	Bragg angle
F	:	Structure factor
S	:	Goodness of fit
R	:	Residual index
CFOM	:	Combined figure of merit
CC	:	Correlation coefficient

s.o.f.	:	Site-occupancy factor
U_{iso}	:	Isotropic thermal parameter
e.s.d.	:	Estimated standard deviation
α	:	Angle between **b** and **c** unit cell axes
β	:	Angle between **a** and **c** unit cell axes
γ	:	Angle between **a** and **b** unit cell axes
$\Delta\rho$	:	Residual electron density
M_r	:	Molecular mass
Z	:	Number of formula units in the unit cell
V	:	Unit cell volume
D_{calc}	:	Calculated crystal density
W	:	Water
D	:	Hydrogen donor atom involved in hydrogen bonding
A	:	Hydrogen acceptor atom involved in hydrogen bonding

ABSTRACT

The first part of this dissertation is an update on the isostructurality method of PXRD analysis (IsoPXRD), the last update having been published in 2001. The scope of the isostructurality part of this dissertation includes organic inclusion complexes of all three natural cyclodextrins (α-, β- and γ-CDs), and their derivatives. PXRD patterns of these complexes were computed from their atomic coordinates available on the Cambridge Structural Database (CSD).

The use of this method is further demonstrated as exemplified by CD inclusion complexes of drugs of the salicylic acid derivative type. Thus it is herein shown, using this method, that the monoclinic form of sulfasalazine can produce inclusion complexes with β- and γ-cyclodextrins, while the triclinic form did not result in an inclusion complex when kneaded with any of the three natural cyclodextrins.

The second part of this dissertation is the synthesis, characterisation, and crystal structure determination of inclusion complexes of the potassium and the caesium salts of the commonly used nonsteroidal anti-inflammatory drug (NSAID) diclofenac (2-[2,6-dichlorophenyl)amino]benzeneacetic acid), with β-cyclodextrin. The potassium- and the caesium–diclofenac•β-cyclodextrin complexes were prepared by the co-precipitation method at elevated temperatures, and their crystals were grown by the slow evaporation method at room temperature. A comparison of these two complexes with the sodium analogue (previously studied) is also given, together with the thermal behaviour of all three complexes, as studied by HSM, TGA and DSC. The synthesised complexes were studied by X-ray diffraction techniques and characterised by the Karl-Fischer method and elemental analysis, in addition to the thermal analysis methods.

The potassium diclofenac•β-CD and the caesium diclofenac•β-CD crystal structures were found to be isostructural in the orthorhombic space group $P2_12_12_1$ but are not isostructural with the sodium analogue, which crystallizes in the hexagonal system, space group $P6_1$.

CHAPTER 1: INTRODUCTION

1.1 Introduction to Cyclodextrins

1.1.1 Discovery and Nature of Cyclodextrins

Just as the enzyme amylase is known to convert starch and glycogen into simple sugars such as glucose and maltose, the enzyme glucosyltransferase degrades the amylose fraction of starch into cyclic oligosaccharides, called cyclodextrins (CDs), composed of 1,4-linked α-D-glucopyranose units [1-3]. Figure 1.1 below shows the action of the cyclodextrin glucosyltransferase (CGT) enzyme on starch, resulting in crystalline cyclic dextrins (cyclodextrins) and amorphous linear dextrins.

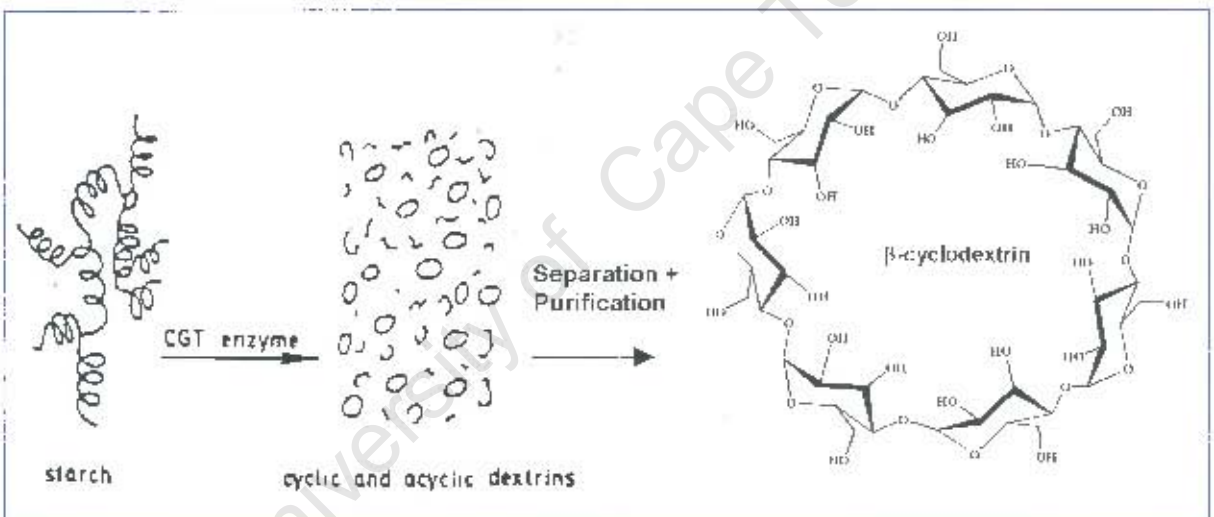

Figure 1.1 – Formation of cyclodextrin from starch (adapted from reference 4), and the chemical structure of β-cyclodextrin.

Since their discovery in 1891 by Villiers, at least three major forms of this group of compounds have been fully characterised and their inclusion complexes are currently being studied in detail. These three well known, industrially produced major forms of cyclodextrins are most commonly known as α-CD, β-CD and γ-CD, with six, seven and eight glucopyranose units respectively. Because α-, β- and γ-CDs were the first to be discovered and characterised they are collectively

known as 'parent', 'native' or 'natural' cyclodextrins [3]. For the purpose of this work we shall apply the latter two names as the term 'parent' will be used for hydrated-CD inclusion complexes only (i.e. without any other guest molecule/ compound).

1.1.2 Cyclodextrin Derivatives

Rare CDs with fewer than six [4], or more than eight [2,3,5-6], glucopyranose residues per ring are also known to occur but little has been published on their inclusion compounds and their practical utility. This is probably because they are less likely to form inclusion complexes with most organic compounds, either because their cavities are too small, as in the case of CDs with fewer than six glucopyranose units, or because they have poorly defined cavities due to their flexible structures, as would be the case for CDs with more than eight glucopyranose units per ring.

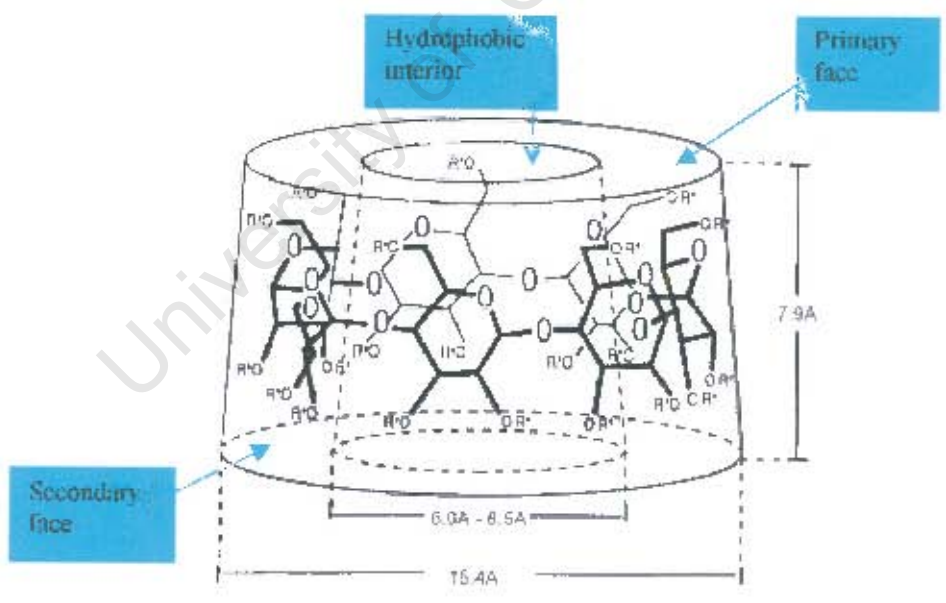

Figure 1.2 – The structure of a derivatised β-cyclodextrin. For the parent molecule, R' = H.

As shown in both Figures 1.1 and 1.2, natural cyclodextrins have hydroxyl groups protruding from both sides of their faces (primary and secondary faces). Modification of these OH groups results in CDs with different physical and chemical properties. Thus trimethylated β-CD (TRIMEB) is one such example in which all three hydroxyl groups per glucopyranose unit of a β-CD molecule are methylated (where R = CH_3 in Figure 1.2). Methylated CDs are usually more soluble in water than their non-methylated counterparts, whereas triacetyl β-cyclodextrin is regarded as being insoluble in water [2,7].

1.1.3 Cyclodextrin Structural Features

As seen in Figure 1.2, natural cyclodextrins have the shape of a truncated cone, with a hydrophobic interior, hydrophilic exterior, and twice as many hydroxyl groups on the secondary face as there are on the primary face [5,8]. These cyclodextrins are thus highly soluble in polar solvents and yet can accommodate nonpolar organic compounds in their apolar hydrophobic cavity, yielding inclusion complexes which are soluble in aqueous media. Alternatively, relatively water insoluble CDs can be designed and have been applied in reducing the side effects of flufenamic acid, a nonsteroidal anti-inflammatory drug, by simply slowing down the release of the drug [7]. Structural features of most natural cyclodextrins in terms of the **principal torsion angle indices**, **glucopyranose conformational descriptors** and **macrocyclic geometry** are well known and have been documented elsewhere [2,6,9]. Here, only a brief description is given together with the average values as have been reported. Figure 1.3 is a reminder of the conventional numbering scheme for CD molecules and Table 1.1 is a list of the average values of the descriptors of the three natural cyclodextrins as defined below.

The **principal torsion angles** include the *primary hydroxyl torsion angle*, the *glycosidic torsion angles* and the *pyranoid torsion angles*. The *primary hydroxyl torsion angle (ω)* quantifies the O_6H rotation along the C_5–C_6 bond and is defined

by the atoms O_5–C_5–C_6–O_6. Two *glycosidic torsion angles* (Φ and ψ) quantify the limited rotational movements of the $C_1(n)$–$O_4(n-1)$–$C_4(n-1)$ glycosidic link and are defined by Φ = **$O_5(n)$–$C_1(n)$–$O_4(n-1)$–$C_4(n-1)$** and ψ = **$C_1(n)$–$O_4(n-1)$–$C_4(n-1)$–$C_3(n-1)$**. The two *pyranoid torsion angles* Θ_1 = **C_2–C_3–C_4–C_5** and Θ_2 = **C_3–C_4–C_5–O_5** describe the conformational relationship around the C_4 atom of each glucose residue.

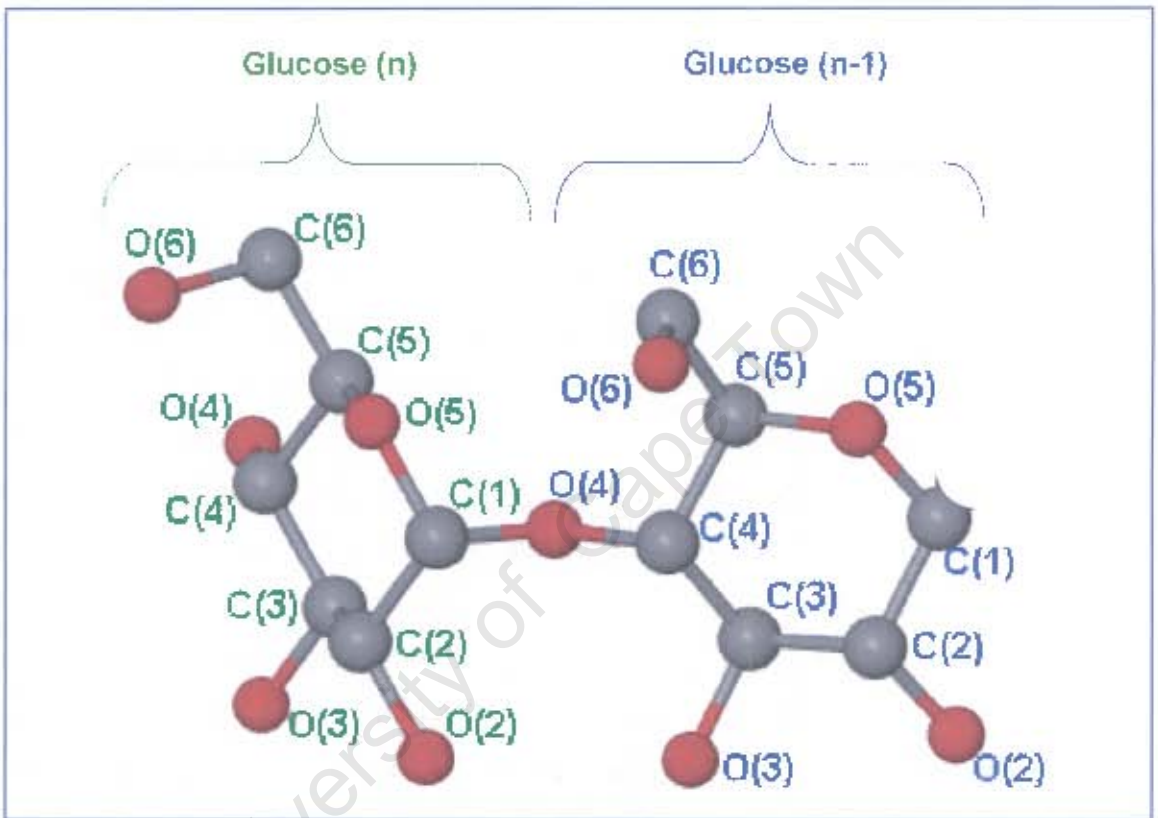

Figure 1.3 – Truncated molecular drawing of a natural cyclodextrin with the conventional numbering scheme. The convention for glucose numbering is an anticlockwise numbering scheme, hence the glucose (n) and the glucose (n-1) on this diagram.

The **glucopyranose conformational descriptors** include the *intersaccharide bond angle* φ = **$C_1(n)$–$O_4(n-1)$–$C_4(n-1)$** describing the angle around the glycosidic link, the **$O_2(n)$---$O_3(n-1)$** distance, and the *tilt angle* τ_1 (or τ_2). The *tilt angle* τ_1 is defined as the angle between the mean glucose plane (i.e. the mean plane through the C_1–C_2–C_3–C_4–C_5–O_5 atoms) and the normal to the mean O_4 polygon

plane, while τ_2 is defined as the angle between the mean O_4 polygon plane and the mean plane through the **$O_4(n)$–$C_4(n)$–$C_1(n)$–$O_4(n-1)$** atoms.

Table 1.1 – Mean indices used to describe the structural features of the three natural cyclodextrins.

Average values of principal torsion angles (rounded off to the nearest integer).

CD	$\lvert\omega\rvert$ (°)	Φ (°)	ψ (°)	Θ_1 (°)	Θ_2 (°)
α	68	108	130	+52	-53
β	64	112	128	+56	-56
γ	68	110	130	+62	-62

Glucopyranose conformational descriptors

CD	φ (°)	$O_2(n)$---$O_3(n-1)$ (Å)	τ_1 (°)
α	118.4	3.05	+11.4
β	117.7	2.92	+9.5
γ	115.0	2.84	+14.5

Average geometric parameters of the O_4 polygon

CD	*l* (Å)	α (°)	$\lvert d\rvert$ (°)	*r* (Å)	$\lvert d\rvert$ (Å)
α	4.2	120	5	4.2	0.07
β	4.3	128	5	5.0	0.08
γ	4.5	132	2	5.9	0.02

The **geometric parameters of the cyclodextrin macrocycle** are best described by an imaginary plane through the O_4 atoms. Thus a planar hexagon is formed by the O_4 atoms of an α-CD molecule, a planar heptagon is formed by the O_4 atoms of a β-CD molecule, and a planar octagon is formed by the O_4 atoms of a γ-CD molecule. The principal geometric parameters of the formed polygon are defined as follows: *l, the side of the O_4 polygon*, is the distance between the neighbouring **O_4** atoms (i.e. between **$O_4(n)$** and **$O_4(n-1)$**); ***a*** is the angle

$O_4(n+1)$–$O_4(n)$–$O_4(n-1)$ (i.e. the acute angle between the two lengths l_1 and l_2); t is the torsion angle **$O_4(n+1)$–$O_4(n)$–$O_4(n-1)$–$O_4(n-2)$**; r is the distance between the apex of the polygon (or the O_4 atom) and the centroid of the polygon; d is the deviation of each O_4 atom from the mean plane of all the other O_4 atoms forming a planar polygon. Average values of these geometric parameters are given in Table 1.1 above.

1.1.4 Uses of Cyclodextrins

Toxicological studies on cyclodextrins have been performed and it has been noted that any of their toxic effects are of secondary character and can be eliminated by selecting the appropriate type of CD or by changing the mode of application [2,3,5]. It is therefore not surprising that CDs are used, or being investigated for use, in a number of fields such as **Biology** *(as enzyme models)*, **Biotechnology** *(in bioconversion of toxic substrates, cell cultivation, antibiotics production)*, **Food Science** *(for flavour and preservation)*, **Agriculture** *(in pesticide delivery)*, **Analytical Chemistry** *(as reagents and in separation methods)*, **Catalysis** *(as substrates or mediators)*, **Technology** *(as chemosensors, in nanotechnology and in liquid crystals)* and **Pharmaceuticals** *(especially in drug formulations)* [2,3,7,10 – 15].

1.2 Inclusion Compounds

1.2.1 Supramolecular Chemistry

Because of the nature and behaviour of cyclodextrins, most cyclodextrin studies fall under the relatively new field called Supramolecular Chemistry. Although supramolecular compounds were first identified in the early 1800s, the discipline of supramolecular chemistry only dates back to the 1960s, with the term 'inclusion compounds' originating in 1950 [3,16,17]. With the foundation laid down by one of its founders, J-M Lehn, Supramolecular Chemistry is defined as

the chemistry of the intermolecular bond, covering the structures and functions of the entities formed by association of two or more chemical species [18]. Supramolecular chemistry is best explained in terms of the host-guest nomenclature [16], where a macromolecule (either in the form of a macrocycle, or a close-packed solid), termed the host, houses the guest. The guest can be a large molecular compound, an atom, an ion, or even a radical [17]. This concept is not far removed from the lock and key concept of molecular recognition, first proposed for biological systems in 1894 [19].

Two types of supramolecular compound exist [16]:

1. Molecular complexes, where the guest molecule is included within the molecular structure of a macrocyclic host; and
2. Lattice clathrates, where the guest forms part of the closely packed structure of a crystalline host.

Forces keeping such molecular entities together include *ion-dipole interactions*, *cation-π interactions*, *van der Waals forces*, *hydrophobic interactions*, *hydrogen bonding*, and are complemented by *preorganisation and complementarity*, *chelate and macrocyclic effects*, *Lewis acid-base pairs* and *close packing in the solid state* [16,20]. With regard to cyclodextrins, which have been described as the most important hosts in supramolecular chemistry [5], **electrostatic, van der Waals, hydrophobic, hydrogen bonding, charge transfer** and **π–π stacking** are the most dominant interactions [21,22]. **The exclusion of cavity-bound high-energy water** and **the relief of conformational strain** are also believed to affect cyclodextrin complexation. Hydrogen bonding has been termed the masterkey interaction in supramolecular chemistry [16].

1.2.2 Cyclodextrin Inclusion Compounds

Of the CD applications mentioned under section ***1.1.4***, we are particularly interested in the use of CDs in pharmacy as drug carriers, through CD-drug inclusion complex formation. In the 1930s, Pringsheim and a number of co-

authors noticed that crystalline dextrins, which were later found to be CDs, and their acetates have a high tendency to form complexes with various organic compounds [2,3,5]. Although modes of inclusion of many CD-drug inclusion complexes are known, the main driving force for inclusion remains controversial [20-22]. Usually, molecular association is made possible not by a single weak interaction, but through the simultaneous cooperation of several weak interactions [23].

All factors listed under section *1.2.1* above contribute, where they apply, in determining whether a CD inclusion complex will form, and water has been found necessary for CD inclusion complex formation [3]. The substitution of the high-enthalpy water molecules by an appropriate guest molecule has also been generally taken as one of the main driving forces for CD inclusion complex formation as represented in Figure 1.4 below, reproduced from ref. [5].

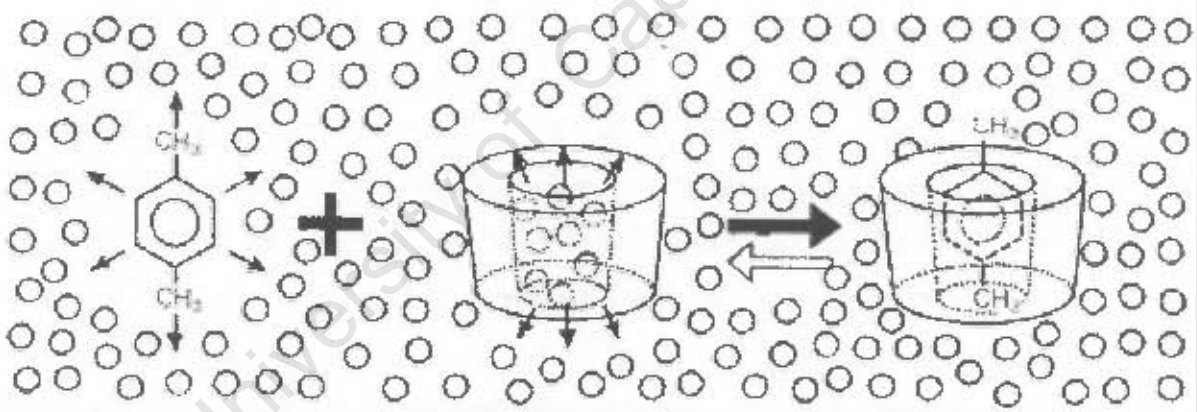

Figure 1.4 – Schematic representation of CD inclusion complex formation. *p*-Xylene is the guest molecule; the circles represent the water molecules.

In Figure 1.4, both the water inside the hydrophobic cavity of the parent cyclodextrin and the hydrophobic xylene surrounded by water molecules, on the left hand side of the reaction scheme, represent an unfavoured high energy state. On the right hand side of the reaction scheme is the *p*-xylene-CD complex, in which the hydrophilic part of the cyclodextrin molecule is interacting with water

and the hydrophobic cavity encapsulates the hydrophobic *p*-xylene molecule. This represents a relatively low energy state.

Contrary to the general concept of the substitution of high-enthalpy water molecules by an appropriate guest molecule as the driving force for CD inclusion complexes, Liu *et al* [21] argue that the release of high energy water from the CD cavity into the bulk of the water solution should not be taken as a driving force for CD inclusion, as the negative enthalpy accompanying the release of this 'high enthalpy' water, is cancelled by the loss of entropy. The result is a negligible change in Gibbs free energy.

Water can be used as a reaction medium for complexation to occur [7], while other complexes can be prepared in the solid state [24]. However, the presence of water in most CD complex crystal structures maintains the integrity of the complex [7,21,22]. Water molecules do so either by participating in the hydrogen bonding network of the complex or by 'filling the holes' in the crystal structure of a particular complex.

1.2.3 Cyclodextrin Complex Preparation

CD inclusion complexes can be prepared quite easily, although not necessarily routinely, in homogeneous solution, in suspension, under pressure, by melting the potential guest with cyclodextrin, or by simply mixing of the components in the solid state [2,7,24]. The controversy around the driving forces for CD-inclusion complex formation makes it difficult for one method to be preferred for a particular type of cyclodextrin, or for a certain set of drugs. The practice therefore has been not to depend on standard methods but to tailor-make one for each system on a 'trial and error' basis [24].

In view of the driving forces for the complexation of drugs with cyclodextrins [2,3,5,21], together with techniques for growing crystals that are suitable for

crystal structure determination [25,26], **'coprecipitation or cocrystallization'** and **'kneading'** methods are frequently used for the preparation of crystalline CD-drug inclusion complexes of pharmaceutical interest.

In the **coprecipitation/ cocrystallization method**, cyclodextrin is dissolved to a near saturation point in water, at room temperature or at elevated temperature (usually 60 to 80 °C), and an equimolar amount of the drug is added as a powder while stirring. The complex either precipitates during the stirring time, or is formed during the crystal growth after filtration. Variations of the coprecipitation method include co-solvent coprecipitation, in which a drug is pre-dissolved in an organic solvent in which it is soluble before being added to the cyclodextrin water solution. Other variations include changing the molar ratios of the cyclodextrin and the drug to be reacted.

The **'slurry method'** can be taken as a variant of the coprecipitation method in which a drug is added to a supersaturated CD-water mixture while stirring. Complex formation is the same as for the coprecipitation method.

In the **kneading method**, a drug is added to a cyclodextrin-water paste, either as a powder or pre-dissolved in the solvent of choice (equimolar or variations). A few drops of water are added to the mixture, to avoid drying as the kneading continues. The kneading experiment is complete when the test, e.g. PXRD pattern or IR (infrared) spectrum of the kneaded material indicates complex formation. Although the kneading time is unpredictable from one drug to another, or from one CD type to the next, a kneading time of about an hour is typical. The kneaded complex may then be redissolved in water, often at moderately elevated temperature, filtered, and subjected to crystal growth. Variations of this method include the use of a water-organic solvent mixture in complex preparation.

1.2.4 Cyclodextrin Crystal Packing

The first X-ray crystal structure of a CD-inclusion complex was published in 1965 [27]. As early as 1984 [28] conclusions were drawn that α-, β-, and γ-cyclodextrin inclusion complexes crystallize in basically two different patterns, the **cage** type (composed of *fishbone (or herringbone)-type* and *brick (or layer)-type*) and the **channel type** (with two kinds of arrangements, the *head-to-head* and the *head-to-tail* arrangements), as shown in Figure 1.5.

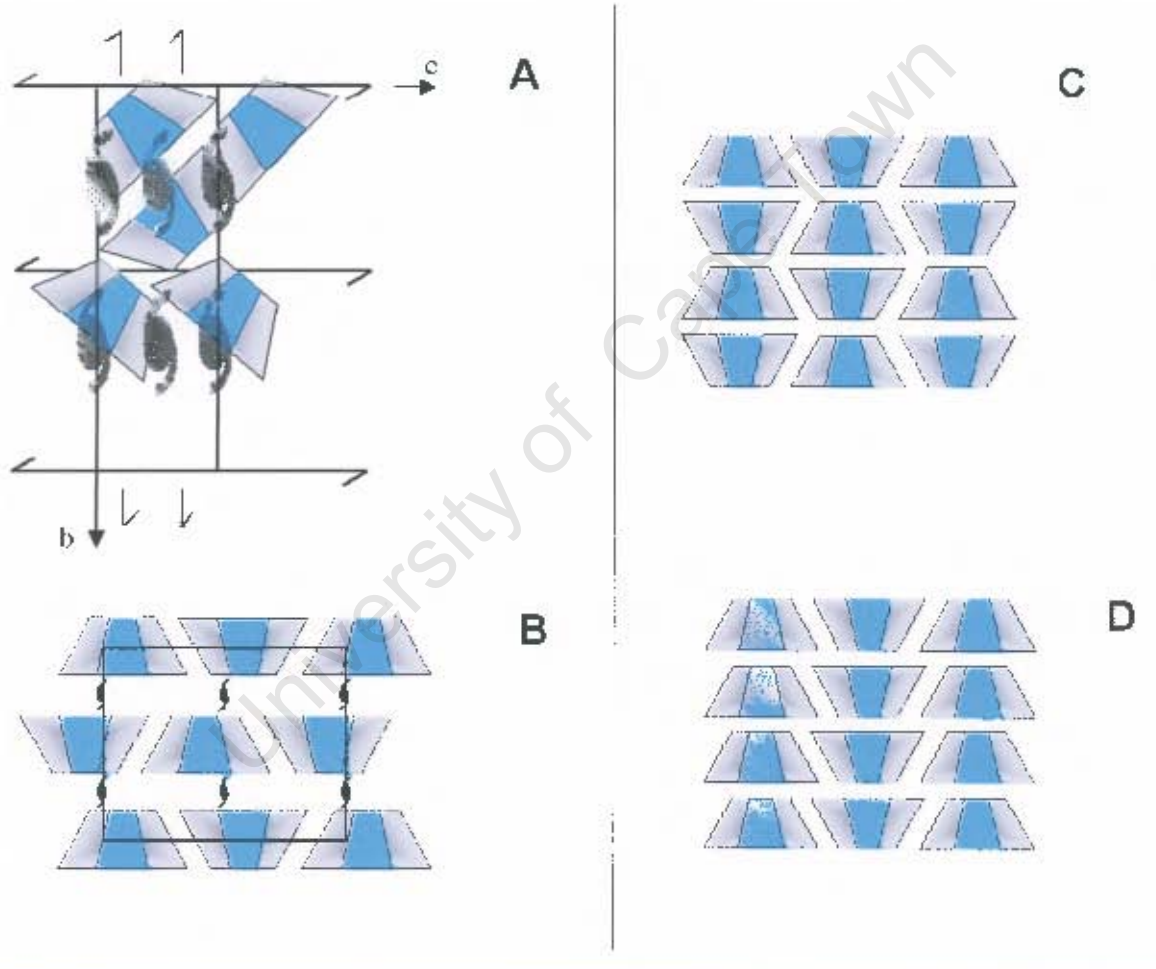

Figure 1.5 – Diagrammatic representation of commonly observed CD packing arrangements in all three natural cyclodextrin complexes. **A** = fishbone or herringbone cage type, **B** = brick or layer cage type, **C** = head-to-head channel type and **D** = head-to-tail channel type.

The cage type is usually formed when small organic guests such as methanol and the like, are included in either α or β-cyclodextrins. With γ-CD the cage type has only been observed for complexes with water as the guest, otherwise the channel type is commonly observed even with small molecules such as methanol [6]. For the larger organic guests (larger than *n*-propanol), and ionic guests, channel or layer structures are frequently observed for α-cyclodextrin. Head-to-head and head-to-tail dimeric structures have also been observed in α-CD complexes with aromatic guests [9].

In the case of the widely studied natural CD, β-cyclodextrin, all forms of packing arrangements have been observed. With the exception of the diclofenac sodium•β-CD complex [29], and other similar crystal structures reported in this dissertation, β-cyclodextrin prefers a head-to-head arrangement, with CD molecules held together by the hydrogen bonds between the O2-H and O3-H atoms of the wider secondary rim for larger organic guest molecules [6,9,28]. These dimers can either pack in cages of larger dimensions than the monomers, or can form channels, or even layers [9]. Noteworthy, and pertinent to our study, is the preference of CD complexes of organic salts to form channel structures regardless of the guest size [6,9,28].

Tetrameric β-CD inclusion complexes have also been observed. In these complexes, two dimers are arranged to form a tetrameric channel, which can either pack in **IM** mode or in **CB** mode (see the description of **IM** and **CB** below) [30].

For the β-CD dimeric complexes, a more systematic approach in the classification of their packing arrangements has led to four distinct arrangements. These have been designated as the **channel type (CH),** the **chessboard (CB),** the **intermediate (IM)** (so-called because it is intermediate between **CH** and **CB**), and the **screw channel (SC)** [31]. Figure 1.6 illustrates these four predominant packing arrangements of β-CD dimeric complexes. The **CH** structures crystallize

in space groups C2 or P1, and the **CB**, **IM** and **SC** in $C222_1$, P1 and $P2_1$ respectively [31]. The implications are that each packing arrangement (or class) with a particular space group forms an isostructural series as demonstrated by Caira [32]. The isostructurality concept is defined in the subsequent section (section **1.3**).

In the **SC** packing mode each dimer packs above another dimer as in the **CH** mode but the consecutive dimers are not parallel [31]. The stacking of the dimers is along the *b* axis such that they form layers along the *a* and the *c* axes.

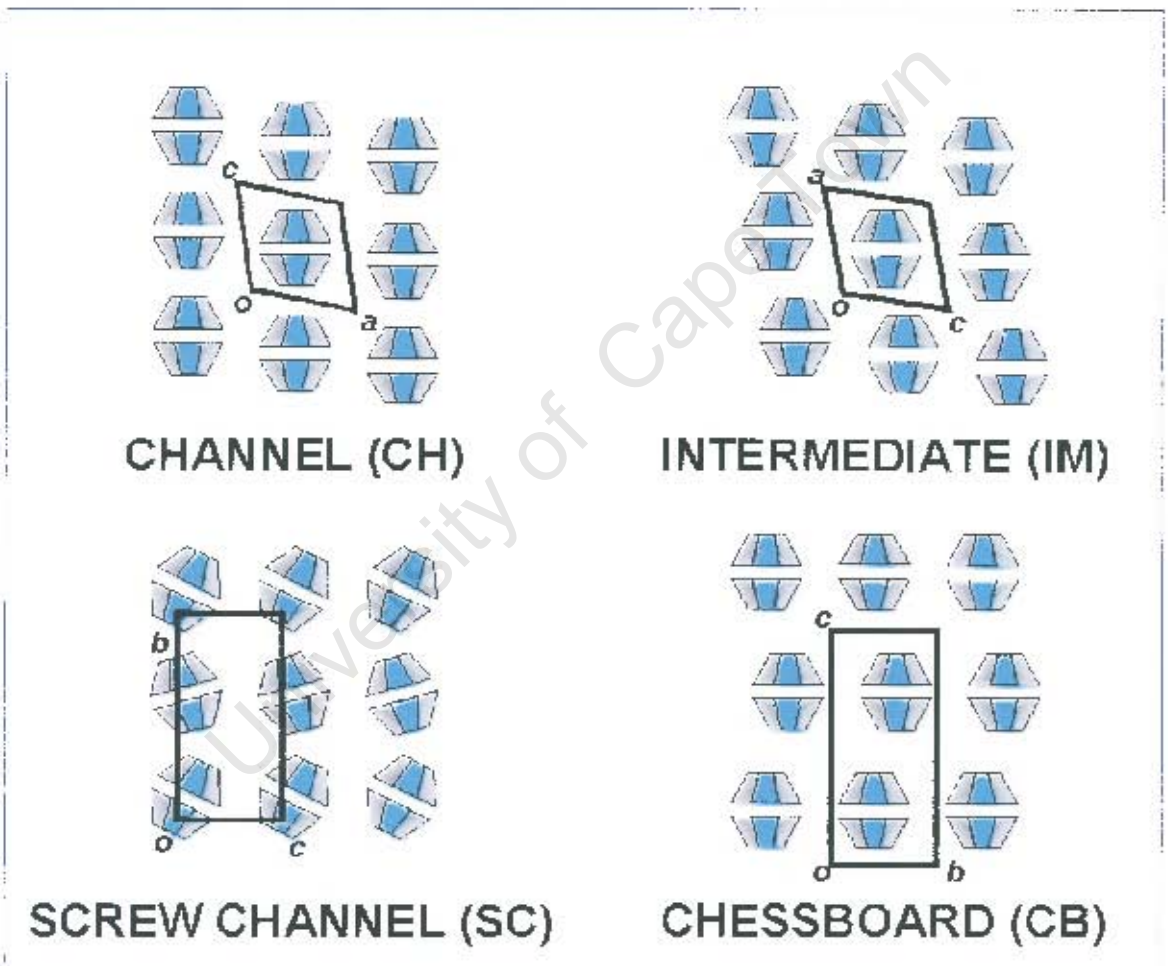

Figure 1.6 – Classification of β-CD dimeric stacking arrangements

A recent review reveals that these dimers can be displaced by a shift of layers along the *ac* plane to some extent [33]. A significant shift of these layers can result in a structure that is no longer isostructural with the others although it may have similar unit cell dimensions. Another structure has recently been reported in which its unit cell edges resemble those of the unit cell for the **CB** mode, but has a packing arrangement somewhat between the **CH** and **SC** modes [34]. These subtle variations in the packing modes of CD inclusion complexes can be attributed to the differences in the conformation and molecular nature of the included guest molecules.

1.3 Introduction to Isostructurality

1.3.1 Definition of Isostructurality

The crystal structure of a given crystalline solid may be assigned to only one of the seven crystal systems, to only one of the 14 Bravais lattices, and to only one of the 230 crystallographic space groups [35]. If a particular compound can be structurally classified in more than one way, it is said to be polymorphic. In this case, the different crystalline forms may or may not crystallize in the same space group. The opposite is also possible – two or more chemically different compounds can have their atoms arranged in the same type of crystal structure (i.e. same crystal system, same Bravais lattice, and same space group) and such compounds are termed isostructural [36,37].

Isomorphism was first discovered by Mitscherlich in 1819 [38,39], when he noticed that certain pairs of salts (e.g. KH_2PO_4, KH_2AsO_4, etc.) developed the same crystalline form [40]. These morphologically similar pairs of salt were then termed isomorphous, meaning 'same form'. This term has been applied to inorganic and organic compounds, and to describe crystal morphological similarities and crystal lattice similarities. To avoid ambiguity, IUPAC agreed on the use of the terms as explained in the following section. However, it remains

unlikely that the term 'isomorphous replacement' will ever be replaced by the more appropriate term 'isostructural replacement' although the replacement is at an isostructural level.

1.3.2 Use of the Term 'Isostructurality'

Although the term 'isomorphous' is still used interchangeably with 'isostructural' and 'isotypic' by some authors, isomorphism is more appropriately used to describe external morphological similarities of crystalline substances [36,40]. Isotypism is more appropriate for inorganic materials, where isotypic salts are usually obtained by replacing an ion in the crystalline lattice of one compound by a spherically similar ion in the lattice of the other [41]. The situation is different for organic crystals, as strict geometrical similarity never occurs where molecules replace one another in isostructural crystals [41]. Thus for organic crystals, the term isostructural has been adopted.

Because we deal with organic compounds, or salts of organic compounds, and their inclusion complexes in this dissertation, only the term isostructural is appropriate in our work. Isostructuralism has further been sub-divided into "main-part isostructuralism" and "homeostructuralism" by Kálmán and co-workers [39,40,42]. Main part isostructurality, also called quasi-isostructurality or isometricity or approximate isomorphism, refers to isostructurality in which the isostructural molecules differ only due to small chemical differences, resulting in negligible change in the volumes occupied by the molecules. The term homeostructural refers to two or more isostructural compounds that have significantly different molecular shape and size.

1.4 Descriptors of Isostructurality

As seen under section *1.3.1*, for two or more crystals to be isostructural, they should have similar molecular shapes (molecular geometry of the non-hydrogen

atoms, sometimes referred to as 'molecular isometricity'), similar unit cell dimensions (unit cell edges and interaxial angles) and they must belong to the same space group (implying similar arrangement of the unit cell contents). Indeed three isostructural indices have been derived by Kálmán and co-workers [39,40,42-43] based on these requirements:

a) ***Packing coefficient increment, Δ(pc)***, denotes a change in the volume of the asymmetric unit as a result of a change in the molecular shape of an isostructural pair:

$$\Delta(pc) = \{\Delta(rst) - \Delta V'\} / V'$$

where $\Delta V'$ is the change in the volume of the asymmetric unit while $\Delta(rst)$ is the net difference between the volume of the newly added and/or deleted atoms. A low $\Delta(pc)$, approximately $\pm$ 2.0 %, and a low $\Delta(rst)$ suggest a high degree of isostructurality.

b) ***Unit cell similarity index, Π***, describes the extent to which the unit cell parameters of two or more isostructural compounds match. The lattice parameters, axial ratios and interaxial angles can be used to estimate Π by the following equation:

$$\Pi = \left| (a + b + c)/(a' + b' + c') - 1 \right|$$

a, b, c and **a', b', c'** are the orthogonalised lattice parameters of the related crystals. Although Π values of 0.001 – 0.03 are normal, Π should be practically zero for highly isostructural crystals.

c) ***Isostructurality Index, I_i (n)***, quantifies the fit of the absolute coordinates of the identical non-hydrogen atoms of an isostructural pair:

$$I_i(n) = [\, 1 - (\Sigma \Delta R_i^2 / n)^{1/2} \,] \times 100\ \%$$

where **n** is the number of the distance differences (ΔR_i) between the absolute coordinates of the identical non-hydrogen atoms within the same section of the asymmetric units of the related (A and B) structures. I_i values of 50 – 95 % have

been reported for isostructural crystals. The higher the I_i values for a certain pair of anticipated isostructures, the higher the degree of isostructurality.

The above three descriptors of isostructurality have been reduced to two, Π and I_i. The increment of the packing coefficient, Δ**(pc)**, has become redundant since it is closely related to the unit cell similarity index [39].

An alternative way of comparing unit cell parameters has also been proposed [44,45], in which the difference in cell size is described by the mean elongation (ε) and the cell shape distortion is accounted for by the asphericity index (A):

$$\varepsilon = (V' / V)^{1/3} - 1 \qquad (V' > V)$$

where **V** and **V'** are the volumes of the respective unit cells.

$$A = \tfrac{2}{3} [1 - \Sigma_{j>i} \{((1 + \varepsilon)M_i - 1) \times ((1 + \varepsilon) M_j - 1)/ 3\varepsilon^2\}]^{\frac{1}{2}}$$

where the M_i's are the principal axes of matrix **M**, which gives the pure shear component of the transformation between the two crystallographic coordinate systems. The closer the relationship between the structures, the closer ε and A are to zero.

Applications of the above definitions have been demonstrated by Kálmán and others [39,40,42] and resulted in the so-called the volumetric measure of isostructurality (I_v) [45], in which the fit of the non-hydrogen atoms in supposed isostructures is modelled by the overlap of their atomic volumes, not by the matching of the absolute coordinates of the common atoms between A and B isostructures:

$$I_v = 2V_0/(V_1+V_2) \times 100\%$$

where V_1 and V_2 are the volumes of the compared fragments and V_0 is the intersection of these volumes. A value of I_v = 100% is obtained for identical structures and I_v = 0% results in the case of no overlap between structures A and B [45]. This calculation should be performed on a whole unit cell to avoid the problem raised by unit cell dissimilarity [40].

1.5 Conditions and Limits of Isostructurality

Apart from the descriptors of isostructurality defined in the preceding section (i.e. similar molecular shape, similar unit cell parameters and similar atomic coordinates), the conditions and limits of isostructurality have been observed in some cases. These include **substituent pairs that can be tolerated by isostructural crystals** (e.g. CH_3 substituted by H without altering the crystal packing), **substituent to molecular size ratio** (e.g. CH_4N_2O not isostructural with CH_4N_2S as the difference in S and O volumes is significant with respect to the CH_4N_2X molecule), **the elimination (or generation) of hydrogen bonding properties** (e.g. H substitution with OH can result in a change in the crystal packing as a result of a change in the hydrogen bonding properties of the molecule), **generation (or elimination) of a chiral molecule** (this changes the configuration of the molecule and often results in different packing arrangements), and **the existence of polymorphism** in which crystals of the same molecule result in different packing arrangements when grown under different conditions [39,40,46-47].

The danger of relying solely on one descriptor of isostructurality has also been highlighted, where near equality of unit cell parameters does not necessarily imply isostructurality [33].

1.6 Implications of isostructurality

Correlation between isostructurality and co-crystallization has been reported [40,43], in which the co-crystallization of some steroid pairs (yielding 'mixed crystals' or 'co-crystals') depended on the degree of their isostructurality, as measured by the indices defined under section **1.4** above. Thus the degree of isostructurality can be a useful indicator in predicting the outcome of co-crystallization reactions. Anomalies in the solubilities of substituted alkylparabens, in which ethyl- and propylparabens had abnormally low solubilities

compared to methyl- and butylparabens, could be explained by the concept of isostructurality [48].

A review highlighting similarities or differences in physicochemical properties or behaviour observed in various series of isostructural compounds has been published [36]. For metal-containing inclusion compounds, the nature of the metal centre and the coordination to the host molecule were found to correlate with the thermal stability order of an isostructural series. Host-guest hydrogen bonding was found to affect thermal stabilities of isostructural clathrates [36].

Unlike the concept of isomorphism (a term used to indicate similarity in crystal morphology) which has been applied in crystal engineering, in particular in crystal seeding via epitaxial growth [49], there are limited publications on the chemical applications of the concept of isostructurality [36]. The use of isostructurality is prominent mainly in chemical crystallography where it is used as the basis of the 'isomorphous replacement' method of X-ray crystal structure solution.

1.7 Isostructurality of Cyclodextrin Inclusion Compounds and X-Ray Powder Diffraction Analysis

X-ray powder diffraction is routinely used as a complementary technique to identify new CD inclusion complexes. The usual procedure involves the recording of the PXRD pattern of the presumed complex (HG), the individual patterns of the guest (G) and the host (H), and that of a physical mixture of the reactants in a chosen stoichiometric ratio (H:G). If the trace of HG appears to differ from the other three traces, in both peak intensities and peak angular positions, then the presumed HG complex has probably formed. This traditional way of identifying newly synthesised CD inclusion complexes suffers from a number of disadvantages, notwithstanding that it is normally complemented by other techniques such as HSM, TGA, infrared spectroscopy, thin layer chromatography and ultraviolet analysis, to demonstrate inclusion.

One deficiency of this way of analysis is the relatively large amount of material (H, G, H+G, HG) used in just one analysis, which may be a concern in pharmaceutical materials that may not be readily available in such quantities. The preparation of H+G alone requires careful attention as one does not want to induce a reaction or to encourage the phase transformation of one species in the process. Some authors ignore the recording of the H + G trace and that has led to the misclassification as a complex [50], of a material found to be a physical mixture. The second deficiency is that attempted inclusion preparations may fail and rather induce polymorphism of either the host or the guest as has been found with attempted TRIMEB inclusion preparations [51]. A further source of complication is that even when inclusion does occur it may not do so quantitatively and the resultant precipitate may be a mixture of HG and H, or HG and G. All these complications may result in the false classification of an unknown species as being an inclusion complex.

Clearly, a more definitive way of using PXRD for the analysis of newly synthesised CD inclusion complexes is desirable. Based on the isostructural behaviour exhibited by most of the cyclodextrin inclusion complexes as analysed from the CSD, Caira has pioneered a systematic classification of cyclodextrin inclusion compounds into distinct isostructural series and demonstrated their practical utility in X-ray powder diffraction studies [32,48]. In brief, the method development is as follows. CD inclusion complexes that display isostructural behaviour, on the basis of isostructural descriptors explained in section 1.4, are grouped into an isostructural class and are represented by a unique PXRD trace, averaged from individual PXRD traces within a class. A number of such PXRD traces, each distinct and characteristic of its class (or series), are then documented for each cyclodextrin type. In this dissertation, this method is referred to as the isostructural method of PXRD analysis, or in short IsoPXRD method.

Once the method has been developed, its application is quite straightforward. Only the PXRD trace of the suspected complex needs to be recorded. If the PXRD trace of a newly synthesised complex can be matched with that of an existing isostructural series, then not only can the new complex be identified unambiguously, but structural features characteristic of that class can be assumed for the new complex. Complex characterisation in this way should carry more weight in, for example, strengthening patent claims and may complement a thorough structural characterisation as legally required by drug-regulation agencies [10]. The condition for a 'match' between the PXRD pattern of a putative complex and a reference pattern is that the majority of the peaks should correspond in angular position to within approximately 0.2° 2θ. Considerable latitude is exercised with regard to correspondence in peak intensities, on the other hand, since the reference pattern is an artefact (average of several computed patterns).

Although the wealth of information obtained from single crystal X-ray diffraction (SCXRD) analysis supercedes that obtained by any other technique used for the structural analysis of crystalline CD inclusion complexes, the difficulty of growing single crystals suitable for crystal structure determination, and the amount of work accompanying each crystal structure solution limit the use of the SCXRD technique. Thus in complexes where crystal growth attempts fail to produce monocrystals with good diffracting qualities suitable for SCXRD analysis, the IsoPXRD method may be necessary. A major advantage of the IsoPXRD method over the traditional use of PXRD for complex identification is the significant reduction of the sample material, as well as the sample preparation time and effort used in the analysis.

A major disadvantage of the IsoPXRD method is the possibility that the X-ray diffractogram of a new inclusion complex does not match any of the available reference patterns. However, it may happen that subsequently a second complex, isostructural with the first, is isolated, leading to the establishment of a

new isostructural series. This clearly indicates that in order for the IsoPXRD method to be useful, continual updating of the isostructural series by incorporation of newly published structures is necessary.

1.8 Motivations and Objectives of this Study

1.8.1 Isostructurality and PXRD Analysis

As we noted in section 1.7 above, the IsoPXRD method needs to be updated for its optimum use. Ideally, any new CD complex would need to be incorporated into the library of reference patterns, as this may result in the generation of a series. In practice, this calls for a constant update. Another reason for this is the increasing number of redeterminations of CD complexes under a different space group [52], which may result in re-assignment to a different isostructural series or the elimination of a series.

The IsoPXRD method was last updated in 2001 [48] and a number of CD inclusion complexes, some of which display novel properties, have been synthesised since then. The aim of the first part of this dissertation therefore is to repeat the survey that was done in 2001 on the currently available data and thus update the 2001 version. The objective of this particular study has been to focus on natural cyclodextrins and their derivatives, and to use the crystal data found in the CSD as well as other data we may have access to. A detailed plan and execution of this part of the project can be found in Chapter 2, and the results are in Chapter 3.

We further intend to demonstrate the ease of application of the IsoPXRD method to materials obtained by kneading CDs and selected guest compounds, where recrystallization of the kneaded materials failed to produce complex monocrystals. Finally, we tested the influence of guest polymorphism on isostructurality of CD inclusion compounds by attempting to prepare inclusion

complexes of the triclinic and monoclinic tautomerisational polymorphs of sulfasalazine with all three natural cyclodextrins. Application of the IsoPXRD method as well as the influence of guest tautomerism are reported in Chapter 4.

1.8.2 Diclofenac Salts: Inclusion in β-Cyclodextrin

It has been a common practice to advance the therapeutic properties of many organic drugs by making salt forms of the drug before tableting, or making solid forms or solutions, for dispensing or storage [53-55]. The discovery of cyclodextrins opened another branch of masking the unpleasant properties of many drugs either by micro-encapsulation, crystalline inclusion, or by simply making mixtures, or solutions, of the drug with one of the cyclodextrins [2]. In some cases, drug salt formation or CD-inclusion by itself has been inadequate in diminishing the undesirable properties of some drugs [56,57]. Thus the pharmaceutical performance of several acidic [58] and basic [59] drugs has been improved by simultaneous CD complexation and salt formation. The β-CD complex of the sodium salt of diclofenac exhibits an aqueous solubility exceeding 10 mg/mL at 20°, pH 5-7 [60]. X-ray analysis of the complex showed that it is monomeric, with host-guest stoichiometry 1:1 and that it crystallizes in the hexagonal space group $P6_1$ [29].

Our aim in this part of the project was to synthesise β-CD complexes of diclofenac salts with different monovalent cations with the intention of investigating the influence of changing the cation, in simultaneous CD inclusion and salt formation, on the crystal isostructurality of these complexes. The plan was to grow crystals of the potassium and the caesium salt inclusion complexes with the host β-CD, solve their structures by SCXRD, and further characterise them by other techniques such as HSM, TGA, DSC, and microanalysis, so as to provide a detailed comparison with the existing sodium analogue. A detailed report of the findings is given in Chapter 5.

1.9 References

1. R. H. Garrett and C. M. Grisham, *Biochemistry*, Saunders College Publishing, Orlando, 1995, 322 – 680.
2. K-H. Frömming and J. Szejtli, *Topics in Inclusion Science,* **Vol 5**, Kluwer Academic Publishers, The Netherlands, 1994, 1 – 218.
3. J. Szejtli and T. Osa, *Comprehensive Supramolecular Chemistry,* **Vol 3**, 1996, vii – 624.
4. T. Nakagawa, K. Ueno, M. Kashiwa, J. Watanabe, *Tetrahedron Lett.,* 1994, **35**, 1921 – 1924.
5. J. Szejtli, *Chem. Rev.,* 1998, **98**, 1743 – 1753.
6. W. Saenger, J. Jacob, K. Gessler, T. Steiner, D. Hoffmann, H. Sunbe, K. Koizumi, S. M. Smith, T. Takaha, *Chem. Rev.,* 1998, **98**, 1787 – 1802.
7. A. R. Hedges, *Chem. Rev.,* 1998, **98**, 2035 – 2044.
8. W. Saenger, *Biochem. Soc. T.*, 1983, **11**, 136 – 139.
9. K. Harata, *Chem. Rev.,* 1998, **98**, 1803 – 1827.
10. H-J. Schneider, F. Hacket, V. Rüdiger, *Chem. Rev.,* 1998, **98**, 1755–1785.
11. M. A. Hossain, K. Hamasaki, K. Takahashi, H. Mihara, A. Ueno, *J. Am. Chem. Soc.,* 2001, **123**, 7435 – 7436.
12. R. Yang, K. Li, K. Wang, F. Zhao, N. Li, F. Liu, *Anal. Chem.,* 2003, **75**, 612– 621.
13. K. Takahashi, *Chem. Rev.,* 1998, **98**, 2013 – 2033.
14. Z. H. Qi, C. C. Sikorski, *NutraCos*, 2002, **1**, 18 – 24.
15. G. Toth, J. Szejtli, I. Toth, L. Szente, E. Pasztor, H. E. Radvany, W. E. Tanko, *Pat. Appl.*, DE 3614275, 1986.
16. J. W. Steed, J. L. Atwood, *Supramolecular Chemistry,* John Wiley and Sons Ltd, Chichester, 2000, ix – 713.
17. H. Dodziuk, *Introduction to Supramolecular Chemistry,* Kluwer Academic Publishers, 2002, xi – 323.
18. J-M. Lehn, *Angew. Chem. Int. Edit.,* 1988, **27**, 89 – 112.

19. J-P. Behr, *Perspectives in Supramolecular Chemistry,* **Vol. 1**, John Wiley and Sons, Chichester, 1994, ix – 316.
20. H-J. Schneider and A. Yatsimirsky, *Principles and Methods in Supramolecular Chemistry,* John Wiley and Sons Ltd, Chichester, 2000, 1– 335.
21. L. Liu and Q-X. Guo, *J. Incl. Phenom. Macro.*, 2002, **42**, 1–14.
22. M. V. Rekharsky and Y. Inoue, *Chem. Rev.,* 1998, **98**, 1875 – 1917.
23. M. S. Searle, M. S. Westwell and D. H. Williams, *J. Chem. Soc. Perk. T. 2,* 1995, 141 – 151.
24. L. Szente, *Comprehensive Supramolecular Chemistry,* 1996, **3**, 243 –252.
25. P. G. Jones, *Chem. Brit.,* 1981, **17**, 222 – 225.
26. A. Holden and P. Singer, *Crystals and Crystal Growing,* Heinemann Education Books Ltd., London, 1961, 17 – 297.
27. A. Hybl, R. E. Rundle and D. E. Williams, *J. Am. Chem. Soc.,* 1965, **87,** 2779 – 2788.
28. W. Saenger, *J. Inclusion Phenom.,* 1984, **2**, 445 – 454.
29. M. R. Caira, V. J. Griffith, L. R. Nassimbeni and B. van Oudtshoorn, *J. Chem. Soc. Chem. Comm.*, 1994, 1061 – 1062.
30. D. R. Dodds, *PhD Thesis, Physicochemical Study of Inclusion of Drug Molecules in Cyclodextrins*, University of Cape Town, South Africa, 1999.
31. D. Mentzafos, I. M. Mavridis, G. Le Bas and G. Tsoucaris, *Acta Crystallogr.*, 1991, **B47**, 746 – 757.
32. M. R. Caira, *Roum. Chem. Quart. Rev.,* 2000, **8**, 221 – 344.
33. M. R. Caira, E. De Vries, L. R. Nassimbeni and V. W. Jacewicz, *J. Incl. Phenom. Macro.,* 2003, **46**, 37 – 42.
34. P. Giastas, K. Yannakopoulou and I. M. Mavridis, *Acta Crystallogr.*, 2003, **B59**, 287 – 299.
35. S. R. Vippagunta, H. G. Brittain, D. J. W. Grant, *Adv. Drug Deliv. Rev.,* 2001, **48**, 3 – 6.
36. M. R. Caira, *Encyclopaedia of Supramolecular Chemistry,* Marcel Dekker Inc., 2004, 767 – 775.

37. F. D. Bloss, *Crystallography and Crystal Chemistry,* Holt, Rinehart and Winston, Inc., New York, 1971, 249 – 250.
38. J. Lima-de-Faria, *Historical Atlas of Crystallography,* Kluwer Academic Publishers, Dordrecht, 1990, 1 – 141.
39. A. Kálmán, L. Párkányi, and G. Argay, *Acta Crystallogr.,* 1993, **B49**, 1039– 1049.
40. A. Kálmán and L. Párkányi, *Adv. Mol. Struct. Res.,* 1997, **3**, 189 – 226.
41. A. I. Kitaigorodskii, *Organic Chemical Crystallography,* Consultants Bureau Enterprises Inc., New York, 1961, 222 – 231.
42. A. Kálmán, G. Argay, D. Scharfenberg-Pfeiffer, E. Höhne and B. Ribár, *Acta Crystallogr.*, 1991, **B47**, 68 – 77.
43. A. Kálmán, G. Argay, D. Živanov-Stakić, S. Vladimirov and B. Ribár, *Acta Crystallogr.*, 1992, **B48**, 812 – 819.
44. J. S. Rutherford, *Acta Chim. Hung.*, 1997, **134**, 395 – 405.
45. L. Fábián and A. Kálmán, *Acta Crystallogr.,* 1999, **B55**, 1099 – 1108.
46. L. Fábián, G. Argay, A. Kálmán, and M. Báthori, *Acta Crystallogr.,* 2002, **B58**, 710 – 720.
47. M. R. Caira, E. J. C. de Vries and L. R. Nassimbeni, *Chem. Commun.*, 2003, 2058 – 2059.
48. M. R. Caira, *Rev. Roum. Chim.,* 2001, **46**, 371 – 386.
49. C. Liu, S. Komarneni and R. Roy, *Mater. Res. Soc., Symposium Proceedings,* 1994, **346**, 721 – 726.
50. L. Filip, D. Bogdan, M. Bojita and M. Bogdan, *Studia Universitatis Babes-Bolyai, Physica,* 2001, 362 – 366.
51. M. R. Caira, S. A. Bourne, W. T. Mhlongo and P. M. Dean, *Chem. Commun.*, 2004, **19**, 2216 – 2217.
52. R. E. Marsh, M. Kapon, S. Hu and F. H. Herbstein, *Acta Crystallogr.*, 2002, **B58**, 62 – 77.
53. M. B. Fawzi and M. Mahjour, *PCT Int. Appl.*, WO 9215332, 1992.
54. L. Gu and R. G. Strickley, *Pharm. Res.*, 1987, **4**, 255 – 257.
55. P. S. Cardaciotto and E. A. Vitalis, *Pat. Appl.,* US 19590127, 1959.

56. K. Csabai, M. Vikmon, J. Szejtli, E. Redenti, G. Poli and P. Ventura, *J. Inclus. Phenom. Mol.*, 1998, **31**, 169 – 178.
57. K. Uekama, F. Hirayama and T. Irie, *Chem. Rev.*, 1998, **98**, 2045 – 2076.
58. E. Redenti, L. Szente and J. Szejtli, *J. Pharm. Sci.* 2001, **90**, 979 – 986.
59. P. Chilesi, P. Ventura, M. Pasini, E. Redenti, J. Szejtli and M. Vikmon, *PCT Int. Pat. Appl.*, WO 94/16733, 1994.
60. V. J. Griffith, L. R. Nassimbeni, D. G. M. Nicholson, M. D. Bodley, M. R. Caira, L. A. Glintenkamp, L. J. Penkler and M. C. van Oudtshoorn. *Eur. Pat. Appl.*, 647451, 1995.

CHAPTER 2: EXPERIMENTAL MATERIALS AND METHODS

2.1 Isostructurality Data Handling

2.1.1 Cambridge Structural Database Search

The Cambridge Structural Database (CSD) is a collection of structural data, viz. X-ray crystallographic and neutron diffraction studies, on small molecules (i.e. not biological macromolecules such as proteins) containing organic carbon (organics, organometallics, coordination compounds, etc.) [1]. Documenting more than 320 000 crystal structures currently, the CSD enables the statistical analysis of the reported data. We used the most recent version of the CSD [1], to analyse isostructurality in cyclodextrins and their organic inclusion compounds, and hence to update the isostructurality method of X-ray powder diffraction analysis (the IsoPXRD method) [2].

Natural cyclodextrin inclusion complexes were searched using a template of each of the α-, β- and γ-CDs with all hydroxyl groups attached. Derivatised CDs were searched by deleting both the primary and the secondary hydroxyl groups in the searching template. Rare cyclodextrins, i.e. those with fewer than six or more than eight glucopyranose residues per cyclodextrin unit, were not included in this study as few data are available for them. With the exception of parent cyclodextrins, CD complexes that had no matching X-ray powder diffractograms were excluded in this survey, as at least two complexes are required for an isostructural series to exist. Cyclodextrin inclusion compounds whose three-dimensional coordinates were not available on the CSD were filtered out of the survey since atomic coordinates are required for the computation of PXRD patterns. Also filtered out during the CSD search were inclusion complexes with inorganic and organometallic compounds as guests, as our interest is on isostructurality of cyclodextrin compounds with organic compounds as guests.

Inclusion complexes indicated in the CSD as having R factors greater than 15 % were considered less accurate and thus excluded from the survey. For inclusion complexes with similar unit cell parameters and possessing identical guests and for which X-ray analyses were performed under the same experimental conditions, the analysis with the lowest R factor (this was often the most recent determination) was chosen. In some redeterminations, some parent CD compounds were chosen based on their water content being the one frequently encountered. In the case of inclusion complexes of the same cyclodextrin form and with similar organic guests, but having different unit cell parameters, which could imply polymorphism, the papers in which such complexes were reported were checked and the one in which the unit cell determinations were measured under the usual experimental conditions (i.e. under usual temperatures and pressures) was taken as a representative complex.

2.1.2 Computation of the Isostructural Series

All the complexes that survived the selection criteria described above were grouped according to their unit cell similarities, and by the space groups in which they crystallize. Atomic coordinates of the crystal structures of the accepted isostructural groups were then used to compute their respective PXRD patterns. Very closely matching PXRD patterns, by visual inspection, were finally grouped into isostructural series, from which an average PXRD pattern was calculated. The calculated PXRD traces were normalised such that the largest peak height in each computed pattern has a relative intensity of 1000 units. Isostructurality of compounds in a series was also confirmed by plotting and overlaying packing diagrams projected along at least two axes. This was done to ensure that all isostructural indices (see section **1.4** of the introduction of this dissertation) are satisfied in grouping each isostructural series.

'Lazy pulverix', a program to calculate theoretical X-ray and neutron diffraction powder patterns [3], was used to calculate PXRD patterns from atomic

coordinates of the published crystal structures. This program calculates reflection intensities I_{hkl} from the formula $I_{hkl} = mLp(F_{hkl})^2$ where m is the reflection multiplicity, L is the Lorentz factor, p is the polarisation factor, and F is the structure factor. The program 'Lazy pulverix' is included in the 'X-Seed' interface program system for crystal structure solution and refinement [4].

The isostructural indices (Π, ε, A and I_v) were calculated using the programs '*cellcmp*' and '*iso*' supplied by their author, Dr. L. Fábián (Institute of Chemistry, Chemical Research Center of the Hungarian Academy of Sciences, Budapest, Hungary) [5]. The program for I_v calculations is based on the method of Gavezzotti [6] for computation of molecular volumes. The programs read SHELX or PDB files. Symmetry transformations and/or unit cell origin shifts are necessary for structures with arbitrarily sequenced symmetry operations and/or with differently set unit cell origins. All calculations were performed over the entire unit cell to avoid the problem raised by cell dissimilarities. Calculations were done on the CD host only, as the guest molecules often occupied different positions in the pairs compared. Hydrogen atoms were deleted as some hosts were reported without, or with incompletely assigned, hydrogen atoms.

2.2 Cyclodextrin-Drug Inclusion Complexes

2.2.1 Compounds Used

The host compounds (α-, β- and γ-cyclodextrins) were obtained from Cyclolab (Budapest, Hungary) and their water content was confirmed by TG analysis prior to their use. TGA is discussed in section ***2.2.4*** below.

All organic solvents used in the experiments for this dissertation were of the pure analytical grades and were dried with molecular sieves for at least 24 hours prior to usage. Salicylamide (≥ 99 % purity) and aspirin (≥ 99.0 % purity) were

purchased from Sigma (St. Louis, U.S.A.) and Fluka Chemika (Steinheim, Switzerland), respectively, and were used as received.

Sulfasalazine was purchased from Aldrich (Milwaukee, U.S.A.) and PXRD confirmed that it was the monoclinic polymorph. Monoclinic sulfasalazine was therefore used without further purification. The triclinic form of sulfasalazine was prepared by recrystallization of the monoclinic polymorph [7]. Details of the preparation are given in Chapter 4.

The diclofenac sodium salt was purchased from Sigma (Steinheim, Germany) and was used as received. Caesium chloride (99%) was purchased from Aldrich (Johannesburg, South Africa) and potassium chloride (99.5%) was acquired from Laboratory and Scientific Equipment Company (Cape Town, South Africa). Both KCl and CsCl were used as received.

2.2.2 Inclusion Complex Preparation and Crystal Growth

For complexes prepared by the kneading method using a pestle and mortar (see Chapter 1 section ***1.2.3*** for details on this method), the kneaded material was analysed by X-ray powder diffraction while moist.

Inclusion complexes from which single crystals were obtained were prepared by the co-precipitation method (detailed in section ***1.2.3***). Details of the procedures, as well as quantities used, are in Chapter 5.

2.2.3 Hot Stage Microscopy (HSM)

HSM can be used to observe visual physical changes of a compound as it is heated over a given temperature range. The events thus recorded can then be linked to the physicochemical changes such as dehydration, melting and decomposition of the analyte in question.

Crystals were submerged in an inert medium of silicone oil and were placed on a Linkam THMS600 hot stage fitted with a Linkam TP92 temperature control unit and a Nikon SMZ-10 stereoscopic microscope. Images were captured using a real-time Sony Digital Hyper HAD colour video camera and viewed using the Soft Imaging System program, AnalySIS [8]. The opacity, colour change and charring of the crystals were also recorded for interpretation of the physicochemical changes and for comparison with the TGA and DSC results.

2.2.4 Thermogravimetric Analysis (TGA)

Thermogravimetric analysis (TGA) measures the weight loss of a solid while it is subjected to a selected temperature programme under a controlled atmosphere. A Mettler Toledo TGA analyser was employed in this study. A nitrogen purge of 30 ml/min was used to provide an inert atmosphere and an empty platinum pan was used as a reference. About 2 to 6 mg of the CD-drug inclusion complex samples were heated in an open platinum pan from 30°C till decomposition (350°C).

2.2.5 Differential Scanning Calorimetry (DSC)

Differential scanning calorimetry (DSC) measures the enthalpy changes as a result of the loss of guest, or any phase transformation, which occurs on heating a solid sample at a selected temperature programme under a controlled atmosphere. A Perkin Elmer DSC 7 thermal analysis system was used to record DSC traces whose features could be interpreted as thermal dehydration and decomposition of the inclusion complexes by correlation with the information obtained from TG and HSM. Sample sizes of 2 – 5 mg were placed in 50 μl pierced aluminium pans and the nitrogen purge gas was used to provide an inert atmosphere.

2.2.6 *Elemental Analysis (Microanalysis)*

In an elemental analysis (also called microanalysis) experiment, the sample is combusted at about 990°C into CO_2, H_2O, NO_x and SO_2 using oxygen as an oxidising agent. Masses of these oxidation products are then used to calculate the respective amounts of C, H, N and S in the sample. In all cases, C, H and N microanalyses were performed on a Fison EA1108CHNS-O Elemental Analyser. Samples were analysed in duplicate and the analysis was repeated until satisfactory results were obtained. Microanalysis results served to indicate the purity of the sample and to confirm the stoichiometric ratio of CD:drug in the inclusion compounds.

2.2.7 *Karl-Fischer Method*

This method was used to estimate water content in cyclodextrin inclusion complexes. In a Karl-Fischer experiment, I_2 oxidises SO_2, with an equimolar amount of H_2O, in an excess of pyridine, according to the following reaction:

$$C_5H_5N{\bullet}I_2 + C_5H_5N{\bullet}SO_2 + C_5H_5N + H_2O \rightarrow 2C_5H_5N{\bullet}HI + C_5H_5N{\bullet}SO_3 \quad \{Eq.\ 1\}$$

An excess of methanol is then used to react with the pyridine/sulphur trioxide complex as shown below:

$$C_5H_5N{\bullet}SO_3 + CH_3OH \rightarrow C_5H_5N(H)SO_4CH_3 \quad \{Eq.\ 2\}$$

In the absence of the analyte water, the redox reaction {Eq. 1} does not occur. Thus when all the analyte water has been consumed, the reagents in Eq. 1 (without water) are the same as the products. The potentiometric end point of a Karl-Fischer titration experiment therefore is when the reduction of I_2 to HI ceases, or when SO_2 is no longer oxidised to SO_3.

A fully automated Mettler Toledo DL 31 Karl-Fischer potentiometric titrator was used. The Karl-Fischer experiment was used to determine the stoichiometric amount of crystal water in the compounds from which single crystals were obtained.

2.2.8 X-Ray Powder Diffraction (PXRD)

Kneaded samples were placed on X-ray insensitive Mylar film, supplied by Chemplex (Palm City, U.S.A.), while single crystals were crushed and packed in Markröhrchen non-diffracting glass capillaries, supplied by Hilgenberg (Germany), prior to being mounted. Samples were then mounted on a Huber D-83253 Imaging Plate appliance fitted with a Guinier Camera 670, a Huber MC 9300 power supply unit and a Philips X-ray generator. With the exception of the Philips X-ray generator, which was from Holland, the rest of the machine and accessories were from Germany. The generator settings were kept constant at 20 mA and 40 kV while the sample was being bombarded with CuK_{α} radiation (λ = 1.5418 Å). The display and manipulation of the PXRD data thus generated were performed on a desktop computer, which was also linked to the instrument.

Exposure times of 10 – 60 min and multiscans of 10 times were used, and the 2θ range was truncated from 4 to 40°. This technique was very useful in many respects. It was used as initial proof of complex formation by matching the experimental X-ray powder pattern of the newly synthesised complex with that of a known isostructural series. For single crystals, this technique was used in determining the purity of the sample, the completeness of the structure refinement, as well as the stability of the synthesised complex. This was done by careful comparison of the experimental PXRD patterns with the PXRD traces calculated from the refined crystallographic data of the respective complexes.

2.2.9 X-Ray Crystal Structure Data-Collection and Data-Reduction

A single crystal with good extinction qualities, as revealed by a polarising microscope, was selected and cut to a near cubic shape (see Chapter 5 for crystal dimensions). The selected crystal was mounted on a glass fibre and coated with Paratone N oil obtained from Exxon Chemical Co. (TX, U.S.A.) so as to keep the crystal rigidly mounted under the extremely low temperatures

required for data-collection. Preliminary unit cell parameters and crystal system were determined on a Nonius Kappa CCD diffractometer using 1.2 kW graphite-monochromated MoK_{α}-radiation (λ = 0.71069 Å) generated by a Nonius FR590 generator operated at 53 kV and 23 mA.

Crystal X-ray diffraction data were collected on the same apparatus, using the same radiation, with the crystal cooled to 113 K, by a constant stream of nitrogen gas produced by a Cryostream cooler (Oxford Cryosystems, UK), so as to reduce atomic thermal motion. Strategies for data-collections were evaluated using the COLLECT software [9]. Data were collected by the standard phi- and omega- scan techniques and were corrected for Lorentz-polarisation effects. Unit cell refinement and data scaling and reduction were performed using the programs DENZO-SMN and SCALEPACK [10]. The data were collected with direction cosines to address the absorption problem encountered with crystals containing atoms with high scattering powers. The data were then corrected for absorption using the program SADABS [11]. No obvious signs of crystal degradation were observed during the data-collection periods of about 48 hours.

The space group was determined by using the collected intensities and pre-determined cell parameters as inputs to the XPREP program [12]. XPREP was also used to prepare instruction files (*.ins) required by SHELX [13] programs for structure solution and refinement.

2.2.10 Crystal Structure Solution and Refinement

One crystal structure (DKBCD, section 5.4.3) in this dissertation was solved by *ab initio* direct methods using SHELXD [14]. SHELXD is a stand-alone executable used to solve structures containing several hundred independent non-hydrogen atoms in the crystallographic asymmetric unit, larger than those amenable to SHELXS-97 [15]. This program is based on the dual-space iteration strategy, called 'Shake-and-Bake' (meaning simultaneous phase refinement,

Shake, and density modification, *Bake*) [16,17], in which alternations in reciprocal space phase refinements are constrained with imposition of an atomic model in real space [18,19]. The program has two main instruction codes. The **FIND** instruction code, which is used to search for a specified number of atoms in the dual-space cycles, and the peak list optimisation (**PLOP**) instruction code used to specify the number of peaks to start with in each cycle [20]. Both the *.ins* and the *.hkl* files were used as inputs to the SHELXD program.

The other crystal structure reported in this dissertation was solved by the isomorphous replacement (molecular replacement) method using atomic coordinates of the rigid part of a cyclodextrin molecule of an isostructural compound to generate an initial phasing model.

Structural models were refined in SHELXL-97 [21], which was incorporated into the X-SEED program interface [4]. Model refinements were performed using full-matrix least-squares minimization of the function $\Sigma w(F_o^2 - kF_c^2)^2$ (the weighted sum of the squares of the differences between the observed and the calculated intensities). The agreement between the observed (F_o^2) and the calculated (F_c^2) structure factors was monitored by assessing the residual index **R**, defined by R_1 or wR_2:

$$R_1 = \frac{\Sigma \left| |F_o| - |F_c| \right|}{\Sigma |F_o|} \qquad wR_2 = \left[\frac{\Sigma\, w(F_o^2 - F_c^2)^2}{\Sigma\, w(F_o^2)^2} \right]^{1/2}$$

where the weighting scheme $w = \dfrac{1}{\sigma^2 (F_o^2) + (aP)^2 + bP}$

and $P = \dfrac{\max(0, F_o^2) + 2F_c^2}{3}$

The residual index, R_1, is a measure of the agreement between the observed structure factors obtained from the measured reflection intensities and calculated structure factors computed from the model which is being refined. The weighted residual index, wR_2, expresses the agreement between the calculated intensities for the refinement against the observed intensities, where the measured structure factors are weighted according to their reliability. For a satisfactory model, both the R_1 and the wR_2 indices should be low.

The terms ***a*** and ***b*** in the weighting scheme are chosen to yield constant distributions of $w(F_o^2 - F_c^2)^2$ with $\sin\theta$ and $(F_o/F_{max})^{1/2}$. Constants ***a*** and ***b*** were refined while the structural model was being refined and the weighting scheme (***w***) was applied in the final cycles of structure refinement.

SHELXL-97 [21] always refines against F^2, which leads to greater deviations of the Goodness of Fit, **S**, from unity than the refinement against **F**. The Goodness of Fit is given by the expression:

$$S = \left[\frac{\Sigma\, w\,(|F_o^2| - |F_c|^2)^2}{(N - n_p)} \right]^{1/2}$$

where **N** is the number of reflections and n_p is the total number of parameters refined. For a good fit of the model to the measured data, **S** should be close to unity and the overdetermination ratio should be of the order $N / n_p \approx 10$.

A measure of the agreement between all equivalent reflections is given by R_{int}:

$$R_{int} = \frac{\Sigma\, |F_o^2 - F_{o\,mean}^2|}{\Sigma\, |F_o^2|}$$

2.2.11 Additional Resources

In addition to other programs already mentioned, the following computer packages were also used in the analysis and presentation of the crystal structures:

- **PLATON for Windows** [22], which was run on **Platon for Windows Taskbar (PWT)** [23], was used to calculate molecular geometric parameters and non-bonded interactions together with their associated standard deviations (e.s.d.s.). This program was also used to expand the contents of the orthorgonalised unit cells in space group P1 for I_v calculations.
- **POV-Ray** [24] and **Weblab ViewerPro** [25] were used to create molecular drawings and crystal packing diagrams.
- **CS ChemDraw Pro™** [26] was used for molecule line drawing diagrams.
- **ORTEP-3** [27] was used to obtain the signs of the tilt angles (τ_1 and τ_2) by viewing the cyclodextrin molecule perpendicular to the O_4 atoms with the least deviation to the mean O_4 plane, and observing the tilt of each glucose monomer with respect to the CD cavity.
- **LAYER** [28] was used to examine simulated graphic representations of the reciprocal lattice layers in order to confirm Laue symmetries and reflection conditions.

Legacy CSD Crystallographic format (FDAT) files for all cyclodextrin compounds and complexes obtained from the Cambridge Structural Database system can be found on a compact disc attached to the inside back cover of this dissertation. Also appended, on the same disc, are crystallographic information files for each of the solved structures reported in Chapter 5 of this dissertation. The file names, types and the information that they contain are listed in Table 2.1 below.

Table 2.1 – A list of crystallographic data files found in the disc appended to the inside back cover of this dissertation.

File Extension	Contents
acd.dat	FDAT file containing all compounds and complexes of the natural α-CD form as found in the CSD
acd_d.dat	FDAT file with all complexes and compounds of derivatised α-CDs as captured from the CSD
bcd.dat	FDAT file containing all compounds and complexes of the natural β-CD form as obtained from the CSD
bcd_d.dat	FDAT file with all complexes and compounds of derivatised β-CDs obtained from the CSD
gcd.dat	FDAT file with all compounds and complexes of the natural γ-CD form as found in the CSD
gcd+d.dat	FDAT file containing all complexes and compounds of the natural γ-CD form and of γ-CD derivatives
.hkl	The collected and reduced crystal data containing intensities of the captured reflections
.ins	SHELX instruction file with refinement information
.res	SHELX coordinate file used containing refinement history
.xl	SHELX output file with refined atomic coordinates and temperature factors, including data on the tilt of each glucose monomer with respect to mean O_4 plane of a CD molecule
.fcf	List of F_o^2, F_c^2 values following final structure refinement
.cif	Crystallographic information file used as input to PLATON
.lis	PLATON output file with atomic coordinates and geometric parameters such as bond distances, bond angles, torsion angles, potential hydrogen bonds and intermolecular contact distances
.htm	Summary of diffractometric data-collection parameters

2.3 References

1. *Cambridge Structural Database and Cambridge Structural Database System*, **Version 5.26**, November 2004, Cambridge Crystallographic Data Centre, University Chemical Laboratory, 12 Union Road, Cambridge, England.
2. M. R. Caira, *Rev. Roum. Chim.*, 2001, **46**, 371 – 386.
3. K. Yvon, W. Jeitschko and E. J. Parthé, *J. Appl. Crystallogr.*, 1977, **10**, 73– 74.
4. L. J. Barbour, *X-SEED – A graphical interface to SHELX*, University of Missouri, Columbia, U.S.A., 1999.
5. L. Fábián and A. Kálmán, *Acta Crystallogr.*, 1999, **B55**, 1099 – 1108.
6. A. Gavezzotti, *J. Am. Chem. Soc.*, 1983, **105**, 5220 – 5225.
7. L. A. Filip, M. R. Caira, S. I. Fărcaş and M. T. Bojiță, *Acta Crystallogr.*, 2001, **C57**, 435 – 436.
8. *Analysis®*, **3.1** (Build 496), Soft Imaging System GmbH, © 1986 – 2000.
9. *COLLECT – Data-collection Software*, Nonius, Delft, The Netherlands, 1998.
10. Z. Otwinowski and W. Minor, *Methods Enzymol.*, **vol 276**, C. W. Carter and R.M. Sweet (eds.), Academic Press, New York, 1997, 307 – 326.
11. G. Sheldrick, *SADABS – Bruker/ Siemens area detector absorption and other corrections*, **V2.03**.
12. *XPREP – Data Preparation and Reciprocal Space Exploration*, **Version 5.1/NT**, Bruker Analytical X-ray Systems, 1997.
13. G. M. Sheldrick, *SHELX in Comput. Crystallogr.*, 1978, 34 – 42.
14. G. M. Sheldrick, *Direct Methods for Solving Macromolecular Structures*, Kluwer Academic Publishers, Dordrecht, 1998.
15. G. M. Sheldrick, *SHELXS-97 – A Program for Crystal Structure Solution*, Institüt für Anorganische Chemie der Universität, Tammanstrasse 4, D-3400 Göttingen, Germany, 1997.

16. R. Miller, G. T. DeTitta, R. Jones, D. A. Langs, C.M. Weeks and H. A. Hauptman, *Science*, 1993, **259**, 1430 – 1433.
17. C. M. Weeks and R. Miller, *Acta Crystallogr.*, 1999, **D55**, 492 – 500.
18. R. Miller and C. M. Weeks, *Mathematical and Physical Sciences, Series C,* **507**-*Direct Methods for Solving Macromolecular Structures*, 1998, 389– 400.
19. G. M. Sheldrick and T. R. Schneider, *Methods Macromol. Crystallogr.*, 2001, **325**, 72 – 81.
20. G. M. Sheldrick and R. O. Gould, *Acta Crystallogr.* 1995, **B51**, 423 – 431.
21. G. M. Sheldrick and T. R. Schneider, *Macromol. Crystallogr.*, 1997, **B277**, 319 – 343.
22. A. L. Spek, PLATON – A Multipurpose Crystallographic Tool, **Version 20604**, © 1980 – 2004 (A. L. Spek, *J. Appl. Crystallogr.*, 2003, **36**, 7-13).
23. Platon for Windows Taskbar, **version 1.07**, © University of Glasgow, 2003.
24. *Pov-Ray for Windows*, **Version 3.1e**, The persistence of vision development team, © 1991 – 1999.
25. *Weblab ViewerPro*, **Version 3.5**, Molecular Simulations Inc., San Diego, CA, 1999.
26. S. Rubenstein, *CS ChemDraw Pro*™, **Version 4.0.1**, CambridgeSoft Corporation, Massachusetts, © 1985 – 1997.
27. L. J. Farrugia, *ORTEP-3 for Windows*, **Version 1.076**, University of Glasgow, © 1997 – 2002, (L. J. Farrugia, *J. Appl. Crystallogr.*, 1997, **30**, 565).
28. L. J. Barbour, *J. Appl. Crystallogr.*, 1999, **32**, 351 – 352.

CHAPTER 3: AN UPDATE ON THE ISOSTRUCTURALITY OF CYCLODEXTRIN INCLUSION COMPOUNDS

3.1 Introduction

The isostructural nature of crystalline compounds or molecules has prompted certain crystallographers to examine this phenomenon more critically and with a view to quantifying it. Thus Kálmán and his co-workers have been involved in logically reasoning out the conditions required for two or more compounds to be described as isostructural. (A detailed discussion with references was given in Chapter 1, sections 1.3 – 1.6). Amongst other outputs of their research, they derived clear and unambiguous definitions of isostructurality, its descriptors, as well as numerical indices with which to quantify the extent of isostructurality. Caira, on the other hand, has introduced the concept of isostructurality into cyclodextrin research and has pioneered the isostructurality method of PXRD analysis [1,2] (referred to as the IsoPXRD method throughout this dissertation). This method is not only used extensively by members of the Supramolecular Chemistry Research Unit at the University of Cape Town [3-5], but the concept has also been applied by other authors involved in cyclodextrin research [6]. The method has not been updated since 2001 [2] and a number of crystal structures have been deposited in the CSD [7] since then. This Chapter is dedicated to updating and reporting the findings on the IsoPXRD method with respect to cyclodextrin hosts and their inclusion complexes.

3.2 The CSD Search

Our search of the CSD, which targeted CD complexes with organic guests only, including parent cyclodextrins, and whose three-dimensional coordinates have been determined resulted in 94 α-CD compounds, 59 of which were complexes and parent compounds of native α-CD (with the rest being the derivatised α-CD species). Similarly 178 hits were obtained for the β-CD compounds, 96 of which were parents and inclusion complexes of the native β-CD form (the rest were the

unusually derivatised β-CDs plus parents and inclusion complexes of the usually derivatised β-cyclodextrins). A search for γ-CD complexes resulted in 17 hits of which 9 were complexes and parent compounds of the native γ-CD form. After applying the selection criteria described in section **2.1**, the structures were grouped into isostructural series and are discussed in the subsequent sections (sections **3.3** to **3.7**).

3.3 Isostructurality Amongst Parent Cyclodextrins

Since the last update of the IsoPXRD method [2], we have captured 12 new crystal forms of parent cyclodextrins. Two of these are parent CDs of the native α-CD type, two are parents of α-CD derivatives, six are parents of β-CD derivatives and two are the trimethylated γ-CD parents. Crystallographic data of the newly captured parent CDs, together with the existing ones, are presented in Table 3.1. The corresponding PXRD traces are in Figure 3.1.

The captured data for parent cyclodextrins exclude unusually derivatised parent CDs in which a bulky substituent has been covalently attached to one or more of the exposed O_2, O_3 and/or O_6 atoms of a cyclodextrin molecule (e.g the compounds with CSD refcodes BEVKAO, CURJUY, FEDKUU, KAYLAX, KOYYUS, LEDROB, LEDRUH, MINKUQ and HAGMOS01) including 2,3,6-Tri-O-propanoyl-β-CD (ICUFIV) and 2,3,6-Tri-O-butanoyl-β-CD (ICUFOB). Some of these unusual CDs are found to be isostructural with each other and thus constitute series of their own. Consequently, they appear in section **3.6** as unusually derivatised β-CDs (Table 3.8 and Figure 3.11).

Table 3.1 – Crystal data for all parent cyclodextrins. The data for new parent CDs are highlighted in yellow. The host terminology is explained on page iii.

Host: Space Group	mol H_2O / mol CD	a (Å)	b (Å)	c (Å)	α (°)	β (°)	γ (°)	REFCODE
α-CD I : $P2_12_12_1$	6 H_2O	14.858	34.038	9.529	90	90	90	CHXAMH02
α-CD II : $P2_12_12_1$	6 H_2O	13.700	29.350	11.920	90	90	90	CHXAMH03
α-CD III : $P2_12_12_1$	7.57 H_2O	14.356	37.538	9.400	90	90	90	BANXUJ
α-CD IV : $P2_12_12_1$	11 H_2O	13.839	15.398	24.207	90	90	90	GOQZUH
α-CD V : $P6_3$	21 H_2O	17.241	17.241	13.323	90	90	120	RIRZUN
β-CD : $P2_1$	9.35 H_2O	20.857	10.158	15.140	90	110.94	90	POBRON
γ-CD : $P2_1$	14 H_2O	16.847	11.098	20.271	90	104.97	90	CIWMIE10
DIMEA : $P2_12_12_1$	----	15.239	17.089	22.848	90	90	90	ROQVUO
TRIMEA: $P2_12_12_1$	----	15.424	18.167	23.128	90	90	90	TEVCEC
RAMEA: $P2_12_12_1$	6.7 H_2O	13.957	29.162	12.965	90	90	90	PEZKAG
AcetylA: $P2_12_12$	2 H_2O	15.563	20.667	13.393	90	90	90	HEHQAM
MONOMEB: $P2_12_12_1$	12 H_2O	12.663	17.679	31.271	90	90	90	IQOZIX
DIMEB I : $P2_12_12_1$	1.08 H_2O	13.328	17.410	29.760	90	90	90	QIYKEO
DIMEB II : $P2_12_12_1$	15 H_2O	14.163	20.828	29.261	90	90	90	BOYFOK04
DIMEB III : $P2_1$	2 H_2O	15.242	10.639	23.324	90	101.80	90	CEQCUW
TRIMEB I : $P2_12_12_1$	1 H_2O	14.823	19.382	26.534	90	90	90	HEZWAK01
TRIMEB II : $P2_12_12_1$	3 H_2O	16.205	16.287	30.099	90	90	90	Form 2 *
TRIMEB III : $P2_12_12_1$	-----	15.951	16.577	28.941	90	90	90	Form 3 *
MONOBrB : $P2_1$	1 H_2O	15.714	15.917	30.102	90	90.55	90	HAXMUO
TRIMEG I : $P2_1$	9.3 H_2O	29.872	18.018	33.170	90	98.15	90	BEBJAT
TRIMEG II : $P2_12_12_1$	2.5 H_2O	16.730	16.875	32.172	90	90	90	GIWMAA
TRIMEG III: $P2_12_12_1$	4.5 H_2O	10.788	29.058	32.291	90	90	90	XERSIW

* The compounds do not have CSD refcodes as they had not been captured on the CSD at the time the search was conducted. The nomenclature, form 2 and form 3 used here, is the same as that used in the publication describing these compounds [8].

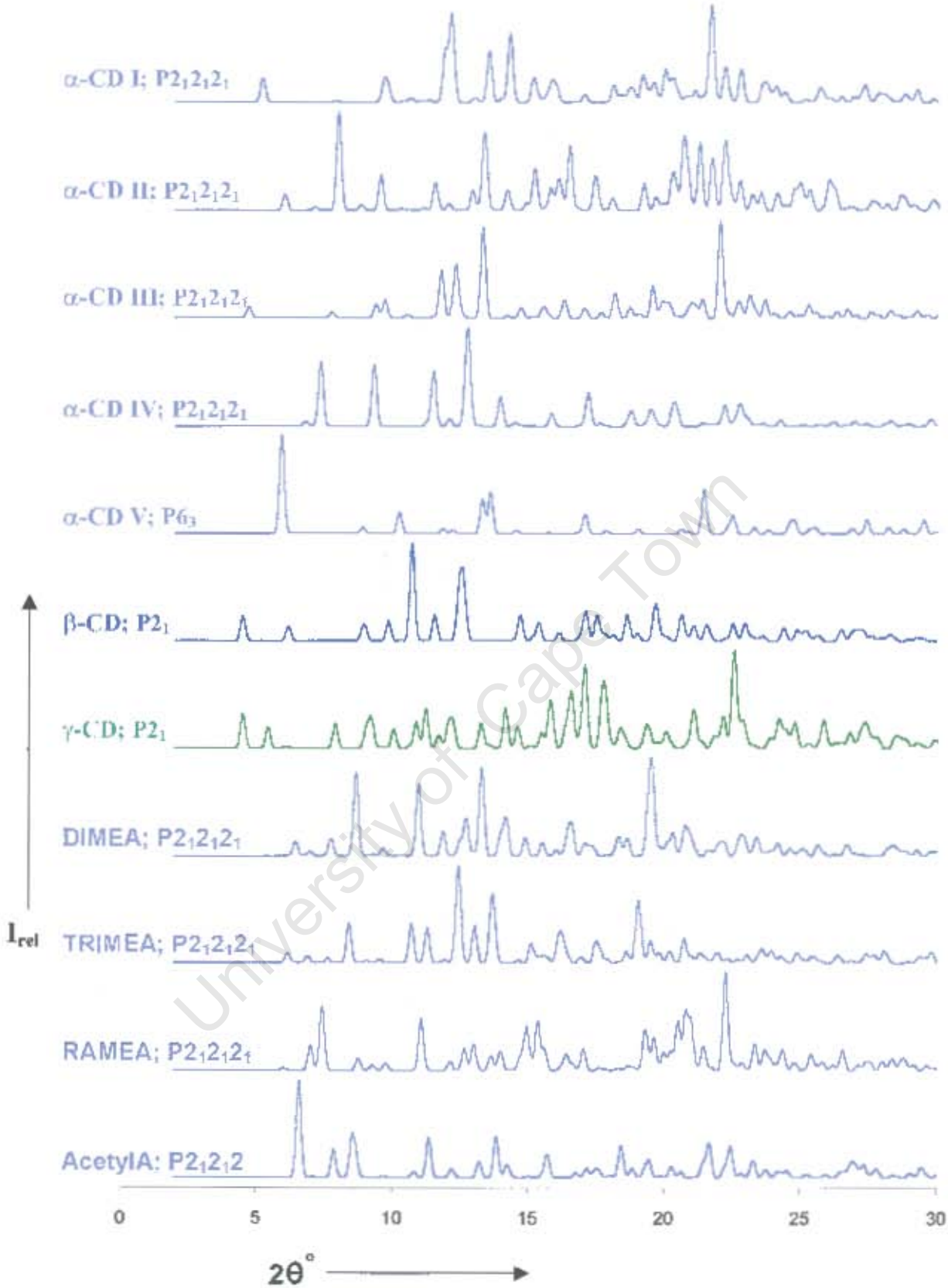

(PXRD traces continue on the next page ...)

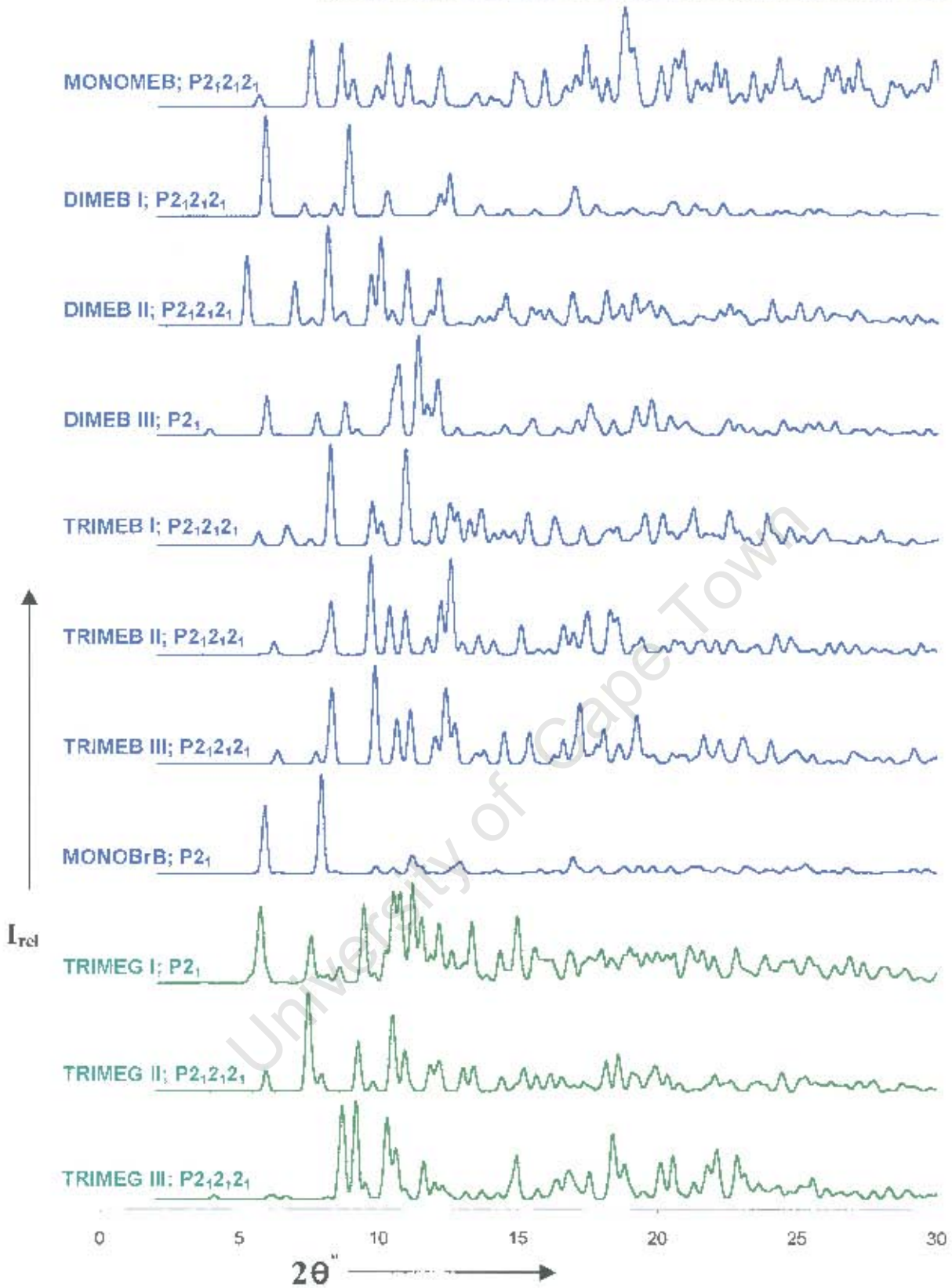

Figure 3.1 – Computed PXRD patterns of all parent cyclodextrins. α-CDs and their derivatives are in pale blue, β-CDs in blue and γ-CDs in green.

Almost all parent cyclodextrins listed in Table 3.1 have the cage-type packing arrangements of CD monomers. This is not surprising as water molecules are small guests that can be accommodated in monomeric cage packing arrangements. Exceptions are α-CD IV, α-CD V, MONOBrB and TRIMEG III. The parents α-CD IV, α-CD V have the layer-type packing arrangements while TRIMEG III crystallizes in channels with CD molecules arranged in a head-to-tail fashion along the *a*-axis. The MONOBrB parent, HAXMUO, is the only dimeric parent CD compound we have identified so far. This dimeric β-CD parent, with bromine atoms attached to all its O_6 atoms of the primary CD side of each CD ring, has a packing arrangement intermediate between the screw channel (**SC**) and the chessboard (**CB**) packing modes of dimeric β-CD complexes (sections ***1.2.4*** and **3.5** give a description of **SC** and **CB** packing modes).

The monoclinic TRIMEG I parent CD, BEBJAT, has four cyclodextrin molecules in its asymmetric unit. All other parent cyclodextrins have one CD molecule in the crystallographic asymmetric unit, except for the dimeric MONOBrB parent compound, which has two.

3.3.1 Isostructurality of parent α-CD species

As has been noted before [2], α-CD I and α-CD III demonstrate some degree of isostructurality. These two α-CD parents belong to the same crystal system (orthorhombic), and have similar unit cell parameters and identical space groups implying that they should have similar packing arrangements. The packing arrangements of cyclodextrin molecules in these two α-CD parents are both of the herringbone cage type, with slightly different orientations of their CD rings so that their crystal structures are non-superimposable (Figure 3.2). In addition, these compounds display a significant difference of 3.5 Å in one of their unit cell lengths, the *b*-axis (Table 3.1), which is enough to result in the two crystals diffracting at different angular positions so that the PXRD diffractograms of these compounds register as distinct patterns, rendering the two crystal structures non-isostructural.

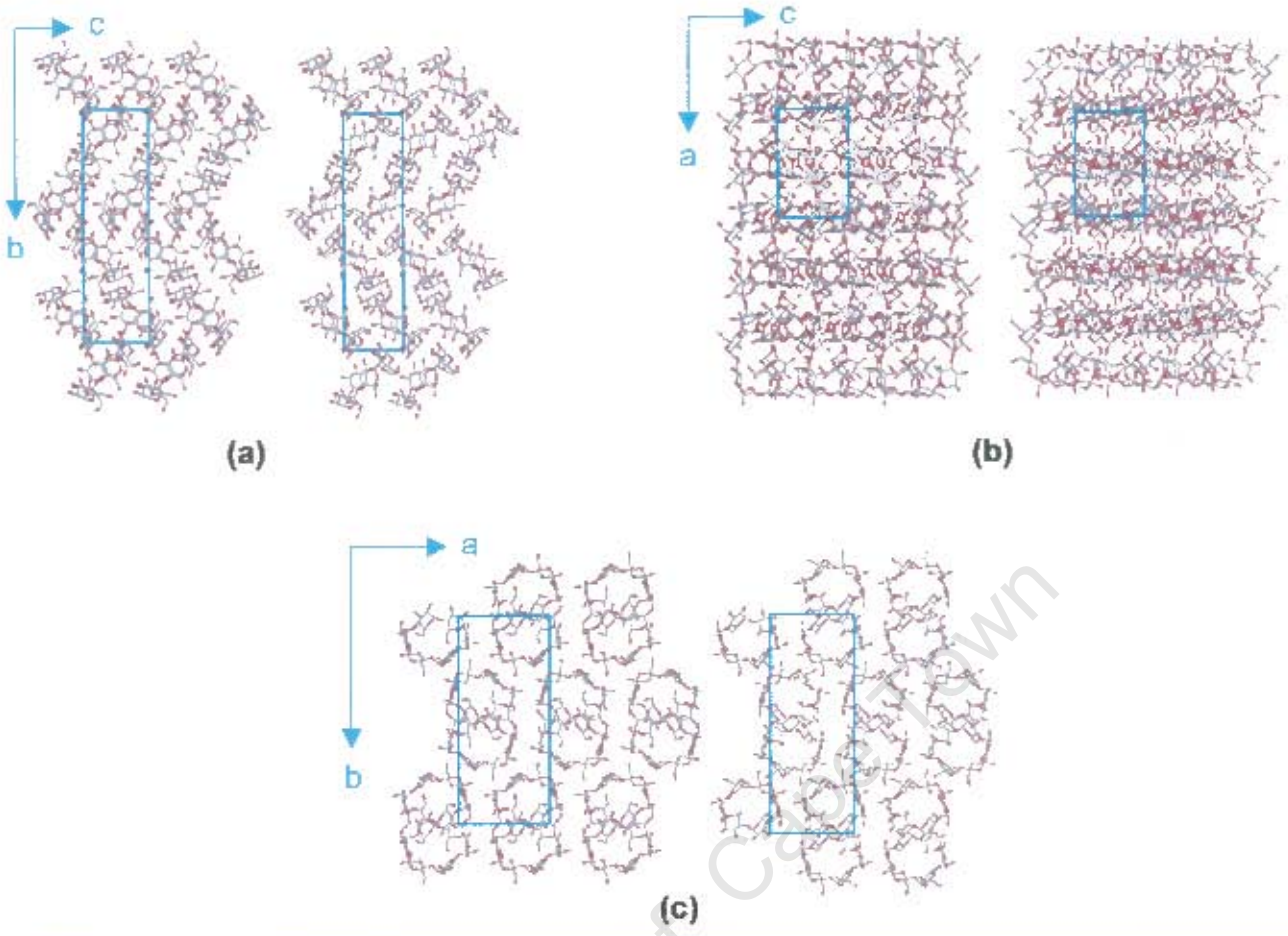

Figure 3.2 – Comparison of crystal packing diagrams of α-CD I (on the left of each comparison pair) and α-CD III (on the right of each pair) forms. Projections are made down the *a*-axis **(a)**, down the *b*-axis **(b)**, and down the *c*-axis **(c)**.

We further calculated Π (the unit cell similarity index) and the I_v (volumetric measure of isostructurality) values of these two α-CD forms to be 0.0491 and 58.6 % respectively (Table 3.2). The reader is referred to Chapter 1 (section 1.4) for definitions of Π and I_v. These values further emphasise that the two forms are not strictly isostructural. For highly isostructural compounds, we have found Π values between 0.000 and 0.005 and I_v values above 90 % (Table 3.5). We also mentioned in Chapter 1 that although Π should be practically zero for highly isostructural compounds, Π values of 0.001 – 0.03 are typical. The I_v value of 58.6 %, which is found between α-CD I and α-CD III is not surprising as the two structures have a very close similarity in their packing arrangements (Figure 3.2).

The relatively high value of **A** (= 1.664) in Table 3.2 implies that there exist differences in the cell shape distortions of the two structures.

Table 3.2 – Isostructurality indices calculated for closely isostructural α-CD parent compounds and those displaying a lower level of isostructurality

Comparison	Π	ε	A	εA	I_v (%)	I_{max} (%)
α-CD I and α-CD III	0.049	0.017	1.664	0.028	58.6	99.9
α-CD II and RAMEA	0.021	0.033	0.547	0.018	77.6	96.1
DIMEA and TRIMEA	0.028	0.029	0.380	0.011	22.7	95.4

Similar to the above example of α-CD I and α-CD III, α-CD II and RAMEA (6A,6C,6E-tri-O-methylcyclohexaamylose) are isostructural to some extent. Several peaks in the X-ray powder diffractograms α-CD II and RAMEA appear at identical positions (Figure 3.1), and there is apparently little difference in their crystal packing diagrams as shown in Figure 3.3. A clue suggesting that the two parent cyclodextrins might be isostructural to some extent is seen on the close matching of their unit cell parameters, with the maximum difference between the corresponding cell dimensions (*c* in this case) being only 1.05 Å (Table 3.1). The calculated isostructural indices of α-CD II and RAMEA in Table 3.2 reflect these findings. The Π value is within the acceptable range and the I_v value indicates that the two α-CD forms are isostructural.

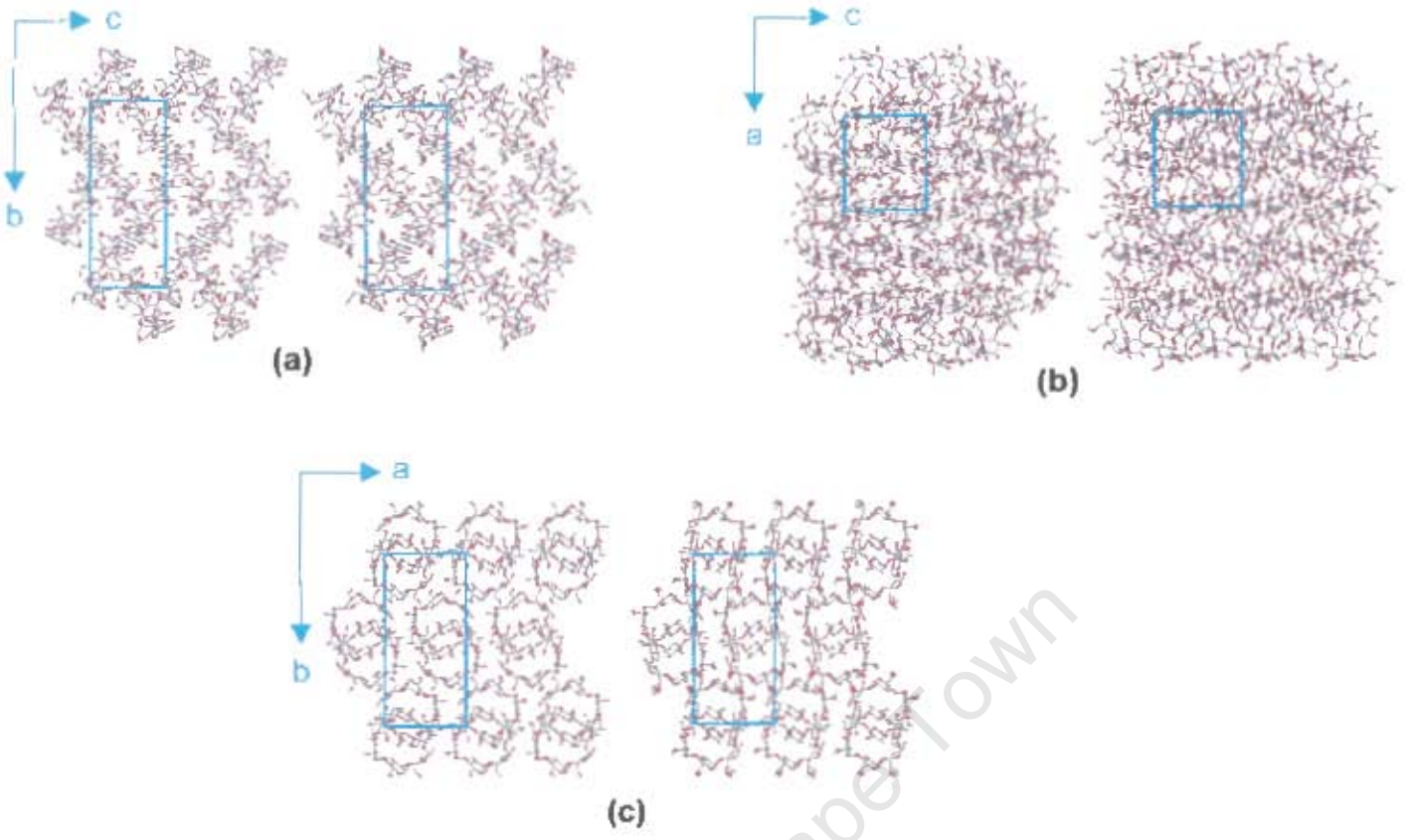

Figure 3.3 – Herringbone cage packing arrangement in α-CD II and RAMEA. α-CD II is on the left of each comparison pair while RAMEA is on the right. Projections are made down the *a*-axis **(a)**, down the *b*-axis **(b)** and down the *c*-axis **(c)**.

The anhydrous parents of α-CD derivatives, DIMEA and TRIMEA exhibit some degree of isostructurality. Their unit cell parameters are similar and they share a common space group as shown in Table 3.1. However, careful examination of their packing diagrams shows that the CD molecules are not arranged in the same way within the unit cells of these two crystal forms. Although they both resemble the cage-type packing arrangement, cyclodextrin molecules occupy different positions (i.e have distinctly different atomic coordinates) and are orientated differently within their respective unit cells. Thus a very low I_v value is obtained on comparing DIMEA and TRIMEA (Table 3.2). PXRD traces of the two compounds show a high resemblance, but the PXRD pattern of TRIMEA is shifted to lower angular positions compared to that of DIMEA since the former

parent CD compound has a larger unit cell volume than the latter. Because DIMEA and TRIMEA have similar unit cell parameters, the indices Π and **εA** in Table 3.2 are low.

3.3.2 Isostructurality of parent β-CD species

In parent β-CD compounds, TRIMEB II and TRIMEB III are isostructural. They have nearly identical unit cell parameters and they share a common space group. The crystal packing diagrams of TRIMEB II and TRIMEB III are superimposable down all three orthogonal axes. PXRD traces of the two matched very well, and more precisely so, at low 2θ values (Figure 3.1). At high 2θ values, the corresponding peaks of TRIMEB II are found to be shifted slightly (by *ca* 1°) to lower 2θ values relative to TRIMEB III, in keeping with the larger unit cell volume of the hydrated species. The two structures have been reported as isostructural [8].

Regarding the other β-CD parent derivatives, there is some similarity in the unit cell parameters of the species belonging to the orthorhombic space group $P2_12_12_1$. This unit cell similarity exists amongst dimethylated CD derivatives, amongst trimethylated CD derivatives and between each, including the monomethylated β-CD parent. However, these compounds display distinct PXRD traces (Figure 3.1).

To investigate this further, crystal packing diagrams of these compounds were compared. The arrangement of cyclodextrin molecules is found to be different, especially for CD derivatives with relatively large differences in their unit cell parameters. For brevity, only one case is illustrated here (Figure 3.4). The chosen example is that of a non-isostructural pair that has the closest match of the unit cell parameters, with the maximum difference between the corresponding cell dimensions (*c* in this case) being 1.51 Å. Both MONOMEB and DIMEB I parent CD compounds have the cage type packing arrangement.

Although the complete disorder of two adjacent glucose monomers in DIMEB I makes the comparison of the projected crystal packing diagrams difficult, the CD molecules were found to be orientated differently with respect to each case (Figure 3.4(a)).

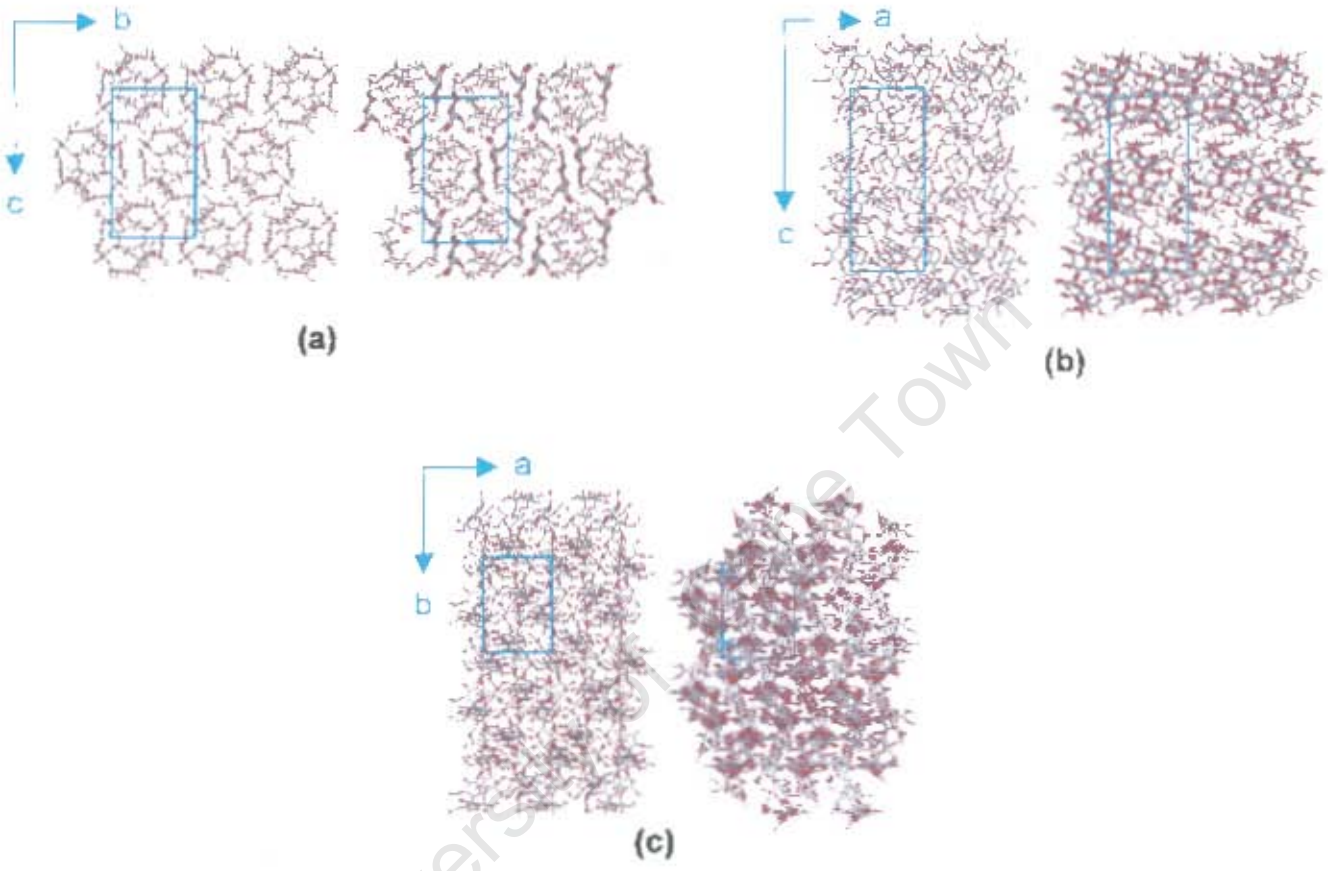

Figure 3.4 – Projections of crystal packing diagrams of MONOMEB and DIMEB I. MONOMEB is on the left of each comparison pair while DIMEB I is on the right. Projections are made down the *a*-axis **(a)**, down the *b*-axis **(b)** and down the *c*-axis **(c)**.

A simple translation, or the introduction of an allowed symmetry operation, does not result in these two structures being superimposable. The herringbone 'tilt' of the cyclodextrin molecules in the packed crystal structures of the two is different (apparent in Figures 3.4(b) and 3.4(c)).

3.3.3 *Isostructurality of parent γ-CD species*

The four γ-CD parents are not isostructural with each other as they have dissimilar unit cell parameters, display distinct PXRD traces and have different crystal packing diagrams.

3.4 Isostructurality in α-CD Inclusion Complexes and in Complexes of the Methylated α-CD Derivatives

Organic inclusion complexes of α-CD and α-CD derivatives were searched as described in Chapter 2. After data reduction (i.e. after the elimination of re-determinations and the exclusion of structures with an R factor exceeding 0.15), the complexes were then grouped into isostructural classes, as described in Chapters 1 and 2, from which average PXRD patterns were calculated. Crystal data for isostructural series of compounds of the α-CD type are listed in Table 3.3 and the corresponding averaged X-ray powder diffractograms are shown in Figure 3.5.

We note that the existing isostructural series have increased in number compared to the last survey [2]. Additional isostructural series were also identified during this update. To accommodate these changes we have introduced a more flexible numbering scheme in which an isostructural class of a native α-CD complex is designated **A'x'** (where 'x' is the series number) while an isostructural class of complexes of a derivatised α-CD is designated **AD'x'** (where 'x' is the isostructural series number). In this way, newly identified CD complexes comprising a class of their own can be easily incorporated into the database by simply incrementing **x** by **1** for each new entry, in either the **Ax** or the **ADx** class.

Table 3.3 – Crystal data for α-CD complexes and for complexes of methylated α-CDs, categorised into isostructural series/ classes. Series **AD1** comprises complexes of the DIMEA exclusively while series **AD2** comprises complexes of the TRIMEA only. The data for new isostructural series are highlighted in yellow.

Series number	Guest	a (Å)	b (Å)	c (Å)	α (°)	β (°)	γ (°)	REFCODE
A1 : $P2_12_12_1$	Pyrrole	9.404	14.294	37.263	90	90	90	QOHMEF
	Acetonitrile	9.479	14.323	37.397	90	90	90	GEVTOQ
	Water	**9.400**	**14.356**	**37.538**	**90**	**90**	**90**	**BANXUJ**
	Methanol	9.465	14.339	37.365	90	90	90	CDEXME10
	Nitromethane	9.452	14.299	37.380	90	90	90	GULTUC
A2 : $P2_12_12$	Sodium 1-propanesulfonate	21.608	16.700	8.302	90	90	90	ACDPRS
	Potassium γ-aminobutyrate	21.861	16.624	8.279	90	90	90	CDKABA
	Potassium acetate	21.890	16.540	8.300	90	90	90	CHAMPA
	Potassium methyl orange	22.120	16.419	8.292	90	90	90	CDXKOM
	Sodium methyl orange	22.099	16.359	8.296	90	90	90	CDXSOM
	Sodium benzenesulfonate	21.832	16.529	8.356	90	90	90	CDXBZS
	2,5-Dihydroxybenzoic acid	21.939	16.786	8.273	90	90	90	WIZQEB
	3,4-Ethylenedioxythiophene	21.794	16.751	8.351	90	90	90	QOHMIJ
	Benzyl alcohol	22.189	16.602	8.256	90	90	90	WILJAC
	m-Nitrophenol	22.231	16.865	8.152	90	90	90	ACDMNP
A3 : $P2_1$	Benzaldehyde	7.932	13.500	24.704	90	90.85	90	BAJJAX
	Hydroquinone	7.909	13.505	24.706	90	90.76	90	PUPTEZ
	p-Cresol	7.927	13.568	24.540	90	90.41	90	WEXLEQ
	4-Fluorophenol	7.845	13.587	24.557	90	91.75	90	JUMYOF
	2-Fluorophenol	7.842	13.615	24.550	90	92.27	90	JUMYUL
A4 : $P2_12_12_1$	*p*-Hydroxybenzoic acid	13.356	15.342	24.896	90	90	90	ACDHBA
	2-Fluoro-4-nitrophenol	13.431	15.299	24.780	90	90	90	ZEJDEX
	p-Nitrophenol	13.455	15.296	24.740	90	90	90	ACDPNP
	Water	**13.839**	**15.398**	**24.209**	**90**	**90**	**90**	**GOQZUH**
	p-Iodophenol	13.477	15.373	24.573	90	90	90	CHAIPL
	2-Pyrrolidone	13.852	15.373	24.353	90	90	90	ACDPRO
	N,N-dimethylformamide	13.750	15.318	24.544	90	90	90	ACDMFM
	p-Iodoaniline	13.681	15.475	24.569	90	90	90	CDEXIA01
	4-Chlorophenol	13.447	15.299	24.795	90	90	90	WEXKOZ
	p-Bromophenol	13.456	15.317	24.733	90	90	90	MESYEO
A5 : P1	*n*-Butylisothiocyanate	13.830	13.880	15.720	93.06	91.72	119.6	XIGBOE
	Acetone	13.852	13.878	15.719	93.01	91.98	119.3	ZASYOH
AD1: $P2_1$	Propan-1-ol	14.136	10.680	21.479	90	106.0	90	KAFGAZ10
	Acetone	14.172	10.707	21.267	90	106.1	90	ROQVOI
AD2: $P2_1$	Benzaldehyde	11.604	23.832	13.593	90	106.1	90	BOHWUQ
	Iodoacetic acid	11.590	23.285	13.901	90	107.0	90	BUPDIZ
	(R)-Mandelic acid	11.624	23.739	13.786	90	106.6	90	CECEMEC10
	(R)-1-Phenylethanol	11.604	23.669	13.824	90	106.7	90	JEJWOK
	(S)-1-Phenylethanol	11.586	23.641	13.762	90	106.5	90	JEJXAX

†For brevity of the data presented here, water has been omitted as a guest molecule except for parent CD complexes shown in bold.

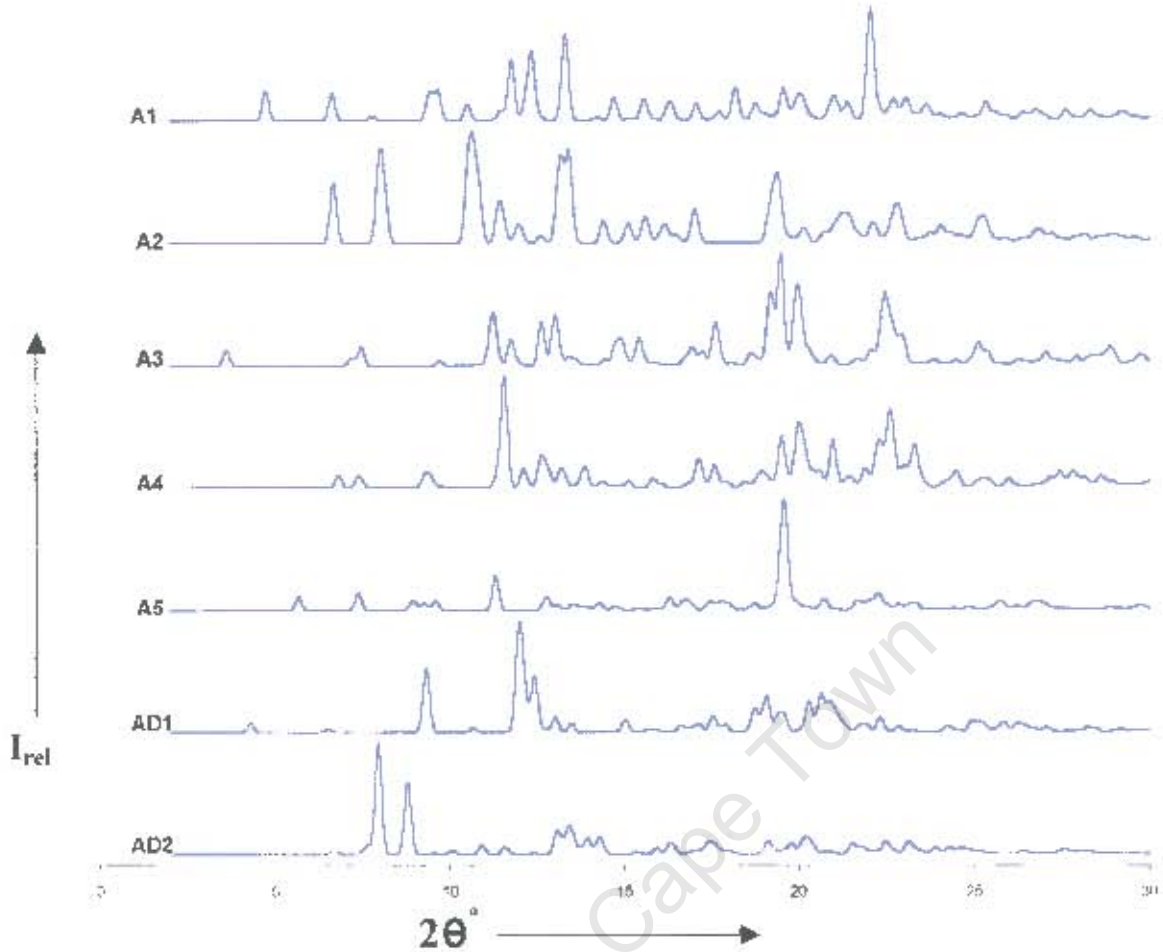

Figure 3.5 – Average computed PXRD reference patterns of isostructural organic inclusion complexes of α-cyclodextrins. The diffractograms shown here are the average patterns for each isostructural series.

As the guest is the only chemically different entity within each class, the extent of isostructurality within each series was evaluated with respect to the guest type. Thus, as shown in Table 3.3, α-CD inclusion complexes with water only as guest molecules have been found to be isostructural not only with α-CD complexes of small organic guest molecules (series **A1**) as previously found [2], but interestingly also with α-CD complexes containing predominantly phenolic guests (series **A4**). As the main requirement for two or more compounds to be isostructural is that they should have very similar arrangements of their unit cell contents, we report here also the packing arrangements in each series.

As usually found for α-CD complexes of small organic guest molecules, series **A1** has a cage-type packing arrangement. Organic salt inclusion complexes comprise series **A2** with a head-to-tail channel-type packing arrangement. The preference of organic salt inclusion complexes to form channels or channel-like structures has been noted (Chapter 1).

Complexes of series **A3** also have a head-to-tail channel packing arrangement. The channels in series **A2** are down the *c*-axis and CD molecules approximate the brick arrangement when crystals are viewed down either the *a*- or the *b*-axis. In series **A3**, channels are down the *a*-axis and CD molecules approximate the layer type when crystals are viewed down the *b*- or the *c*-axis. Series **A3** and **A4**, which are not isostructural with each other, are dominated by the phenolic guest compounds and it is interesting to note that *p*-fluorophenol and *p*-cresol fall under series **A3** while other *p*-halophenols are under series **A4**. Series **A4** has a layer-type packing arrangement with CD molecules forming layers on the *ac*-plane.

A new, additional series that is not isostructural with any of the existing classes, series **A5**, has been discovered in this survey. This series was generated as the compound XIGBOE, which appeared after the last IsoPXRD update, has been found to be isostructural with the known complex ZASYOH. Of the natural α-CD complexes in Table 3.3 and Figure 3.5, series **A5** is the only one in which CD molecules are dimeric. The CD dimers in series **A5** pack in infinite head-to-head channels parallel to the *c*-axis, with continuous layers cutting through the *a*- and *b*-axes. The guests are of small but different molecular sizes.

With regard to the O-methylated CD derivatives, series **AD1** comprises organic inclusion complexes of the host DIMEA exclusively while series **AD2** comprises organic inclusion complexes of the host TRIMEA only. Complexes of series **AD1** arrange in monomeric cage-type packing and contain small organic guest molecules while complexes of series **AD2** are dominated by the monosubstituted

benzenes as guest molecules and pack in monomeric head-to-tail channels parallel to *a*.

We note that the two recently reported [2]rotaxanes of α-CD (as the rotor) and stilbene derivatives (as the axle), with 2,4,6-trinitrophenyl substituents on both ends of the axle as the capping groups [9], display a limited degree of isostructurality. Their PXRD patterns are almost indistinguishable from each other, as shown in Figure 3.6, and they both have a cage type packing arrangement. The two complexes have superimposable crystal stackings down both the *a*- and the *b*-axes, but the relatively large difference in their monoclinic β-angle (Table 3.4) results in the crystal stacking along the *c*-axis being different in the two structures. Although both complexes are monomeric, INUPEM has two complex units in its asymmetric unit while INUPAI has one such unit, resulting in the *c*-axis of INUPEM being double that of INUPAI. Since these two complexes are not completely isostructural, and thus cannot comprise a series, their diffractograms were not averaged.

Table 3.4 – Crystal data of some α-CD complexes demonstrating a high degree of isostructurality and those exhibiting a lower level of isostructurality.

REFCODE: Sp Grp	Guest†	a (Å)	b (Å)	c (Å)	α (°)	β (°)	γ (°)
INUPAI : $P2_1$	[2]-[(E)-4,4'-bis(2,4,6-trinitrophenylamino)-3,3'-dimethoxystilbene]	13.427	17.813	18.448	90	107	90
INUPEM : $P2_1$	[2]-[(E)-4,4'-bis(2,4,6-trinitrophenylamino)stilbene], Methanol	13.429	17.694	35.770	90	95.1	90
QOYLEV : $P2_12_12_1$	(R)-1,7-dioxaspiro[5.5]undecane	23.450	14.636	21.637	90	90	90
RACVIA01: $C222_1$	(R)-(-)-1,7-dioxaspiro[5.5]undecane	24.002	14.812	21.792	90	90	90

†Again, water has been omitted as a guest molecule for brevity

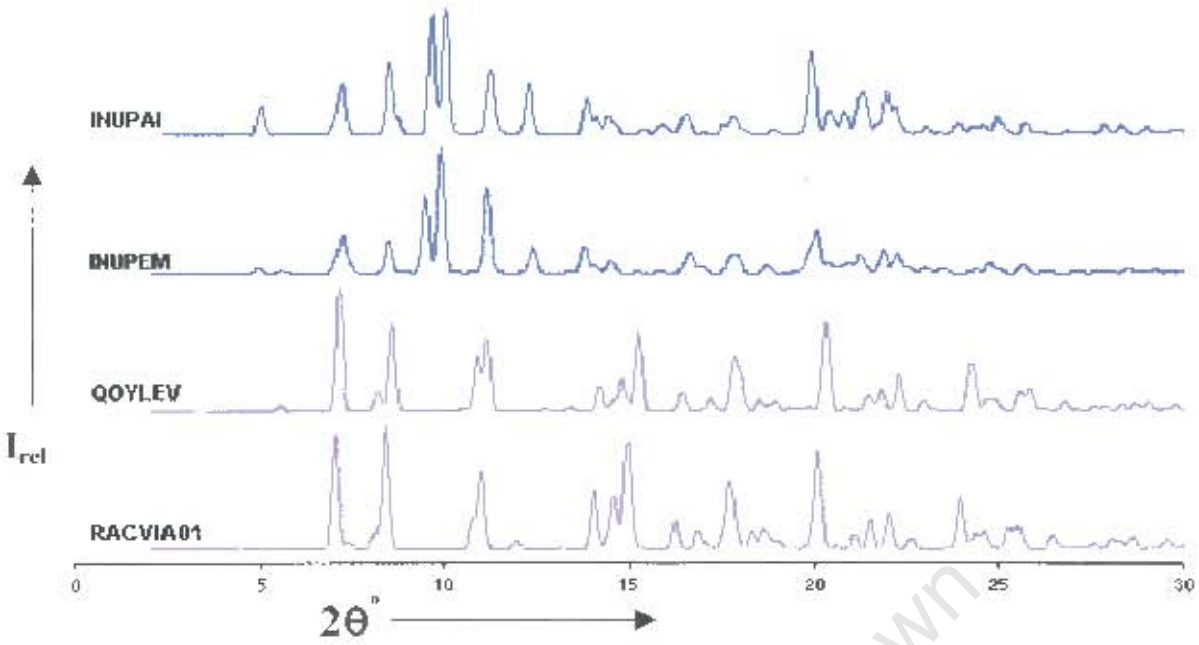

Figure 3.6 – Computed PXRD traces of some α-CD complexes demonstrating a high degree of isostructurality and those exhibiting a lower level of isostructurality.

We also report the two complexes we noted that demonstrated a high degree of isostructurality although they crystallize with different lattice types in the orthorhombic system. As shown in Table 3.4 and Figure 3.6, these α-CD inclusion complexes, QOYLEV (in space group $P2_12_12_1$) and RACVIA01 (with space group $C222_1$), have nearly equal unit cell dimensions, with a maximum difference of 0.5 Å in one of their corresponding unit cell edges, and have very similar X-ray powder diffractograms. The general shift of peaks to lower θ-values for RACVIA01 is consistent with its longer unit cell. Furthermore, and as shown in Figure 3.7, these two isostructural TRIMEA complexes are virtually indistinguishable from their crystal packing diagrams. Besides their possession of different space groups, the two complexes can be taken as isostructural. The close molecular isometricity of the guest compounds of the two complexes is noteworthy.

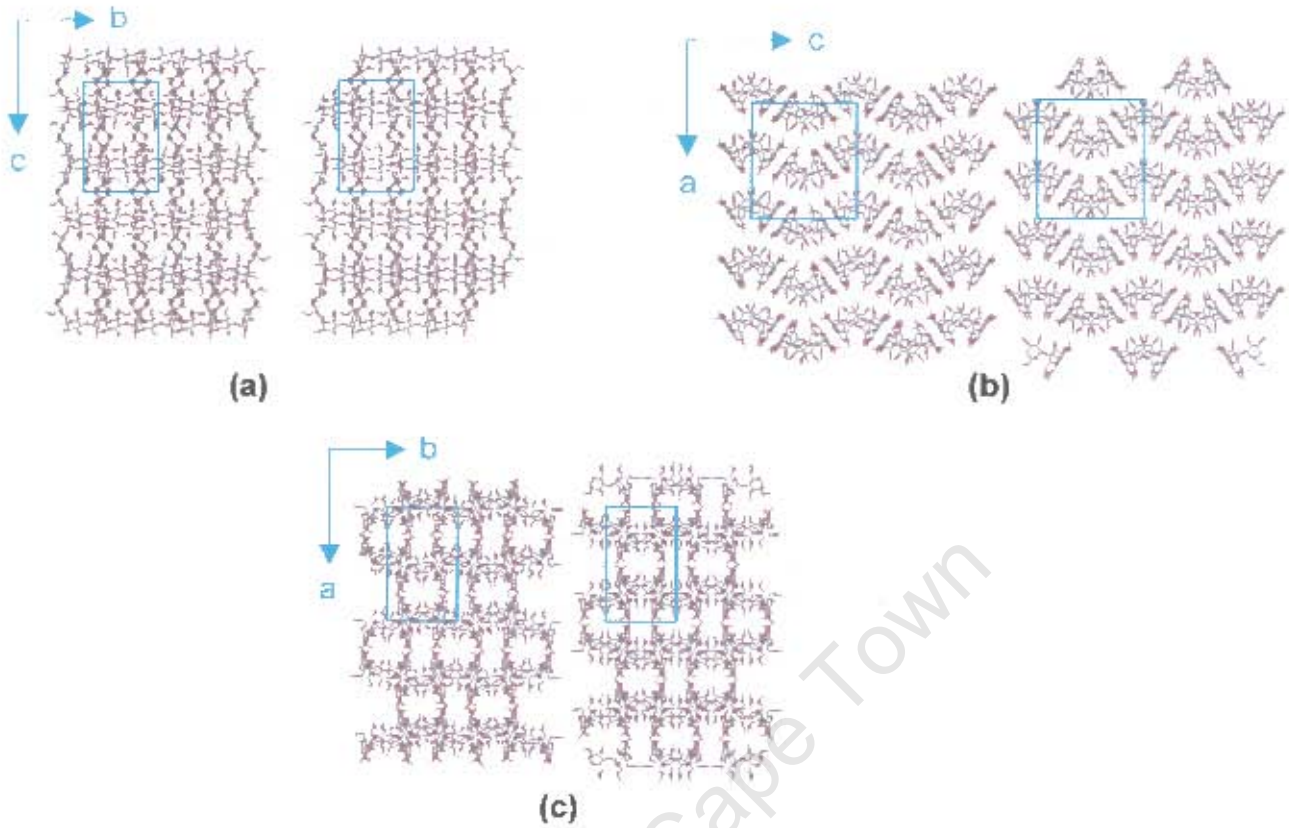

Figure 3.7 – Projections of crystal packing diagrams of TRIMEA complexes with a high degree of isostructurality but with different space groups of the same crystal system QOYLEV is on the left of each pair while RACVIA01 is on the right. Projections are made down the *a-axis* **(a)**, down the *b-axis* **(b)** and down the *c-axis* **(c)**.

Since isostructurality indices have not, to our knowledge, been employed previously to assess isostructurality quantitatively for CD inclusion complexes, it was decided to investigate the merits of doing so in this work. To evaluate the level of isostructurality within a class, isostructural indices were computed for series **A1**, chosen as a representative example, and the results are in Table 3.5. Pairwise comparison of five complexes yields ten sets of indices. Unit cell similarity indices in members of this class are practically zero and the I_v values are well above 90 % indicating a very high level of isostructurality within this series.

Table 3.5 – Isostructural indices within series A1.Unit cell similarity indices are recorded to three decimal places and I_v values are recorded to three significant figures.

A1: $P2_12_12_1$	Π	ε	A	εA	I_v (%)	I_{max} (%)
BANXUJ – GEVTOQ	0.002	0.001	3.323	0.003	95.5	99.8
BANXUJ – QOHMEF	0.005	0.004	0.399	0.002	94.0	99.5
BANXUJ – CDEXME10	0.002	0.000	6.283	0.002	94.9	98.7
BANXUJ – GULTUC	0.003	0.001	2.388	0.002	96.9	99.8
GEVTOQ – QOHMEF	0.004	0.005	0.259	0.001	92.5	99.8
GEVTOQ – CDEXME10	0.000	0.000	1.284	0.000	96.5	98.5
GEVTOQ – GULTUC	0.001	0.002	0.277	0.000	97.3	99.6
QOHMEF – CDEXME10	0.003	0.004	0.190	0.001	92.6	98.2
QOHMEF – GULTUC	0.003	0.003	0.317	0.001	94.7	99.3
CDEXME10 – GULTUC	0.001	0.001	0.490	0.001	96.8	98.9

For simplicity and due to the level of complication that can be encountered in these types of calculations, we selected one series as an example but similar values can be assumed within each series since the averaged PXRD patterns, as well as the matching of crystal packing diagrams, were in good agreement within all series reported in this dissertation. We conclude that the computation of isostructurality indices is a very useful complement to the PXRD patterns in providing a more comprehensive description of isostructurality in CD inclusion complexes.

3.5 Isostructurality in Complexes of Natural β-cyclodextrin

As was done for α-CD inclusion complexes, the data for β-CD complexes were screened for re-determinations and for the R factor limit of 15 %. The isostructural series numbering scheme proposed in the preceding section, section 3.4, is also applied here. Thus the previous series 7 in ref. [2] is replaced by the numbering **B1**, and the old series 8 is now **B2**, and so on. Complexes of the methylated β-CDs, as well as those of β-CD derivatives with substituents other than methyl, are designated by the prefix **BD** followed by the series number. Crystal data for complexes of the native β-CD form are in Table 3.6 and

the corresponding PXRD patterns are in Figure 3.8. The data and PXRD traces for complexes of β-CD derivatives are in Table 3.8 and Figure 3.11 respectively.

Table 3.6 – Crystal data for complexes of natural β-cyclodextrin forming isostructural series. The data for new isostructural series (i.e. not reported previously) are highlighted in yellow.

Series number	Guest	a (Å)	b (Å)	c (Å)	α (°)	β (°)	γ (°)	REFCODE
B1 : $P2_1$	Methanol	15.330	10.110	21.030	90	111.0	90	BOBPIR
	Water	**15.140**	**10.158**	**20.857**	**90**	**110.9**	**90**	**POBRON**
	Benzyl alcohol	15.356	10.101	21.287	90	112.8	90	DEBGOG
	m-Aminophenol, Methanol	15.122	10.335	20.915	90	109.6	90	GUXZOO
	1,4-Butanediol	15.271	9.973	21.199	90	110.9	90	KUTKOZ
	Squaric acid	15.231	10.068	21.117	90	110.2	90	MIFHAK
	Ethylene glycol	15.208	10.021	21.212	90	111.5	90	PIJGIY
	Glycerol	15.251	9.954	21.322	90	111.2	90	PIJGOE
	Dimethylsulfoxide	15.155	10.285	20.906	90	109.9	90	VACZIJ
	Diethanolamine	15.247	9.987	21.310	90	111.9	90	YIYSII
	1,5-Pentanediol	15.240	10.014	21.451	90	111.3	90	YIYSOO
	But-2-yne-1,4-diol	15.223	10.092	20.988	90	110.3	90	ZIGZIY
	Formic acid	15.171	10.169	20.986	90	110.9	90	ARUXIU
	Acetic acid	15.263	10.157	21.044	90	110.7	90	ARUXOA
B2 : $P2_1$	Hexamethylenetetramine	15.285	10.345	20.118	90	102.1	90	DIRVOP
	trans-Cyclohexane-1,4-diol	15.123	10.378	20.042	90	102.3	90	POVSIC
B3 : $P2_1$	1,4-Diazabicyclo(2.2.2)octane	15.395	16.598	15.441	90	117.4	90	BISTAY
	N-(2-thiazolyl)sulfanilamide	15.264	16.500	15.559	90	117.3	90	LILLUN
B4 : P1	4-t-Butyltoluene	15.562	15.564	15.835	102.1	102.2	103.6	KUTJUE
	(Z)-7-Tetradecenal	15.475	15.466	15.720	101.9	101.9	103.8	XUBXUN
B5 : P1	*p*-Bromoacetanilide	15.197	15.613	15.743	87.16	98.29	103.4	XADHIT
	p-Hydroxybenzaldehyde	15.262	15.728	16.350	92.67	96.94	103.3	OKUFOP
B6 : C2	Coumarin	19.322	24.641	16.050	90	108.8	90	GOSQOU
	Naphthyloxyacetic acid	19.341	24.632	15.975	90	108.8	90	ODEJOW
	Pyrene, Octanol	19.327	24.441	15.922	90	109.0	90	PUKPIU
	Pyrene, Cyclohexanol	19.254	24.467	15.914	90	109.5	90	PUKPOA
	(Z)-Tetradec-7-enoic acid	19.316	24.564	15.935	90	108.9	90	SOBJEY02
	S-(+)-Ibuprofen	19.410	24.415	15.898	90	109.0	90	TUXKUS
	3,3-Dimethylbutylamine	19.187	24.560	15.893	90	108.8	90	VIJXAN10
	trans-Cinnamic acid	19.422	24.461	15.941	90	108.7	90	XERTET
	(Z)-9-Dodecen-1-ol, Ethanol	19.238	24.477	15.790	90	109.5	90	ZUZXOH
	Methylparaben	18.863	24.454	15.594	90	110.7	90	AJUVEG
	Butyrophenone	19.352	24.599	15.916	90	109.4	90	DOQPOO
	Tridecanoic acid	19.363	24.597	15.937	90	109.0	90	SOBHUM02
	Spiroacetal	19.368	24.450	15.940	90	108.7	90	TEMCIX
	3,5-Dimethylbenzoic acid	19.374	24.711	15.999	90	108.9	90	YOVVIO01
	Ethanol	19.292	24.691	15.884	90	109.4	90	IJOLUO
	(Poly(tris(ethylene glycol)))	18.726	24.475	15.398	90	110.5	90	BEZLAT

(Table continues on the next page...)

	Valerophenone	19.339	25.581	16.010	90	109.1	90	DOQPUU
B7 : P1	N-acetyl-D-phenylalanine	18.150	15.470	15.410	103.5	113.7	98.7	AGAZUD
	Ethyl cinnamate	18.186	15.486	15.392	102.8	113.6	99.7	BIDMOQ
	1-Adamantane-carboxylic acid	17.747	15.255	15.491	102.5	113.5	98.9	BOGCAB
	4-t-butylbenzoic acid	18.244	15.476	15.417	102.9	113.1	99.7	HEGXUM
	Nonanoic acid	18.056	15.446	15.452	103.2	113.0	99.4	TEJHAR
	1,12-Dodecanediol	17.926	15.399	15.416	103.4	113.4	98.9	TAFZIK
	4,4'-Dipyridine	18.115	15.497	15.364	103.0	113.2	99.5	UKAGOC
	N-acetyl-L-phenylalanine methyl ester	18.129	15.411	15.585	104.0	112.9	98.8	DOCVUM04
	1,13-Tridecanedioic acid. Ethanol	18.207	15.510	15.280	103.0	113.1	99.8	LONGIE
	N-acetyl-L-phenylalanine amide	18.120	15.400	15.530	103.2	112.9	99.2	VOQDOU
	N-acetyl-*p*-methoxy-L phenylalanine methyl ester	18.310	15.510	15.310	102.8	112.7	99.5	VOQDUA
	1,12-Dodecanedioic acid, Ethanol	18.153	15.456	15.251	102.8	113.1	99.9	WISREV
	Methyl-4-hydroxybenzoate	18.019	15.343	15.414	103.5	113.1	99.3	AJUVAC
	1,14-Tetradecanedioic acid, Ethanol	18.242	15.492	15.436	102.8	113.0	99.8	CACPOM
	N-acetyl-L-phenylalanine	17.890	15.390	15.390	102.8	113.4	99.3	AGAZOX
	7-Hydroxy-4-methylcoumarin	18.010	15.530	15.370	103.4	113.2	99.5	MASBIR
	4,7-Dimethylcoumarin	18.133	15.479	15.101	102.9	113.4	99.5	MASBOX
	Aspirin, Salicylic acid	18.312	15.475	15.247	102.6	112.7	99.9	DIFHOP
B8 : $C222_1$	4-t-butylbenzyl alcohol	19.196	24.393	32.808	90	90	90	KOFJEU
	1-Hydroxymethyl-adamantane	19.162	23.965	32.597	90	90	90	FASXUS
	2-Azi-5-hydroxyadamantane	19.144	23.950	32.670	90	90	90	MEGQUK
B9 : $P2_1$	4,4'-Diaminobiphenyl	15.394	31.995	15.621	90	103.7	90	MACDAW
	(RS)-Fenopren	15.277	32.232	15.316	90	101.2	90	DUTLIN10
	(R)-(-)-Fenoprofen	15.260	32.760	15.350	90	101.5	90	GETPAW
	(S)-(+)-Fenoprofen	15.310	32.124	15.277	90	100.8	90	GETPEA
B10: $P2_12_12_1$	Potassium diclofenac	15.478	25.958	36.780	90	90	90	DKBCD *
	Caesium diclofenac	15.467	26.004	36.812	90	90	90	DCsBCD *

†For brevity, water has been omitted as a guest except for parent CD complexes, shown in bold.

‡Unit cell vectors transformed to obtain the reduced cell parameters.

*The compounds have not been submitted to the Cambridge Crystallographic Datacentre yet. The abbreviations used here are those used in the report of these structures [Chapter 5].

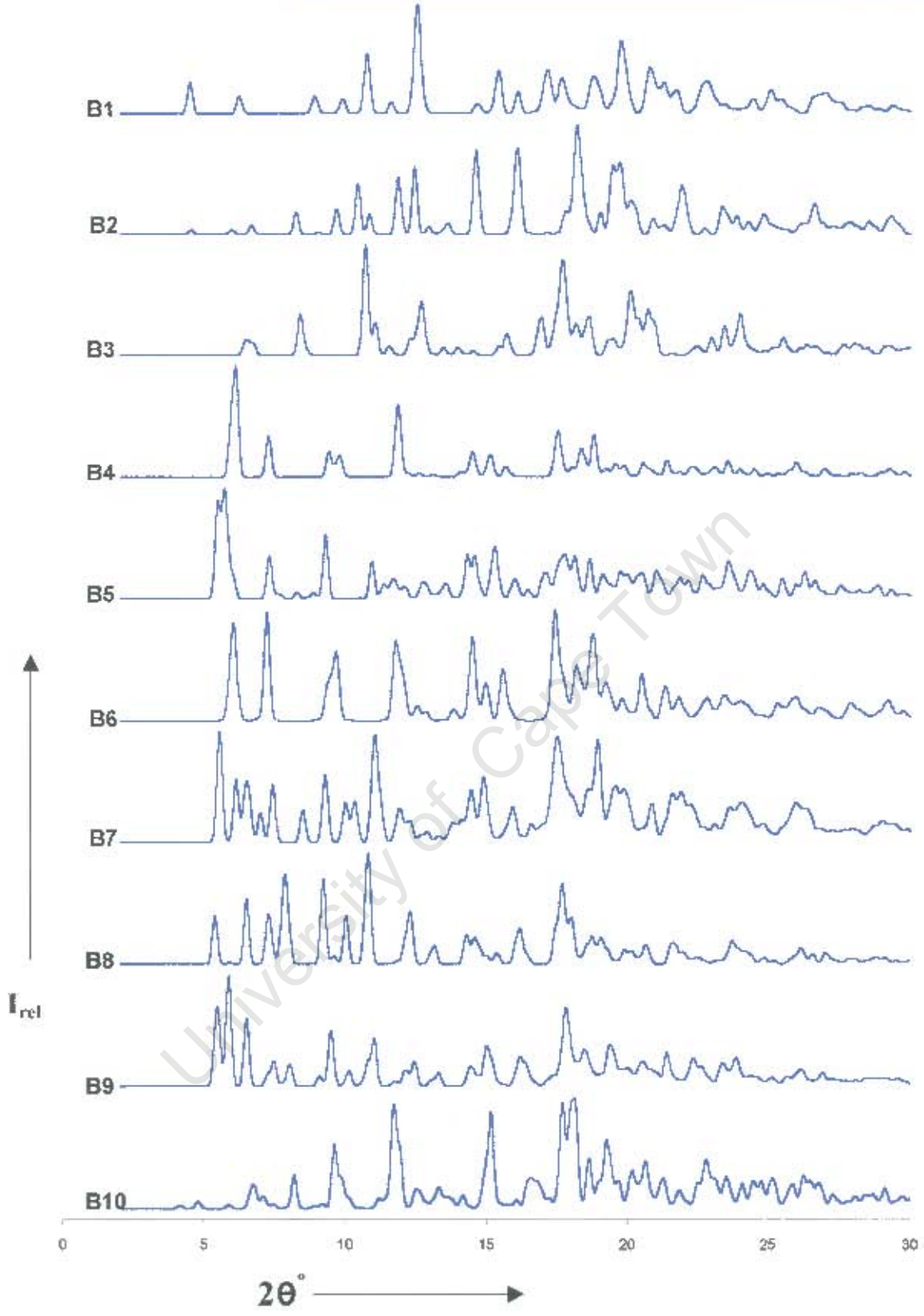

Figure 3.8 – Computed reference X-ray powder diffractograms for series of isostructural organic inclusion complexes of natural β-cyclodextrin.

Most of the new complexes captured were found to be isostructural with the existing classes, in particular with series **B1**, **B6** and **B7**, as indicated in Table 3.6. A few of the new entries were not found to be isostructural with any of the known series. However, two additional isostructural series, **B5** and **B10**, emerged from this survey.

Series **B1** to **B3** comprise the monomeric β-CD complexes while series **B4** to **B9** represent dimeric β-CD complexes. Complexes comprising series **B10** are monomeric with two CD molecules, in a head-to-tail orientation, comprising an asymmetric unit.

Complexes of series **B1** have the herringbone cage packing arrangement of monomeric CD molecules. This series is dominated by organic guest molecules of small and intermediate size and is the only natural β-CD series isostructural with the parent cyclodextrin. It is noteworthy that the large cavity of β-CD, relative to α-CD, results in the former being able to accommodate guest molecules as large as linear compounds of five-carbon chains and some phenyl compounds in monomeric cage packing arrangements (Table 3.6).

Complexes of series **B2** have a similar packing type to complexes of series **B1** but the relatively large difference in the monoclinic β-angles of the two series slightly alters their cage packing arrangements so that the crystal packing diagrams of the two are non-superimposable. Thus the two series are non-isostructural as has been recognised previously [2]; hence they have distinct PXRD traces as seen in Figure 3.8. Series **B2** contains medium-sized guest molecules, comparable in size to the guest molecules of series **B1**.

Series **B3** contains complexes with guests of different molecular sizes that crystallize in monomeric layers perpendicular to the *b*-axis. No new complexes were found for series **B2** and **B3**.

The dimeric β-CD series, series **B4** to **B9**, are dominated by a variety of long chain (up to 14 carbon atoms), large cyclic and polycyclic organic guest compounds in contrast to the relatively small guest compounds of the monomeric β-CD classes, series **B1** to **B3** and **B10**. The β-CD dimers of series **B4** to **B6** have the channel type (**CH**) packing arrangement, series **B7** has the intermediate (**IM**) packing arrangement, series **B8** has the chessboard (**CB**) packing mode, while dimers of series **B9** have the screw channel (**SC**) packing mode. These dimeric packing arrangements have been described in Chapter 1 and their details and isostructural implications can be found elsewhere [1,10].

The newly emerged isostructural series, series **B5**, has a channel type packing arrangement as do complexes of series **B4**, but the large differences in the triclinic α and β interaxial angles between the two series make the stacking of the dimeric channels different in the crystal structures of the two. Thus the two series are non-isostructural and have distinct PXRD traces as shown in Figure 3.8.

Isostructural series **B10** is the second additional series that has been captured in this update of the IsoPXRD method. This series comprises organic salt inclusion complexes that were prepared by the author and whose crystal structures are reported in detail in Chapter 5. The two complexes of this series have identical organic anions as guest molecules, differing only in the nature of the metal counterion. The monomeric β-CD molecules of the two complexes of series **B10** pack in antiparallel head-to-tail screw channels along the *c*-axis. This series is not isostructural with any of the known series and thus has a unique average PXRD pattern as can be seen in Figure 3.8.

Because complexes of series **B4**, **B5** and **B6** all pack in **CH** mode, characterised by head-to-head channel stacking of dimeric β-CD molecules along *c*, varying only in the nature of the dimeric channels, their PXRD traces are not as distinct from each other as are the traces of other series (Figure 3.8). In fact, the PXRD trace of series **B4** has peaks that are in close correspondence with those of

series **B6**. This near coincidence of average PXRD patterns of series **B4** and **B6** can be explained by the near superposition of their lattice points, such that a triclinic unit cell (in series **B4**) can be chosen to fit the monoclinic C-lattice points (of series **B6**). There also exists a twofold symmetry operator (a crystallographic diad, C2) passing through the dimer interface of complexes in series **B6** that is approximated by a pseudo-twofold symmetry operator in the β-CD dimers of series **B4**. This subtle structural relationship also explains the previous misclassification of some complexes, eg. SOBHUM and SOBJEY [11] under series **B4**, whereas they genuinely fall under series **B6** as SOBHUM02 and SOBJEY02 [12].

Another close correspondence of averaged X-ray powder diffractograms exists between complexes of series **B8** and **B9**, with PXRD traces of the two series differing largely in peak relative intensities with only a few differences in their peak angular positions (Figure 3.8). The orthorhombic complexes of series **B8** have the chessboard (**CB**) packing arrangement, while the monoclinic complexes of series **B9** pack in screw channels (**SC**). The close resemblance between PXRD traces of series **B8** and **B9** can be explained by the observation that some complexes with a **SC** packing mode can exhibit a shift of layers along the *ac* plane to an extent that they approximate the **CB** packing mode. (This phenomenon is discussed with illustrations towards the end of this section). It has also been noted that a simple lattice transformation of the primitive monoclinic cell of series **B9** yields a C-centred cell with dimensions very similar to those of the cell for series **B8** [2].

Variations in the triclinic interaxial angles of dimeric P1 β-CD complexes are likely to result in more isostructural series of the **CH** packing mode being generated in the future. This is exemplified by the new isostructural series **B5** that has been identified from the present survey and by the existence of a non-isostructural compound, TAFZEG (Table 3.7), whose unit cell dimensions closely match those of series **B5**, with significant differences only in the interaxial β and γ

angles relative to series **B5**. Thus TAFZEG, although possessing a distinct PXRD pattern, has some of the peaks appearing at similar angular positions to series **B5** (compare Figures 3.8 and 3.9). Whereas complexes of series **B5** pack strictly in **CH** mode, the dimeric **CH** packing arrangement of TAFZEG assumes the **IM** packing mode, resulting in half-blocked channels along the *c*-axis.

Table 3.7 – Crystal data for β-CD complexes with subtle deviations from the current isostructural series

Variant of	Guest†	a (Å)	b (Å)	c (Å)	α (°)	β (°)	γ (°)	REFCODE
B5: P1	Benzoic acid. Ethanol	15.210	15.678	15.687	89.13	74.64	76.40	TAFZEG
B6: C2	4,7-Dimethylcoumarin	19.513	24.024	16.414	90.00	104.5	90.00	MASBAJ
B9: $P2_1$	*p*-Amino-*p*'-nitrobiphenyl	15.454	31.693	15.255	90.00	102.9	90.00	QACXEX
	Paroxetine	15.226	31.477	15.674	90.00	104.3	90.00	BEGWEQ
	Adamantanone	15.428	32.545	15.437	90.00	103.6	90.00	KIFPAQ

†Again, water has been omitted as a guest molecule for brevity in presentation

We have identified one complex with unit cell parameters very similar to those of series **B6**, the only difference being about 5° in the β-angle. This complex, MASBAJ (appearing in table 3.7) has dimeric β-CD molecules shifted with respect to each other so that the channels down the *c*-axis are concealed, as in **IM** mode, in contrast to infinite channels that occur in complexes of series **B6**. Thus the PXRD trace of MASBAJ is unique with only a few peaks matching those of series **B6**, and only so at low 2θ values (Figure 3.9).

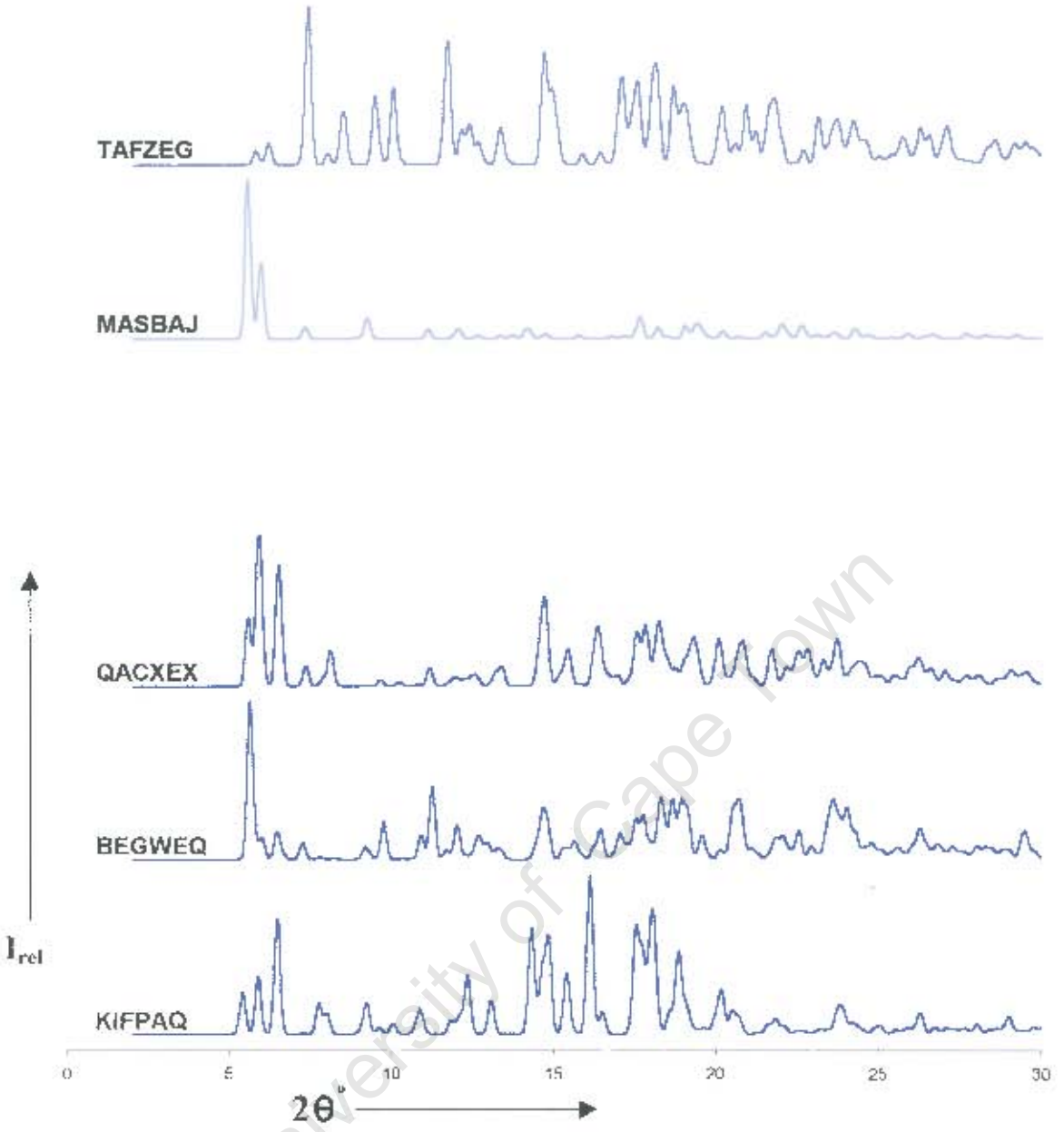

Figure 3.9 – Computed PXRD traces of β-CD complexes with slight variations of their unit cell parameters and/or crystal packing diagrams so that they are not fully isostructural with the established isostructural series.

The monoclinic screw channel (**SC**) packing of β-CD dimeric complexes is another packing arrangement likely to generate more isostructural series in the future. This packing mode, characteristic of complexes of series **B9** and of complexes that are variations of this series (QACXEX and BEGWEQ in Table 3.7), is characterised by the stacking of dimers along the *b*-axis such that they

form layers along the *a*- and the *c*-axes. Depending on the location of the structural motif relative to the 2-fold screw axis parallel to *b*, the successive dimeric layers can be shifted with respect to each other resulting in different channel packing modes [13] as shown in Figure 3.10. Thus QACXEX and BEGWEQ possess the **SC**-type packing, an arrangement found in complexes of series **B9**, while KIFPAQ has the **CB** packing mode (which is characteristic of complexes belonging to series **B8**). This subtlety in the isostructurality of the mentioned compounds has also been noted elsewhere [13] and is clarified in the next paragraph.

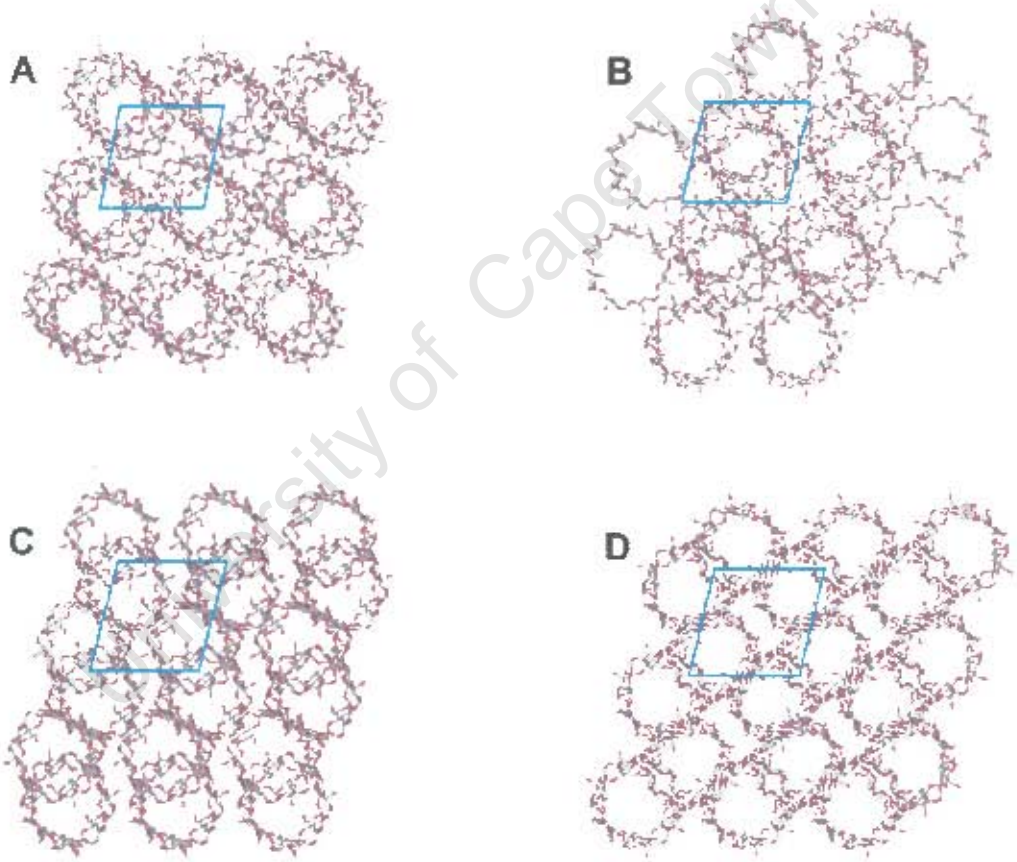

Figure 3.10 – (010) projections of crystal stackings of GETPAW (**A**), QACXEX (**B**), BEGWEQ (**C**) and KIFPAQ (**D**).

Shown in Figure 3.10 is a complex, GETPAW (**A**), representative of isostructural series **B9**, with a typical **SC** packing of β-CD dimeric layers, viewed down the screw channels parallel to *b*. A slight shift of these layers parallel to the *ac*-plane results in the slightly different **SC** stacking found in complex QACXEX (**B**), which is not isostructural with complexes of series **B9**. These layers can be shifted more, so that the β-CD dimeric overlaps in successive layers become even smaller (e.g. BEGWEQ (**C**)), or negligible (e.g. in KIFPAQ (**D**)). As shown in Tables 3.6 and 3.7, all these complexes have nearly identical unit cell parameters, which are also very similar to those of series **B9**, and consequently, show some similarity in their PXRD patterns.

The two coincidental matches of PXRD traces of series **B4** with **B6** and series **B8** with **B9** are noteworthy as the involved series are, by definition, not isostructural. The knowledge of the correct crystal system of a newly prepared complex, belonging to any of the series **B4**, **B6**, **B8** or **B9**, may be required for its unambiguous assignment to an isostructural class. If single crystals of the newly isolated complex are not readily available for determination of the Laue symmetry, these coincidental matches may limit what can be said about the crystalline phase of a newly prepared complex using the IsoPXRD technique alone.

3.6 Isostructurality in Complexes of β-CD Derivatives

Turning to the complexes of derivatised β-cyclodextrin, we have identified six new isostructural series in addition to the previously reported classes [2], half of which are due to the unusually derivatised β-CDs forming classes of their own. The existing two isostructural series (series 15 and 16) [2] are replaced by the numbering **BD1** and **BD3**, respectively. Two complexes, PABNEM and PINMAA, were each found to be isostructural with the existing classes. The data for complexes of derivatised β-cyclodextrin demonstrating isostructural behaviour are presented in Table 3.8 and their averaged PXRD patterns are in Figure 3.11.

Complexes comprising series **BD1** are organic inclusion complexes of the host DIMEB exclusively, with highly isometric guest molecules of halophenyl derivatives, that crystallize in a cage-type packing arrangement. Series **BD3** is exclusively made up of TRIMEB complexes, with a large variety in guest size and shape, that pack in anti-parallel head-to-tail channels along the *a*-axis.

Table 3.8 – Crystal data for isostructural complexes of common derivatives of β-CD and several novel β-CD derivatives. The data for new isostructural series are highlighted in yellow.

Series number	(Guest or CD Derivative)[1]	a (Å)	b (Å)	c (Å)	α (°)	β (°)	γ (°)	REFCODE
BD1: $P2_12_12_1$	*p*-Nitrophenol	14.779	18.965	28.741	90	90	90	DEZMIE10
	p-Iodophenol	14.796	18.853	28.989	90	90	90	DEZMOK10
	2,4-Dichlorophenoxyacetic acid	14.886	18.980	28.515	90	90	90	PABNEM
BD2: $P2_12_12_1$	6-O-(4-Nitrophenyl)-β-CD[‡]	13.207	18.993	28.563	90	90	90	BEFDIA
	6-O-(4-Bromophenyl)-β-CD[‡]	13.401	19.157	28.489	90	90	90	BEFDUM
	6-O-(4-Formylphenyl)-β-CD[‡]	13.204	19.146	28.835	90	90	90	HAGMOS01
	6-Anilino-6-deoxy-β-CD	13.432	19.025	28.041	90	90	90	NATFET
	6-O-((R)-2-Hydroxypropyl)-β-CD[‡]	13.184	19.335	27.261	90	90	90	LEDROB
	6-O-((S)-2-Hydroxypropyl)-β-CD[‡]	12.939	19.528	27.303	90	90	90	LEDRUH
	6-Deoxy-6-(4-carboxyphenyl-amino)-β-CD[‡]	13.588	19.172	28.187	90	90	90	BEDKAX
BD3: $P2_12_12_1$	*p*-Iodophenol	14.997	21.368	28.205	90	90	90	CAMPIP
	(R)-Flurbiprofen	15.092	21.714	28.269	90	90	90	COYXAP10
	(S)-Flurbiprofen	15.271	21.451	27.895	90	90	90	COYXET20
	4-Biphenylacetic acid	14.890	21.407	28.540	90	90	90	PAFSOE
	(S)-Ibuprofen	15.232	21.327	27.597	90	90	90	RONWOG
	(S)-Naproxen	15.179	21.407	27.670	90	90	90	ZIFQOU
	Ethyl laurate	14.796	22.444	27.720	90	90	90	PINMAA
BD4: $P2_12_12_1$	6A,6D-Dideoxy-6A-(t-butylthio)-β-CD[‡]	32.489	15.460	15.172	90	90	90	CURYUJ
	6'-Deoxy-6'-(6-Aminohexyl)amino-β-CD[‡]	32.513	15.387	15.265	90	90	90	TEVCUS
BD5: $P2_12_12_1$	**Water**	**12.663**	**17.679**	**31.271**	**90**	**90**	**90**	**IQOZIX**
	Ethanol	12.761	17.338	30.796	90	90	90	XERTAP
BD6: $P2_1$	**Water**	**15.242**	**10.639**	**23.324**	**90**	**101.8**	**90**	**CEQCUW**
	Acetic acid	15.165	10.613	23.188	90	102.0	90	NITSIS
BD7 : $P2_1$	Methanol	11.567	21.105	20.300	90	93.58	90	ICUFAN
	2,3,6-Tri-O-propanoyl-β-CD[‡]	12.562	21.695	21.451	90	93.98	90	ICUFIV
BD8: $P4_12_12$	6-Deoxy-6-Phenylthio-β-CD[‡]	21.915	21.915	28.337	90	90	90	FEDKOO
	6-Deoxy-6-Phenylseleno-β-CD[‡]	22.074	22.074	28.610	90	90	90	BEFFAU

[1] For brevity, water has been omitted as a guest molecule except for parent CD complexes shown in bold.
[‡] Not a host-guest complex but a derivatised β-CD in which a bulky substituent has been substituted at one or more of the primary hydroxyl groups.

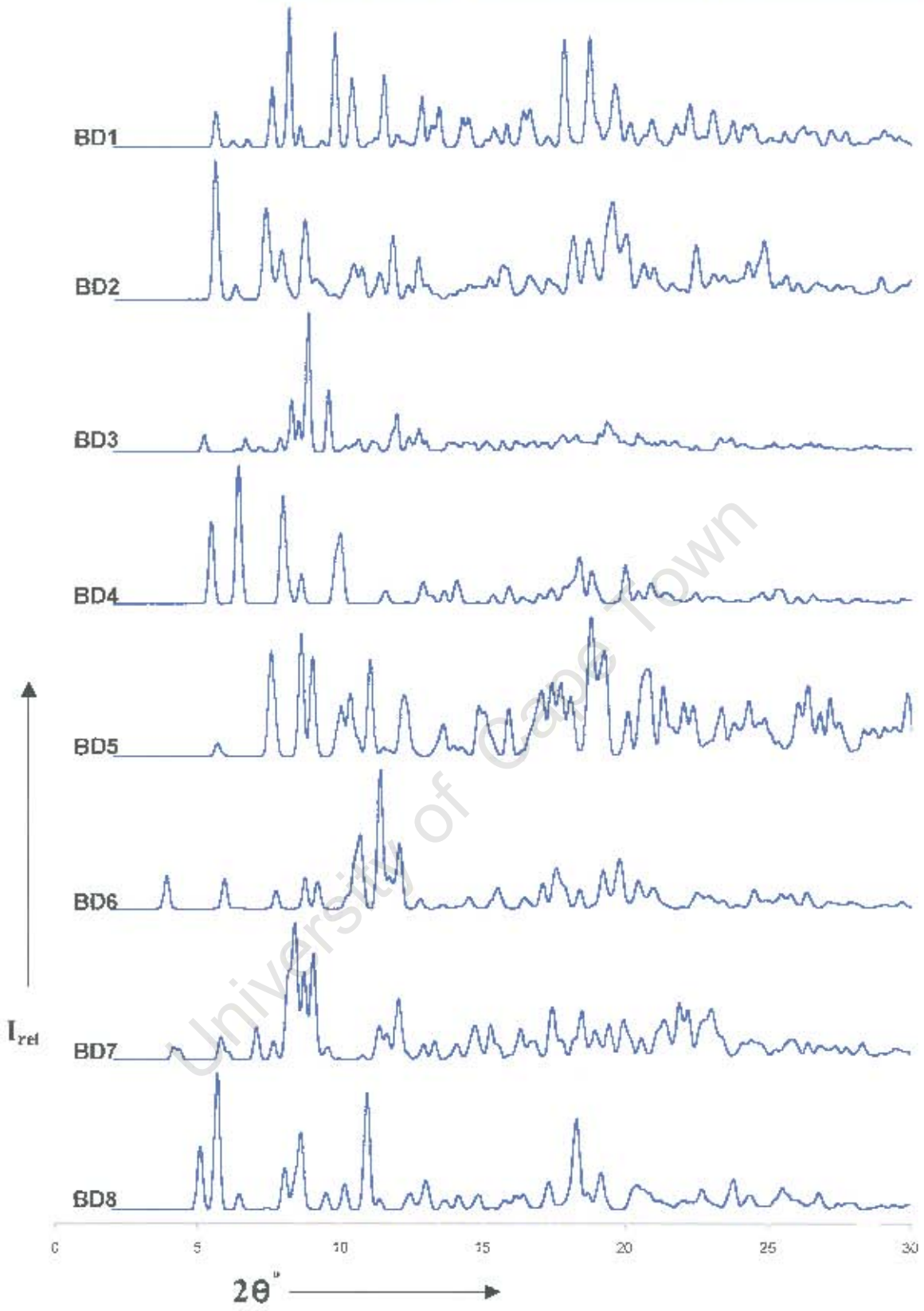

Figure 3.11 – Computed reference PXRD traces of complexes of common derivatives of β-CD and several novel β-CD derivatives forming isostructural series.

Series **BD2** comprises the unusual CD derivatives packing in anti-parallel head-to-tail screw channels along the *a*-axis with the organic substituent inserting into the secondary face of the neighbouring CD molecule. PXRD traces of compounds of series **BD2** with highly isometric substituents on atoms O_6 (LEDROB, LEDRUH, BEDKAX) matched more closely with one another than they did with the rest of series **BD2** compounds, although all members of this series are isostructural. Novel β-CD derivatives, comprising series **BD4**, have the cage type packing arrangement.

Two parent cyclodextrin hosts, MONOMEB and DIMEB III (described earlier in section 3.3), were found to be isostructural with their respective inclusion complexes XERTAP and NITSIS, both of which contain small organic guest molecules (Table 3.8). Consequently, two new series, **BD5** and **BD6** were created. Both series are characterised by cage-type packing arrangements. Cages of series **BD5** are arranged in a different pattern from those of series **BD6**, hence the two series have distinct PXRD patterns as shown in Figure 3.11.

Series **BD7** comprises an inclusion complex of 2,3,6-tri-O-acetyl-β-CD with methanol (ICUFAN) and the host compound 2,3,6-tri-O-propanoyl-β-CD (ICUFIV) with no guest molecule, both of which crystallize in head-to-tail channels along the *a*-axis. **BD8** is one of the series with unusual β-CD derivatives and has the cage-type packing arrangement.

The first three series (**BD1** to **BD3**) differ in their unit cell edges by 2.3 Å in *a*, 3.6 Å in *b* and 1.7 Å in *c*, in the extreme cases. Furthermore, these series belong to the same crystal system (orthorhombic) and possess a common space group, $P2_12_12_1$. As mentioned earlier, crystal packing arrangements in the three series are different and they have distinct PXRD patterns as shown in Figure 3.11. This behaviour was investigated for other compounds that were found to be non-isostructural with one another and non-isostructural with any of the known isostructural series but whose unit cell parameters and/or PXRD traces resemble

each other or resemble one of the currently known isostructural series. The data for the analysed CD compounds are in Table 3.9.

Table 3.9 – Crystal data for some β-CD inclusion complexes and β-CD derivative compounds demonstrating limited isostructural behaviour

Closest series	Guest†	a (Å)	b (Å)	c (Å)	α (°)	β (°)	γ (°)	REFCODE
BD1: $P2_12_12_1$	2-Naphthoic acid	15.463	18.922	27.852	90	90	90	WAGHAN01
BD2: $P2_12_12_1$	6A,6B-Dideoxy-6A-(*p*-methylbenzylthio-6B-phenylthio-β-CD‡	14.464	17.337	29.388	90	90	90	RABZIE
	6-Deoxy-6-(1-*n*-propylamino)-β-CD‡	14.414	19.377	26.997	90	90	90	SUYLAZ
	6-Deoxy-6-N-(N'-(dimethyamino-1-naphthalenesulfonyl)diamino-ethane)-β-CD‡	15.881	17.801	27.293	90	90	90	TADGOU
BD3: $P2_12_12_1$	*m*-Iodophenol	15.669	20.798	25.486	90	90	90	GELKEN10
	Water	**14.823**	**19.382**	**26.534**	**90**	**90**	**90**	HEZWAK01
BD4: $P2_12_12_1$	6-Deoxy-6-(2-(Diphenyl-phosphino)-ethylenethio)-β-CD‡	14.968	15.331	31.808	90	90	90	MEYHON

†For brevity, water has been omitted as a guest molecule except for CD complexes shown in bold.

‡Not a host-guest complex but a derivatised β-CD in which one or more of the primary hydroxyl groups has (have) been replaced by one or more bulky organic substituent(s).

The DIMEB naphthoic acid inclusion complex, WAGHAN01 in Table 3.9, has similar unit cell parameters to DIMEB complexes comprising series **BD1** (Table 3.8) and has a similar type of crystal packing as series **BD1**. However, close inspection of the packing diagrams of WAGHAN01 revealed that it is not isostructural with complexes of series **BD1**, as the relative orientation of the cyclodextrin molecules in each case is different. Thus the PXRD trace of WAGHAN01 resembles that of series **BD1**, with only slight and undirectional shift of peaks along the 2θ scale (compare traces in Figures 3.11 and 3.12).

A few unusual β-CD derivatives have unit cell parameters approximating those of similarly derivatised β-CDs in series **BD2**. These compounds, RABZIE, SUYLAZ, TADGOU and series **BD2** complexes are all characterized by screw channels modulated by one of the screw axes of the space group $P2_12_12_1$. Depending on the direction of this screw axis, the propagation of the channels may be different. The channels of series **BD2**, RABZIE and SUYLAZ vary slightly, but those of TADGOU appear totally different from the rest. Consequently, although all the stated compounds are non-isostructural with each other, the PXRD trace of RABZIE resembles the average trace of complexes in series **BD2** at lower 2θ values (< 9°), while the trace of SUYLAZ resembles that of **BD2** at higher 2θ values (2θ > 18°).

By the same argument as in the above case, the screw channels characteristic of TRIMEB complexes of series **BD3** can be distorted to an extent that they approximate the cage type packing arrangement. Thus GELKEN10 has a packing arrangement intermediate between a screw channel and a cage type while HEZWAK01 has a cage type packing arrangement. The two complexes, although possessing approximately matching unit cell parameters and sharing a common space group, are non-isostructural with each other and are non-isostructural with series **BD3**. As a result, these complexes diffract X-rays differently, and differently from complexes of series **BD3**; hence they have distinct X-ray powder diffractograms as shown in Figures 3.11 and 3.12.

MEYHON in Table 3.9 has unit cell parameters matching those of similarly derivatised β-CD compounds of series **BD4** in Table 3.8 but the relatively large substituent in MEYHON results in a cage packing arrangement that is slightly different from that of compounds comprising series **BD4** so that it is non-isostructural with this series. The consequence of similarity in unit cell dimensions is that the PXRD trace of MEYHON matches closely that of series **BD4** especially at lower Bragg angles.

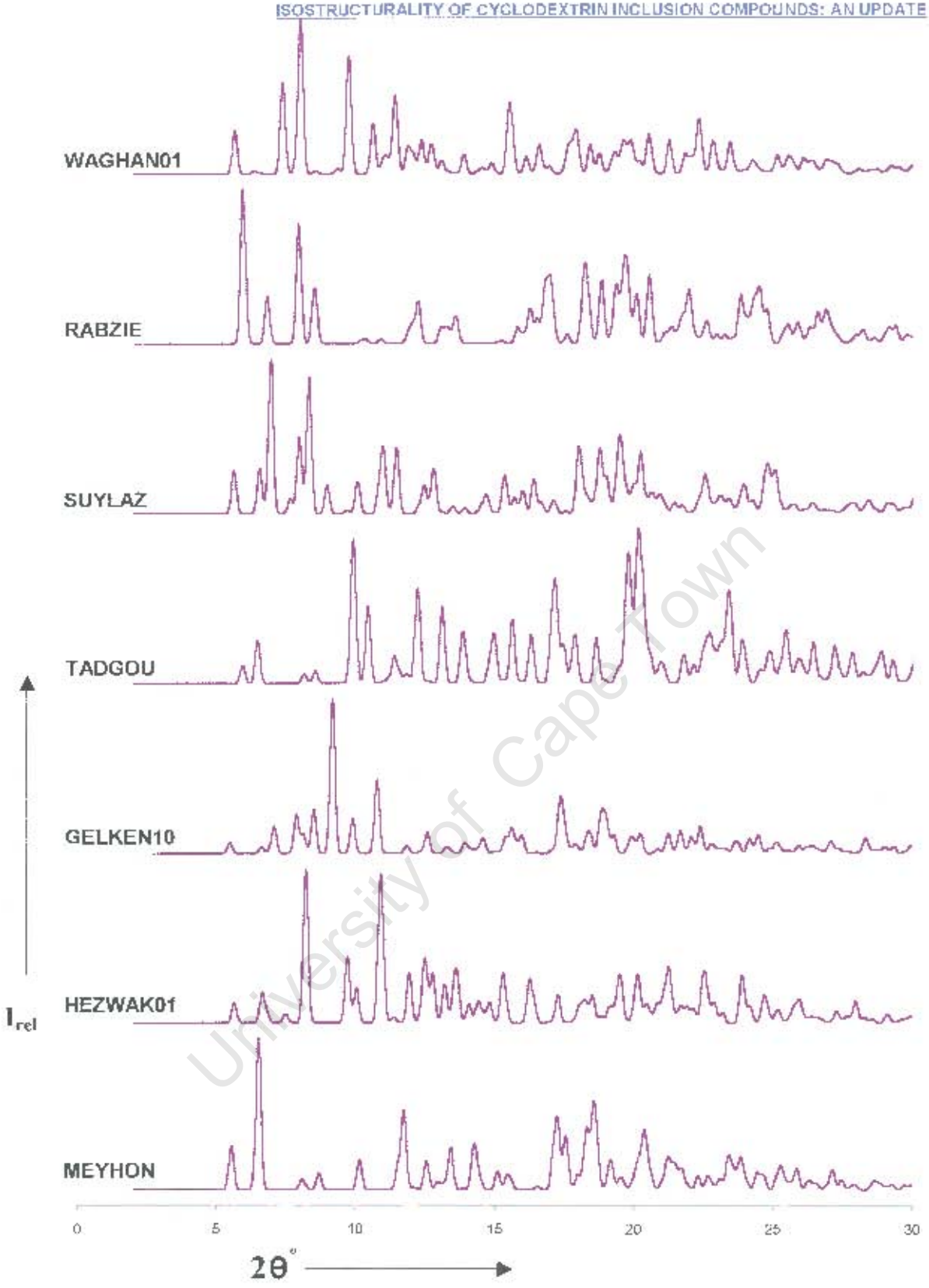

Figure 3.12 – Computed PXRD traces of β-CD inclusion complexes and β-CD derivative compounds demonstrating limited isostructural behaviour.

Two sets of TRIMEB organic inclusion complexes, one set orthorhombic and the other monoclinic, each set with closely matching unit cell parameters and sharing a common space group, were encountered (Table 3.10). The complexes in the first set (space group $P2_12_12_1$) would be expected to be isostructural, as would the complexes in the second set (space group $P2_1$).

Table 3.10 – Crystal data of non-isostructural TRIMEB organic inclusion complexes with very similar unit cell parameters and sharing common space groups.

Space Group	Guest[1]	a (Å)	b (Å)	c (Å)	α (°)	β (°)	γ (°)	REFCODE
$P2_12_12_1$	(S)-1,7-Dioxaspiro[5 5]undecane	10.936	25.530	29.640	90	90	90	QOYLIZ
$P2_12_12_1$	Methylcyclohexane	11.149	25.664	29.427	90	90	90	XAQJII
$P2_1$	2,4-Dichlorophenoxyacetic acid	11.680	28.230	15.020	90	112.6	90	ASIQOI
$P2_1$	Indole-3-butyric acid	11.411	28.629	15.089	90	111.9	90	ASIQUO

[1]Again, water has been omitted as a guest molecule for brevity

In the orthorhombic set, CD molecules of both QOYLIZ and XAQJII pack in head-to-tail channels down the *a*-axis. However, the relative orientation of CD molecules in each structure is different, so that the channels of the two structures do not appear at identical positions. The two orthorhombic TRIMEB inclusion complexes are therefore not fully isostructural and as such cannot comprise a series. Except for two peaks with relatively small intensities (one at about $2\theta = 6°$ and the other at about $2\theta = 7.6°$) that are present in the PXRD pattern of QOYLIZ and not present in the PXRD trace of XAQJII, the two complexes could easily be misclassified as isostructural (Figure 3.13).

In the other set (monoclinic), the two TRIMEB inclusion complexes, as convincingly isostructural as they might appear on matching of their PXRD traces and cell parameters, have different orientations of their CD rings such that the complex ASIQOI forms channels along the *a*- and the *c*-axes while the other complex ASIQUO has head-to-tail antiparallel channels along *a*, with layers parallel to the *bc*-plane. Although possessing closely matching X-ray powder diffractograms, as shown in Figure 3.13, the two complexes are not fully isostructural.

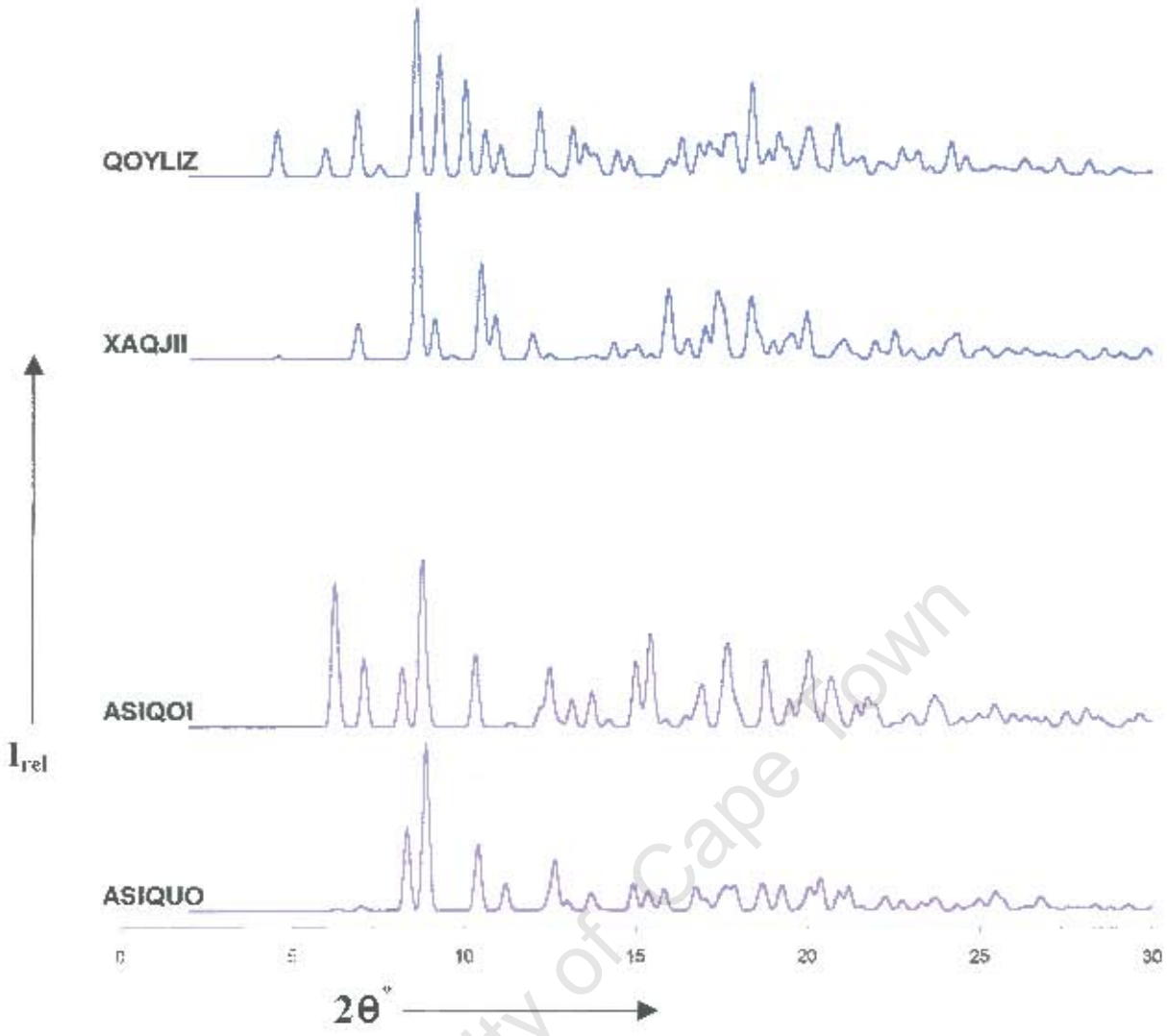

Figure 3.13 – Computed PXRD patterns of non-isostructural TRIMEB organic inclusion complexes with similar unit cell parameters.

3.7 Isostructurality of Gamma Cyclodextrin Organic Inclusion Complexes and Their Derivatives

No new isostructural series were discovered for γ-CD and its derivatives. Thus the data for γ-CD inclusion complexes are the same as previously reported [2], with old series 17 now designated **G1**. Crystal data for organic inclusion complexes of the γ-CD type comprising this isostructural class are listed in Table 3.11 and the corresponding average PXRD trace is shown in Figure 3.14.

Table 3.11 – Crystal data for isostructural γ-CD inclusion complexes

Series number	Guest†	a (Å)	b (Å)	c (Å)	α (°)	β (°)	γ (°)	REFCODE
G1: $P42_12$	Methanol	23.808	23.808	23.140	90.0	90.0	90.0	NUNRIX
	1-Propanol	23.840	23.840	23.227	90.0	90.0	90.0	SIBJAO
	1-Propanol	23.809	23.809	23.207	90.0	90.0	90.0	SIBJES

†Water has been omitted as a guest molecule for brevity

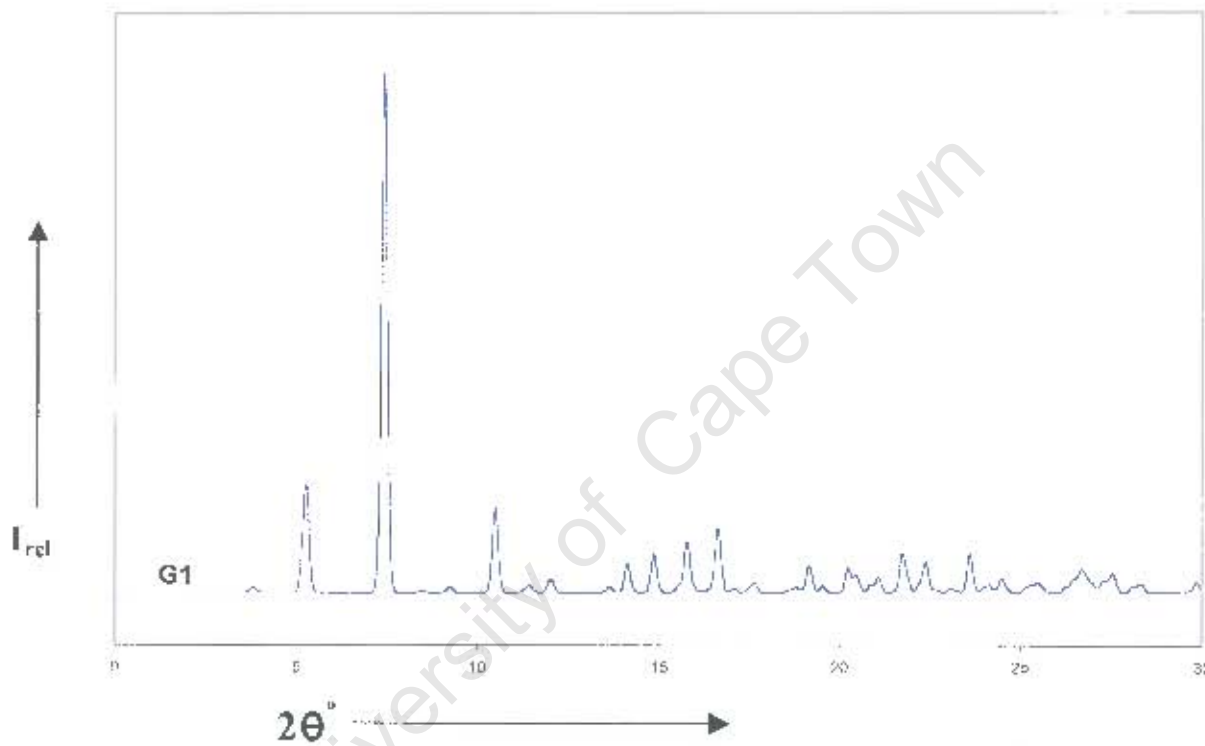

Figure 3.14 – Average computed PXRD reference pattern for isostructural complexes of series G1.

The γ-CD inclusion complexes comprising series **G1** contain small organic guest molecules and crystallize in channel-mode in the tetragonal space group $P42_12$. The propan-1-ol complexes, SIBJAO and SIBJES (Table 3.11), differ slightly in their water content (by 0.12 water molecules per formula unit). The data for these two γ-CD inclusion complexes were collected from crystals of different experimental batches [14].

3.8 References

1. M. R. Caira, *Roum. Chem. Quart. Rev.*, 2000, **8**, 221 – 344.
2. M. R. Caira, *Rev. Roum. Chim.*, 2001, **46**, 371 – 386.
3. E. J. C. de Vries, *PhD Thesis, Inclusion of Alkylparabens in Cyclodextrins*, University of Cape Town, South Africa, 2003.
4. V. J. Smith, *MSc Dissertation, Physicochemical Study of Solid Cyclodextrin Inclusion Complexes of the Antithrombotic Ajoene*, University of Cape Town, South Africa, 2004.
5. P. M. Dean, *MSc Dissertation, Structural and Thermal Characterisation of NSAIDS and Cyclodextrin-NSAID Complexes*, University of Cape Town, South Africa, 2004.
6. L. Cunha-Silva, and J. J. C. Teixeira-Dias, *New J. Chem.*, 2004, **28**, 200–206.
7. *Cambridge Structural Database and Cambridge Structural Database System*, **Version 5.26**, November 2004, Cambridge Crystallographic Data Centre, University Chemical Laboratory, Cambridge, England.
8. M. R. Caira, S. A. Bourne, W. T. Mhlongo and P. M. Dean, *Chem. Commun.*, 2004, **19**, 2216 – 2217.
9. H. Onagi, B. Carrozzini, G. L. Cascarano, C. J. Easton, A. J. Edwards, S. F. Lincoln and A. D. Rae, *Chem. –Eur. J.*, 2003, **9**, 5971 – 5977.
10. D. Mentzafos, I. M. Mavridis, G. Le Bas and G. Tsoucaris, *Acta Crystallogr.*, 1991, **B47**, 746 – 757.
11. S. Makedonopoulou, I. M. Mavridis, K. Yannakopoulou, J. Papaioannou, *Chem. Commun.*, 1998, **19**, 2133 – 2134.
12. R. E. Marsh, M. Kapon, S. Hu, F.H. Herbstein, *Acta Crystallogr.*, 2002, **B58**, 62 – 77.
13. M. R. Caira, E. De Vries, L. R. Nassimbeni and V. W. Jacewicz, *J. Incl. Phenom. Macro.*, 2003, **46**, 37 – 42.
14. J. Ding, T. Steiner, W. Saenger, *Acta Crystallogr.*, 1991, **B47**, 731 – 738.

CHAPTER 4: APPLICATION OF THE ISOPXRD METHOD TO KNEADED SAMPLES OF SALICYLIC ACID DERIVATIVES WITH CYCLODEXTRINS

4.1 Introduction

In this Chapter, the author intends to demonstrate the use of the IsoPXRD method, whose recent update appears in the previous chapter, versus the traditional method of CD complex identification using PXRD. A group of three related drugs has been selected for this study. The selected drugs are the salicylic acid derivatives, namely aspirin, salicylamide and sulfasalazine, which are well known therapeutic agents in particular as analgesics (pain-killers), antipyretics (fever-reducers) and as anti-inflammatories [1].

Aspirin, chemically known as 2-acetoxybenzoic acid or acetylsalicylic acid, has a low aqueous solubility – i.e. 1 g dissolves in 300 ml of water at 25 °C (0.3 % or 3 mg/ml). In addition, this drug spontaneously hydrolyses into salicylic and acetic acids in moist air, according to the reaction scheme shown in Figure 4.1. Aspirin inclusion in cyclodextrin in order to stabilise it and improve its solubility in aqueous media is therefore desirable.

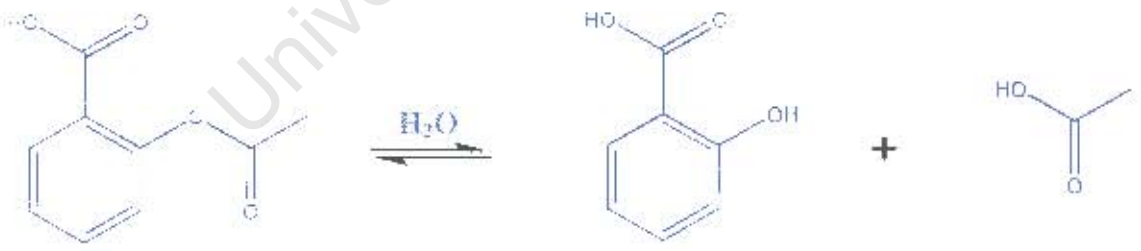

(a) **(b)** **(c)**

Figure 4.1 – Reaction scheme for the conversion of aspirin **(a)** into salicylic **(b)** and acetic **(c)** acids.

Aspirin is the most widely studied of the three drugs and attempts have been made to complex it with cyclodextrins [2-4]. A crystal structure of an inclusion complex of aspirin with β-cyclodextrin has also been reported [5]. However, the deacetylation, or hydrolysis, of aspirin (as shown in Figure 4.1) occurred during the preparation, so that the crystal structure turned out to be a quaternary complex of aspirin, salicylic acid, water and β-CD.

Salicylamide, chemically known as 2-hydroxybenzamide (see Figure 4.2), also exhibits low aqueous solubilities both at room and physiological temperatures. This drug has a 0.2 % (2 mg/ml) water solubility at 30 °C and this increases to 0.8 % (8 mg/ml) at 47 °C. Sulfasalazine, or 5-[*p*-(2-pyridylsulfamoyl)phenylazo]-salicylic acid (Figure 4.2), on the other hand, is practically insoluble in water [1].

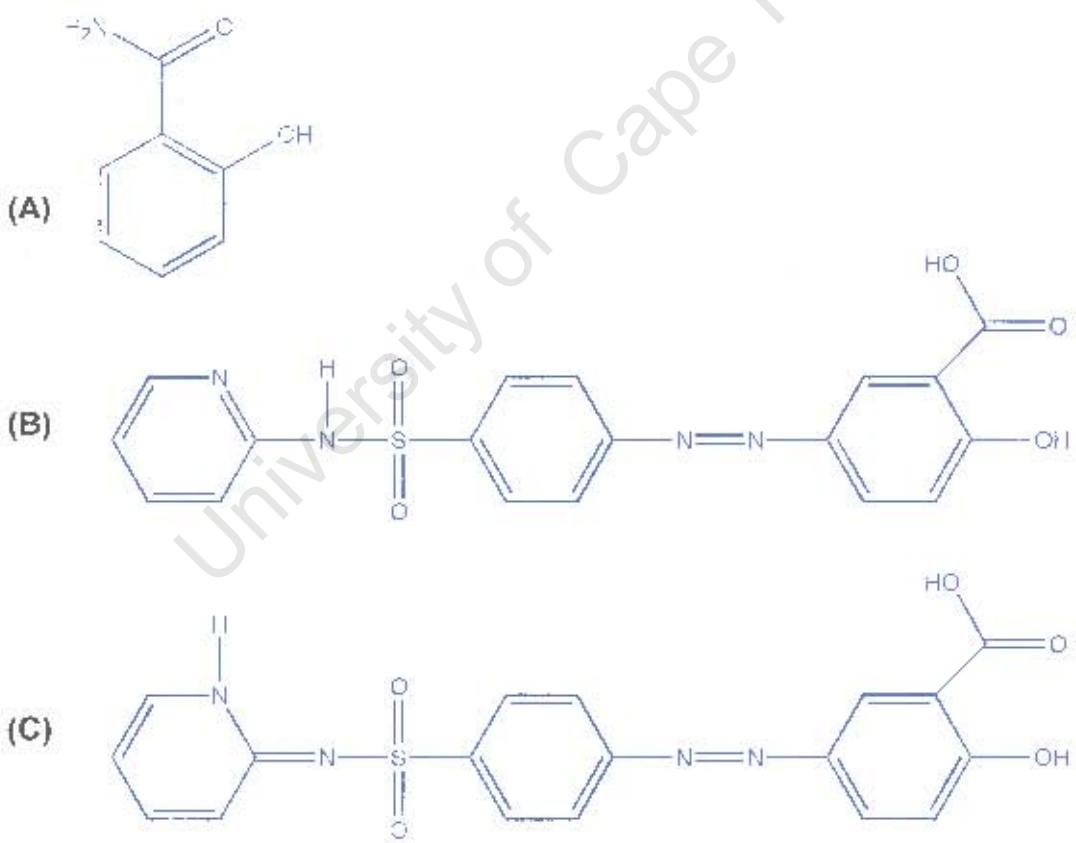

Figure 4.2 – IUPAC line drawings for the chemical structures of salicylamide **(A)** and two tautomers of sulfasalazine, the amide **(B)** and the imide **(C)** forms.

Sulfasalazine (SSAL) is prone to tautomerisation (see Figure 4.2) so that two tautomers of this drug exist [6,7]. The amide tautomer crystallizes in the triclinic space group $P\bar{1}$ while the imide tautomer crystallizes in the monoclinic space group $P2_1/c$. The monoclinic form (MSSAL) can be obtained by recrystallizing the triclinic form (TSSAL) from acetone or THF solvents. The triclinic form results from crystallization of MSSAL from ethanol or MEK. Although studies on the complexation of sulfasalazine with cyclodextrins have been performed [8], isostructural behaviour of CD inclusion complexes of this drug has not been investigated to our knowledge.

4.2 Preparation

All complexes reported in this Chapter were prepared by the kneading method (see section ***1.2.3*** for a description of this method) with H:G molar ratios of 1:1. For all complexes the kneaded material was analysed in its paste form (i.e. no further sample preparation was performed).

4.2.1 Preparation of Aspirin•β-CD Inclusion Complex

Aspirin•β-CD was obtained by slowly adding 10 mg of aspirin to a paste of 72 mg β-CD formed with distilled de-ionised water. The paste was kept wet by the drop-wise addition of distilled water while constantly kneading. This continued until proof of complex formation was evident from PXRD analysis. The complex was obtained after an hour.

4.2.2 Preparation of Salicylamide•β-CD Inclusion Complex

Preparation of a salicylamide•β-CD inclusion complex involved slow addition of 10 mg of the drug to a paste of 95 mg β-cyclodextrin treated with distilled de-ionised water. This was then kneaded while kept moist by the drop-wise addition of distilled de-ionised water. Complete complex formation could be achieved in 40 minutes.

4.2.3 Preparation of Sulfasalazine Tautomers and Sulfasalazine-CD Inclusion Complexes

The triclinic tautomeric form of sulfasalazine was obtained by dissolving 40 mg MSSAL in 20 ml MEK in a closed vial at 60 – 70 °C for 27 hrs. This was then filtered twice with 0.45 μm microfilters and evaporated to dryness at 30 – 32 °C. The evaporation took two weeks. Similar results could be achieved using ethanol instead of MEK, with the amounts kept the same. Seeding with the desired form was also found to be helpful.

Complex formation between sulfasalazine and all three natural cyclodextrins (α-, β- and γ-CDs) was attempted by kneading 10 to 20 mg of each tautomer with an equimolar amount of a cyclodextrin. The paste was kept wet using 50 % (by volume) acetone/water solvent mixture for the MSSAL complexes, and 50 % MEK/water solvent mixture for the TSSAL complexes. Since a particular solvent is known to favour a particular SSAL tautomeric form, these water-solvent mixtures were employed to avoid one tautomer being converted to the other on kneading.

4.3 Aspirin-Cyclodextrin Inclusion Complex

Aspirin•β-CD is an example of an inclusion complex in which the IsoPXRD method cannot be used, as the complex has a unique pattern, different from any of the patterns for established isostructural classes. Thus the classical way of recording at least three PXRD traces (i.e. the trace of the suspected complex (HG), one of either the guest (G) or the host (H) alone, and that of a physical mixture of the reactants in a chosen stoichiometric ratio (H:G)) cannot be avoided in the identification of this complex by X-ray powder diffraction analysis.

The kneaded aspirin•β-CD material obtained in this study can be taken as a true inclusion complex since its PXRD trace is different from that of the host and from that of the physical mixture (see Figure 4.3). The reader is reminded that this

method is based on the assumption that the PXRD trace of the kneaded material, if different from that of a physical mixture and that of at least one of the starting materials, is probably not representative of a new phase of any of the starting materials, but a complex.

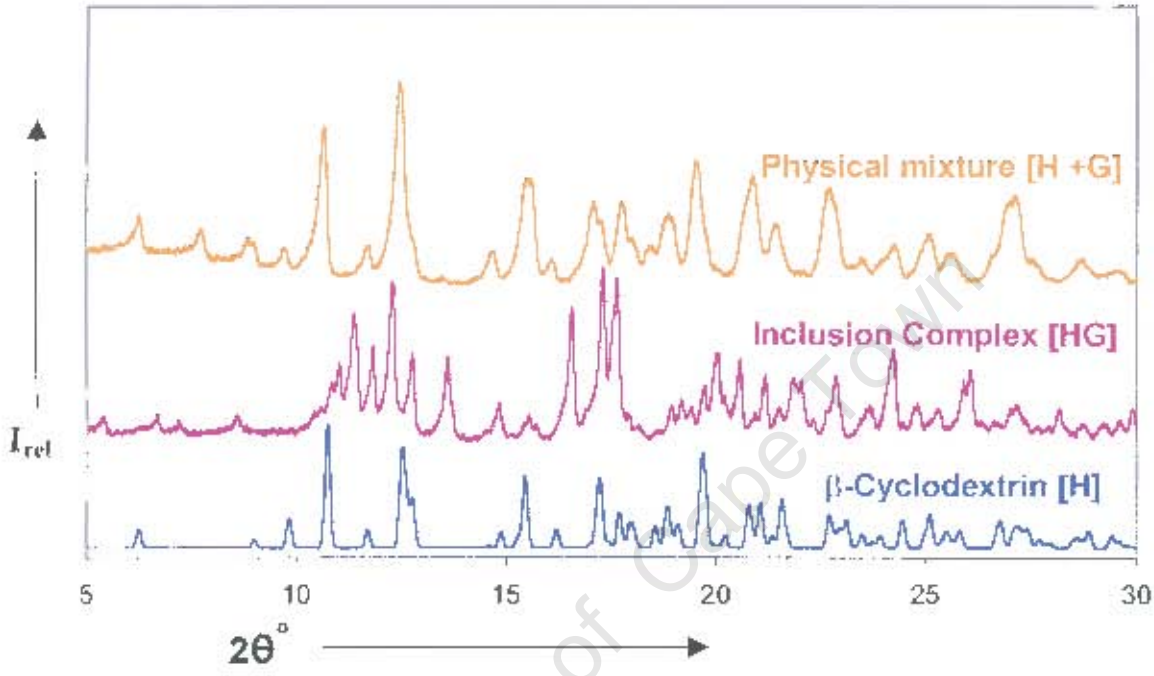

Figure 4.3 – PXRD traces recorded for the identification of an aspirin•β-CD inclusion complex.

Also noted is that the PXRD trace of the prepared complex does not match that of the reported crystal structure [5] of a quaternary aspirin•salicylic acid•β-CD hydrate complex, which belongs to series **B7** (see Chapter 3, section **3.5**).

As no further analysis was performed on the kneaded aspirin•β-CD material, it is not known to what extent it may have contained salicylic acid as a decomposition product of aspirin. Attempts to recrystallize the kneaded material in water yielded crystals of the host cyclodextrin.

4.4 Salicylamide-Cyclodextrin Inclusion Complex

The β-CD•salicylamide inclusion complex (SALMBCD) was identified using the IsoPXRD method. The PXRD trace of this complex registered very closely with the reference pattern **B6** (see Figure 4.4). The peak at 2θ = 10.7°, present in the SALMBCD complex but not in the reference pattern, appears at the same angular position as a prominent peak of the host (see Figure 4.3). Further analysis of the X-ray powder diffractogram of SALMBCD revealed more peaks at 2θ values of 12.5°, 15.4° and 19.7° that coincide with those of the host, implying the presence of the starting material in the kneaded sample. Although the material was kneaded further, up to 2 hrs, to force any uncomplexed host or guest molecules to complex, the diffractogram of SALMBCD did not change.

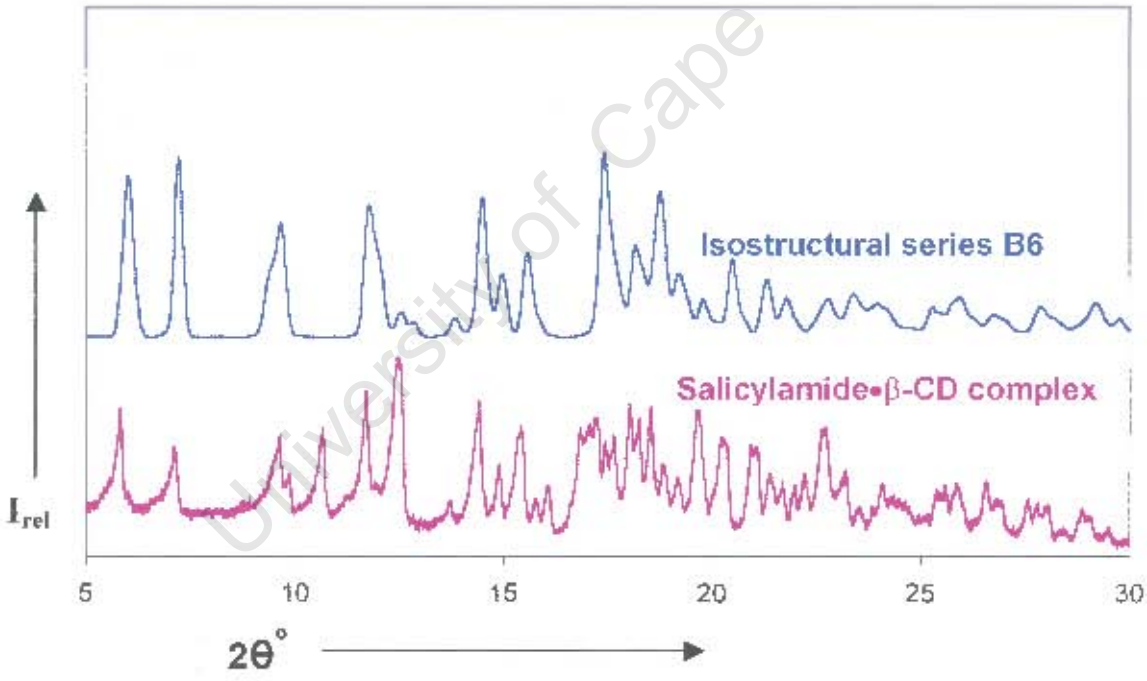

Figure 4.4 – PXRD trace of salicylamide•β-CD inclusion complex compared with the average trace of isostructural complexes comprising series **B6**.

The close similarity between the average PXRD trace for complexes comprising series **B6** and that for series **B4** was mentioned earlier (section **3.5**, Chapter 3). Therefore, great care has been taken in judging the SALMBCD complex as being isostructural with complexes of series **B6**. Consequently, it can be assumed that the prepared complex has a similar crystal structure to complexes comprising series **B6**. Thus it can be said that the solid state of this complex possesses a side-centred lattice with crystallographic space group C2 (monoclinic system). Isostructurality of the prepared complex with complexes of series **B6** also implies that it crystallizes with the approximate unit cell parameters a = 19.5 Å, b = 24.5 Å, c = 15.9 Å and β = 109°. The arrangement of CD molecules in this complex can be assumed to be that of the dimeric channel packing arrangement characteristic of complexes of series **B6**.

4.5 Sulfasalazine-Cyclodextrin Inclusion Complexes

Both the amide and the imide tautomeric forms of SSAL were employed in attempts to form inclusion complexes with the three natural cyclodextrins. However, only the monoclinic form of sulfasalazine could be included in β- and γ-cyclodextrins by the kneading method. Attempts to include the triclinic form via the same method failed. Neither of the two tautomers could be included in α-CD probably due to the relatively small cavity size of this host for a relatively large drug, sulfasalazine. The coprecipitation method was attempted using both forms and, although no complex crystals were obtained in either case, it was noted that TSSAL had difficulty in wetting compared to MSSAL.

The X-ray powder diffractogram of MSSALBCD was found to match that of series **B4** (see Figure 4.5). Thus, by a similar argument as that for the β-CD•salicylamide case appearing in the preceding section, the crystalline material of the new MSSALBCD complex can be assumed to belong to the triclinic space group P1 with approximate unit cell parameters a = 15.5 Å, b = 15.5 Å,

c = 15.8 Å, α = 102°, β = 102° and γ = 104°. CD molecules in the crystalline MSSALBCD material are expected to have a **CH**-type packing arrangement.

Although great care has been taken in matching the diffractograms of SALMBCD and MSSALBCD complexes with the reference patterns of the respective **B6** and **B4** isostructural series, the ambiguity resulting from the closeness of PXRD traces of these two series may call for further analysis of the prepared complexes for the proposed crystal data (space group and unit cell parameters) to be valid. However, since complexes of both series have CD dimers arranged in the **CH** packing mode (see Chapter 3) the topology of the host framework in the prepared complexes can confidently be said to be that of the dimeric **CH** packing arrangement as proposed.

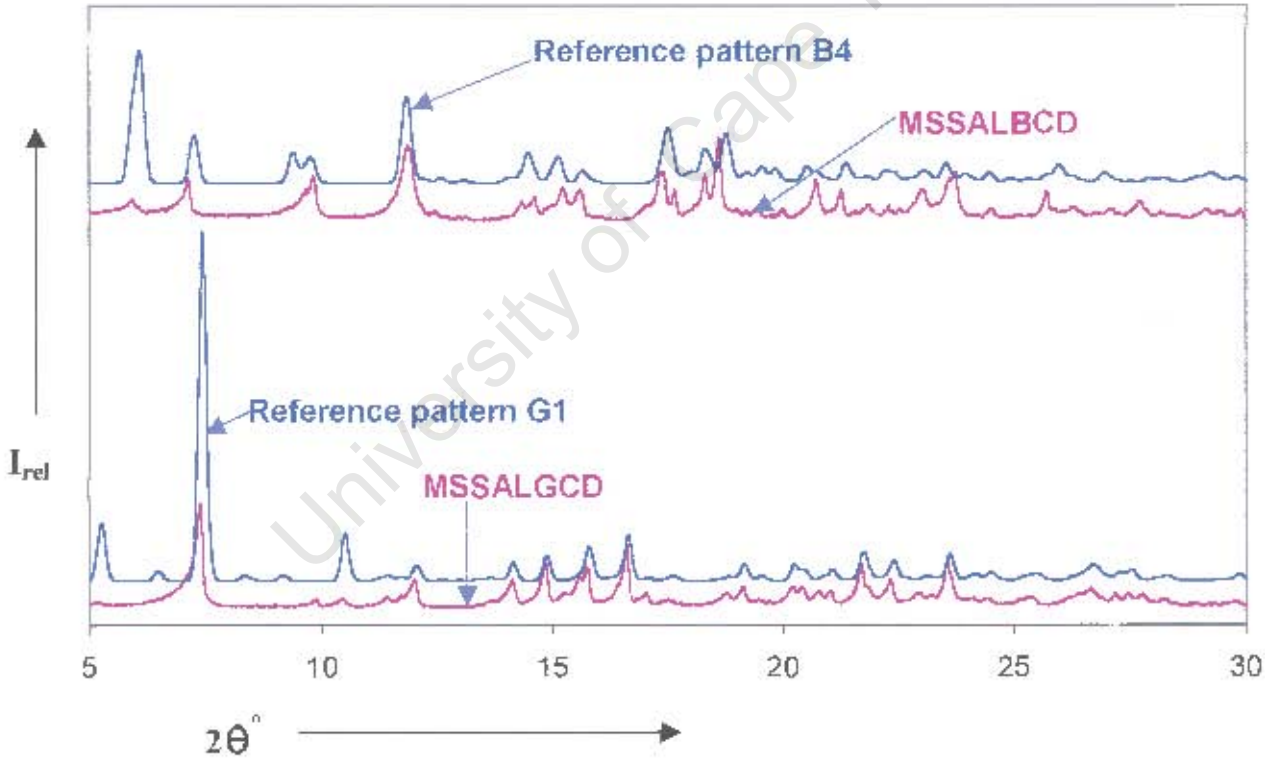

Figure 4.5 – PXRD patterns of monoclinic sulfasalazine-CD inclusion complex versus those of known isostructural series.

The prepared MSSALGCD complex was found to be isostructural with the single isostructural series of γ-CD complexes, series **G1** (see Figure 4.5). Since no ambiguity exists in this isostructural class, the space group, unit cell parameters and host packing of the MSSALGCD complex can confidently be deduced from that of isostructural series **G1**. The new complex, therefore, is expected to belong to the tetragonal space group $P42_12$ with approximate unit cell parameters a = 23.8 Å and c = 23.2 Å. The γ-CD molecules in the MSSALGCD complex can be assumed to pack in channels parallel to the crystallographic c-axis, as do complexes of series **G1**.

The experiments involving sulfasalazine thus yielded an interesting, novel result, namely preferential inclusion of one of the two tautomers of the drug in the natural cyclodextrins β- and γ-CD. As shown in Figure 4.2, the difference between these forms is manifested as an apparently minor proton shift, but this is evidently sufficient to enable their discrimination by the host CD molecules. The two tautomers are known to adopt different conformations and hydrogen bonding arrangements in their respective crystal structures [6,7].

As stated in Chapter 3 (section **3.1**), the notion of the IsoPXRD method is being recognised by other researchers apart from our own routine application of the method. Thus, an inclusion complex of 2-phenoxyethanol in β-cyclodextrin was identified by comparing its PXRD pattern with that computed from the crystal structure of an isostructural compound (Z)-9-Dodecen-1-ol•Ethanol•β-CD [9], which appears in series **B6** of our library of reference patterns. The reaction product between β-CD and 2-phenoxyaniline was also confirmed as an inclusion complex on matching its PXRD trace with that computed from a known β-CD•benzocaine complex [10]. The authors were then able to deduce crystal packing arrangements of the prepared complexes based solely on matching PXRD patterns. Conversely, complexes with different X-ray powder diffractograms could be assumed to possess different crystal packing arrangements [10].

4.6 References

1. S. Budavari, M. J. O'Neil, A. Smith, P. E. Heckelman, *The Merck Index – an encyclopedia of chemicals, drugs and biologicals*, 11th Edition, Merck & Co. Inc., U.S.A., 1989.
2. H. S. Choi, A. H. Coll, K. U. Kon, S. K. Seoul, *B. Kor. Chem. Soc.*, 1992, **13**, 474 – 479.
3. W. Wu, L. Zhuang, Y. Lin, Y. Mo, *Guangdong Yaoxueyuan Xuebao*, 1995, **11**, 1 – 3.
4. Y. Nakai, K. Yamamoto, K. Terada, *Funtai Kogaku Kaishi*, 1983, **20**, 728 – 733.
5. F. Nishioka, I. Nakanishi, T. Fujiwara, K. Tomita, *J. Incl. Phenom. Macro.*, 1984, **2**, 701 – 714.
6. L. A. Filip, M. R. Caira, S. I. Fărcaş, M. T. Bojita, *Acta Crystallogr.*, 2001, **C57**, 435 – 436.
7. A. J. Blake, X. Lin, M. Schroder, C. Wilson, R-X Yuan, *Acta Crystallogr.*, 2004, **C57**, 226 – 228.
8. L. A. Filip, *PhD Thesis, Contribuţii La Studiul Fizico-Chimic Şi Al Unor Complecşi Cu Derivaţi Din Clasa Salazinelor,* Universitatea De Medicină Şi Farmacie "Iuliu Haţieganu" Facultatea De Farmacie, Cluj-Napoca, Romania, 2002.
9. L. Cunha-Silva and J. J. C. Teixeira-Dias, *New J. Chem.*, 2004, **28**, 200 – 206.
10. S. S. Braga, P. Ribeiro-Claro, M. Pillinger, I. S. Gonçalves, F. Pereira, A. C. Fernandes, C. C. Romão, P. B. Correia and J. J. C. Teixeira-Dias, *Org. Biomol. Chem.*, 2003, **1**, 873 – 878.

CHAPTER 5: INCLUSION OF SALTS OF DICLOFENAC IN β-CYCLODEXTRIN

5.1 Introduction

Diclofenac, chemically known as 2-[(2,6-dichlorophenyl)amino]benzeneacetic acid, is a well known NSAID commonly used for the treatment of painful inflammations such as osteoarthritis, rheumatoid arthritis, abdominal cramps, and ankylosing spondylitis. The anti-inflammatory activity of diclofenac is thought to be related to the inhibition of the conversion of arachidonic acid to prostaglandins, which are the mediators of the inflammatory process [1].

Diclofenac is largely administered in its salt form because of the low aqueous solubility associated with its free acid form [2,3]. The pharmaceutical compositions of the potassium and the sodium salts of this drug are available as *cataflam*® and *voltaren*® respectively [4-6]. The potassium salt of this drug is water soluble and is preferred for acute conditions while the sodium salt, which is sparingly soluble in water, is preferred for the treatment of chronic illnesses. Figure 5.1 below shows the IUPAC line drawing of the diclofenac anion.

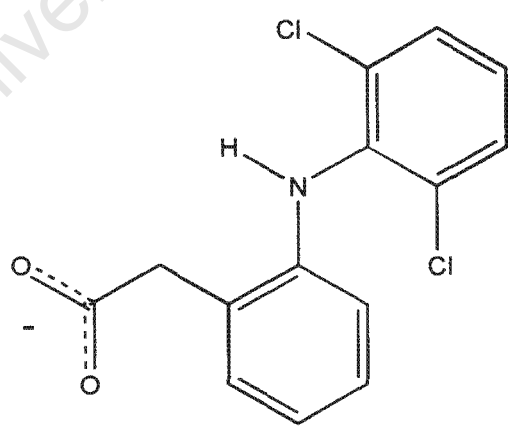

Figure 5.1 – Structure of the diclofenac anion, a drug guest used in β-CD inclusion studies in this dissertation.

Like other NSAIDs, diclofenac is known to cause gastrointestinal ulceration and bleeding [7-9]. Diclofenac has also been suspected to be associated with the development of a variety of disease conditions such as *corneal perforation and melting, hepatitis, autoimmune haemolytic anaemia and thrombocytopenia* [10-13]. Different treatment strategies and a number of pharmaceutical preparations have been developed in order to reduce the undesirable side effects of this drug [14-21]. These include co-administration of diclofenac with other drugs, inorganic and organic salt preparations of diclofenac, and formulations containing lipids, cyclodextrins or other polymers.

Cyclodextrin inclusion complexes of diclofenac have been reported to advance the therapeutic properties of this drug while at the same time masking the undesirable side effects. Consequently, studies of diclofenac inclusion complexes with the three natural cyclodextrins (and some of their derivatives) have been carried out [22-28]. Although interactions between the diclofenac anion and β-CD have been investigated, both in solution [27, 29-33] and in the solid state [34-35], only one crystal structure has been reported thus far, that of the sodium salt of this drug with β-cyclodextrin (DNaBCD) [36].

Thus in this chapter, we report the preparation, characterisation and crystal structure analyses of β-CD inclusion complexes of the potassium and the caesium salts of diclofenac. The isostructural behaviour of these salt inclusion complexes is also highlighted and comparisons are made with the known sodium analogue [36].

5.2 Preparation

For both the caesium and the potassium inclusion complexes, complex preparation was achieved by the following ion exchange reactions (the reader is referred to pages iii and iv for abbreviations and symbols used in the chemical equations below):

$$DNa\ (s) + KCl\ (s) + BCD\ (s) + H_2O\ (l) \rightarrow DKBCD\ (s) \downarrow + NaCl\ (aq)$$

$$DNa\ (s) + CsCl\ (s) + BCD\ (s) + H_2O\ (l) \rightarrow DCsBCD\ (s) \downarrow + NaCl\ (aq)$$

1:1 molar ratios of DNa:β-CD were used in the presence of an excess amount of either KCl or CsCl for the preparation of the potassium and the caesium complexes respectively. Thus 100 mg of β-CD, 30 mg DNa and 75 mg KCl were used for the preparation of the DKBCD complex while 100 mg of β-CD, 30 mg DNa and 168 mg CsCl were used in the preparation of the DCsBCD complex. For each complex, the pre-weighed amounts were dissolved in 4 ml of water at 65 - 70°C with constant stirring for 60 minutes. The resulting clear solution was, in each case, filtered into a glass vial with a 0.45 μm nylon microfilter while hot. The vial was then closed with parafilm, which was punctured a few times using a needle to enhance evaporation while at the same time preventing dust particles from entering the vial. Clear crystals were obtained after leaving the preparations at room temperature for three to four weeks. Similar results could also be achieved within a week by growing crystals at elevated temperatures (55 – 60 °C). Leaving the preparations in the refrigerator resulted in a white powder which we did not characterise further.

5.3 Characterisation

5.3.1 Hot Stage Microscopy

Crystals were taken out of the vials and the excess mother liquor was removed using dry filter paper. These crystals were then placed on a cover slip, submerged in silicone oil and were heated at a rate of 10 K min^{-1}. HSM photographs of both DKBCD and DCsBCD are presented in Figure 5.2. The colour change from colourless to brown, evident at about 215 °C, is attributed to complex decomposition. The presence of a complex is supported by the fact that

for the host alone, the decomposition temperature is considerably higher. Diclofenac sodium has a melting point in the range 283 – 285 °C and its free acid is known to melt at 156 – 158 °C [37], neither of which events was observed in the HSM analysis, implying that the prepared complex is free of the starting materials. Both the DKBCD and DCsBCD complexes displayed similar thermal events. They commenced dehydrating at about 100 °C as indicated by bubbles evolving from the silicone oil, and decomposed at about the same temperature.

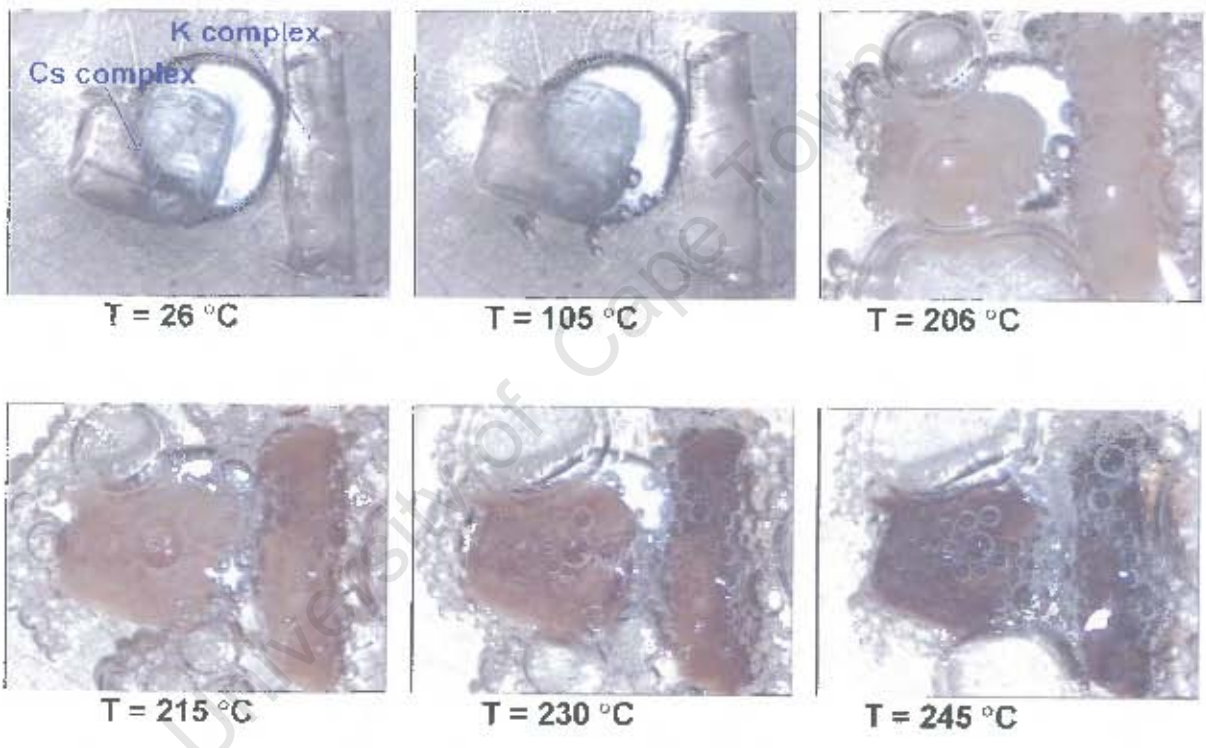

Figure 5.2 – HSM images of both DKBCD (the potassium complex) and DCsBCD (the caesium complex) recorded at various temperatures. Both complexes were heated on the same slide as shown.

5.3.2 TGA, Karl-Fischer and DSC

Karl-Fischer and TGA techniques were used to determine the amount of water of crystallization in each complex. We used both techniques in a complementary way as preliminary results from the TGA analysis had a high variance. Better consistency for TGA results was obtained by allowing samples to equilibrate with the atmospheric conditions overnight following their removal from the mother liquor. For all three analyses (Karl-Fischer, TGA and DSC), samples were crushed into a powder after being left to dry in an open atmosphere overnight. Measurements were taken on the same sample batch for all techniques and analysis results are given in Table 5.1. Although the Karl-Fischer and TGA techniques have overlapping error ranges, the Karl-Fischer technique estimated slightly higher nominal values of **n** (water of crystallization), by about 0.3 H_2O molecules per complex unit, than the number of water molecules that could be located in the crystal structures of both the DKBCD and DCsBCD complexes.

Table 5.1 – TGA and Karl-Fischer results for both the potassium and the caesium complexes.

TECHNIQUE	TGA		KARL-FISCHER	
Complex	% Mass loss	n	% Moisture	n
$C_{42}H_{70}O_{35}\bullet C_{14}H_{10}Cl_2NO_2^-K^+\bullet nH_2O$	10.9 ± 0.5	9.5 – 10.5	12.2 ± 1	10.3 – 12.4
$C_{42}H_{70}O_{35}\bullet C_{14}H_{10}Cl_2NO_2^-Cs^+\bullet nH_2O$	10.0 ± 0.5	9.1 – 10.1	11.3 ± 1	9.9 – 12.1

Good correlation is observed between the DSC and TG traces of both complexes. The DSC endotherm at about 70 – 110 °C in both complexes (Figure 5.3) can be interpreted as an enthalpy change resulting from the loss of complex water. This water loss was also captured on the HSM images (Figure 5.2) as bubbles commencing at 105 °C. Thus the mass loss on the TG traces, from *ca*

30 °C to about 150 °C (Figure 5.3), has been interpreted as due to complex dehydration. This TGA mass loss was used to quantify the hydration of each complex and the values are presented in Table 5.1.

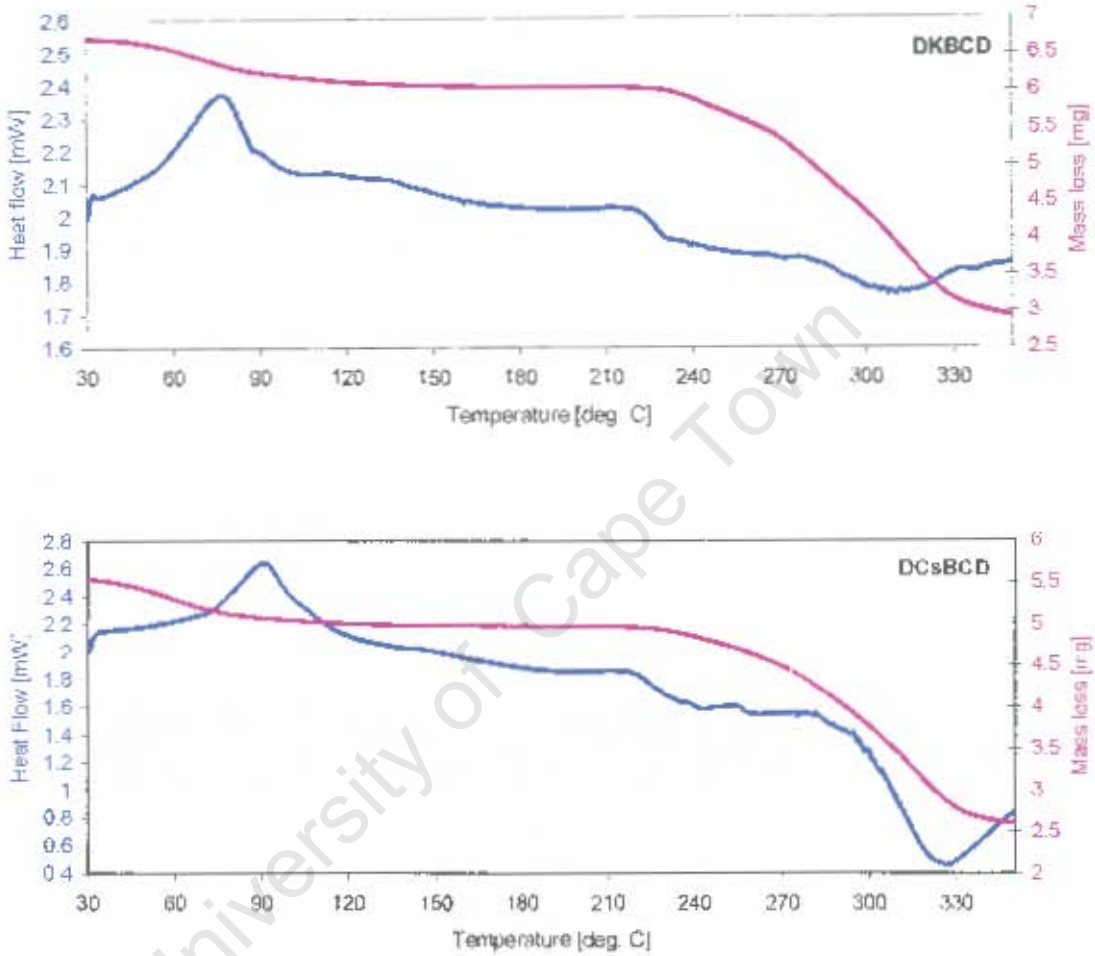

Figure 5.3 – Representative TG (in pink) and DSC (in blue) traces of both DKBCD and DCsBCD complexes.

HSM implied complex decomposition at 215 °C (images in Figure 5.2) and the vast mass loss on the TG (following a plateau from the mass loss due to complex dehydration) indicative of complex degradation starts at about the same

temperature. This decomposition also manifests itself as a broad exothermic peak in the DSC curve, with an onset temperature at about 220 °C. Also notable is the similar trend in the DSC curves of both DKBCD and DCsBCD implying similar thermal events such as complex dehydration and degradation pathways.

5.3.3 Elemental analysis

Further characterisation of the prepared complexes by elemental analysis served two purposes. Firstly, it was to confirm the host:guest:water ratio for the complex formulae in Table 5.1. The second reason was to monitor the completeness of the exchange reaction, i.e. the replacement of the sodium ion by the potassium (or caesium) ion, performed in the preparation of these complexes (refer to chemical equations in section 5.2).

Elemental analysis was performed on the same batch as that used for thermal analyses. For each prepared complex (DKBCD and DCsBCD), the microanalysis results presented in Table 5.2 are in line with the host:guest:water ratios used in calculations of **n** using TG analysis. The good agreement between the calculated and the experimental CHN results also rules out the possibility of an incomplete reaction, or the product being a mixture of reaction species.

Table 5.2 – Calculated and experimental CHN results for both the DKBCD and DCsBCD complexes. Microanalysis data are given as the average of three determinations.[1]

Complex Formula	$C_{42}H_{70}O_{35}•C_{14}H_{10}Cl_2NO_2^-K^+ •10H_2O$		$C_{42}H_{70}O_{35}•C_{14}H_{10}Cl_2NO_2^-Cs^+ •9.6H_2O$	
Element	Calculated	Experimental	Calculated	Experimental
% C	40.78	40.83	38.75	38.82
% H	6.11	6.05	5.76	5.72
% N	0.85	1.03	0.81	0.81

[1]Average e.s.d. for experimental values is ± 0.2 %.

5.4 Crystal Structure Analysis

5.4.1 Preliminary Space Group Determination

Preliminary unit cell parameters and Laue groups of both the DKBCD and DCsBCD complexes were checked on the Nonius Kappa CCD diffractometer with the crystals maintained at room temperature. The findings suggested isostructural behaviour in the two complexes, with the caesium complex having a slightly larger unit cell volume than the potassium complex. The preliminary check indicated a primitive orthorhombic lattice for both complexes.

Monocrystals of high quality (as indicated by their ability to extinguish plane-polarised light uniformly) were then selected and cut to near cubic dimensions of 0.30 x 0.30 x 0.30 mm^3 for the potassium complex and 0.12 x 0.16 x 0.19 mm^3 for the caesium complex. The crystals were then mounted on a glass fibre and covered with Paratone N oil to provide a rigid mounting for low temperature data-

collection. The Paratone N oil also helped to prevent dehydration, which would in turn result in crystal cracking. Crystals were then cooled to -160 °C to reduce atomic thermal vibrational motion. This was necessary to optimise the diffraction quality, ensuring the collection of high-angle data to maximise the resolution.

5.4.2 *Intensity Data-Collection*

After cooling the crystal, the data were then collected on the same Nonius Kappa CCD diffractometer, with instrument settings as described in Chapter 2. It became apparent during the refinement and model optimisation stages of the crystal structures that the reflection intensity data suffered from absorption effects and therefore data recollections with direction cosines were performed. The previous sets of data were thus discarded. Only the results based on the final data sets that were collected with direction cosines and subsequently corrected for absorption are reported here. The default parameters in the SADABS [see Chapter 2 for SADABS reference] program were used in absorption treatment of the data of the two complexes. The intensity data were collected for the θ range of 1.4° – 27.3° for the potassium complex and 1.4° – 25.8° for the caesium complex, with the respective crystal to detector distances of 46 and 52 mm. The completeness of the intensity data-collection was 98.6 % for DKBCD and 99.8 % for DCsBCD with respective exposure times of 30 and 106 seconds per frame. Longer exposure times were deemed necessary for the caesium complex, whose data were collected in P1 but later processed in the correct space group. Data-collection parameters, refinement parameters as well as refined crystal data for the studied diclofenac salt inclusion complexes are presented in Table 5.3.

Table 5.3 – Crystal data, data-collection and refinement parameters for the DKBCD and DCsBCD crystal structures

Complex	DKBCD	DCsBCD
Complex Formula	$C_{42}H_{70}O_{35}•C_{14}H_{10}Cl_2NO_2^-K^+ •10H_2O$	$C_{42}H_{70}O_{35}•C_{14}H_{10}Cl_2NO_2^-Cs^+ •9.6H_2O$
M_r	1649.40 g.mol^{-1}	1736.00 g.mol^{-1}
Crystal System	Orthorhombic	Orthorhombic
Space Group	$P2_12_12_1$	$P2_12_12_1$
a	15.4777(1) Å	15.4668(1) Å
b	25.9583(2) Å	26.0042(2) Å
c	36.7799(2) Å	36.8118(4) Å
V	14777.2(2) Å^3	14805.8(2) Å^3
Z	8	8
D_{calc}	1.483 g.cm^{-3}	1.557 g.cm^{-3}
Mosaicity	0.8°	0.8°
F (000)	6976	7184
μ (MoK_α)	0.25 mm^{-1}	0.68 mm^{-1}
Crystal Size	0.30 x 0.30 x 0.30 mm^3	0.12 x 0.16 x 0.19 mm^3
Temperature	113 K	113 K
θ range scanned (°)	1.4 – 27.3	1.4 – 25.8
Index Ranges	h: –19,19; k: –33,33; l: –44,47	h: –18,18; k: –31,31; l: –44,47
Reflections Collected	148189	342970
Unique Reflections	32677	28243
R_{Int}	0.065	0.113
R_σ	0.077	0.087
Reflections with $I > 2\sigma(I)$	27018	20144
Least-Squares Parameters Refined	1478	1450
S	1.11	1.04
R Indices	R_1 = 0.0902, wR_2 = 0.2114	R_1 = 0.0821, wR_2 = 0.2313
Shift/e.s.d. (Maximum, Average)	0.02, 0.00	0.02, 0.00
Flack x Parameter	0.03(6)	0.04(2)
$(\Delta\rho)_{max}$ final	1.71 e·Å^{-3}	2.55 e·Å^{-3}
$(\Delta\rho)_{min}$ final	-0.86 e·Å^{-3}	-0.64 e·Å^{-3}

5.4.3 Space Group Confirmation and Structure Solution

The space group assignments were confirmed using the program XPREP [referenced in Chapter 2] which indicated a primitive lattice type on input of cell dimensions to the *hkl* files of both DKBCD and DCsBCD. A search for higher symmetry indicated the orthorhombic crystal system, with mean $|E^2 - 1| = 0.682$ for the potassium complex. Further inspection of the DKBCD reflection data using the program LAYER [referenced in Chapter 2] implied the presence of three sets of screw axes as evidenced by the systematic absences h = 2n +1 on h00, k = 2n + 1 on 0k0 and l = 2n + 1 on 00l. There were a few indexed reflections violating this systematic absence behaviour in the collected DKBCD intensity data. We therefore increased the tolerance parameter in XPREP, from 4 to 8, to cater for these violations. This resulted in the space groups P222, $P222_1$, $P2_12_12$ and $P2_12_12_1$ being indicated as possible space groups. However the structure could not be solved in P222, $P222_1$ or $P2_12_12$ as alternative space groups suggested by XPREP, though with lower figures of merit than that for $P2_12_12_1$. The space group chosen for solution of the DKBCD structure was therefore $P2_12_12_1$.

For the caesium complex, the space group $P2_12_12_1$, with mean $|E^2 - 1| = 0.732$, was indicated as having the lowest CFOM by the XPREP computer program. Thus the space group $P2_12_12_1$ was also used for the solution of the DCsBCD crystal structure. In each case, the unit cell volumes were consistent with two complex formula units per asymmetric unit.

The diclofenac potassium•β-CD crystal structure was solved *ab initio* using the SHELXD computer program [referenced in Chapter 2], which revealed the positions of the potassium ions as well as most of the non-hydrogen atoms of the host molecules and guest anions. The DKBCD complex formula as determined from TG and elemental analyses (Table 5.2) had been used to calculate 80 % of the non-hydrogen atoms for the FIND command, with a starting value of 220

(increments of 10 for each subsequent cycle) set for the PLOP command. The run was terminated based on the CC value, which was beyond 85%. The carbon skeleton of the two CD rings comprising an asymmetric unit of the DKBCD crystal structure could be unambiguously located after a SHELXD run, which took several hours.

The diclofenac caesium•β-CD crystal structure was solved by molecular replacement using the rigid part of the host framework of the refined DKBCD structure. All atoms of the starting model (refined DKBCD host) were however assigned isotropic thermal parameters for the starting cycles so that the model was unbiased for the caesium complex.

5.4.4 Key for Complex and Atom Nomenclature

For ease of comparisons, a similar numbering scheme for the host molecules and guest anions of both the DKBCD and DCsBCD structures was followed and is shown in Figure 5.4. Since there are two crystallographically independent complex units comprising an asymmetric unit (in both DKBCD and DCsBCD), one complex unit will henceforth be referred to as the **P** unit and the other the **Q** unit. The **P** unit consists of the host whose glucose residues are labelled $\mathbf{G_A} \rightarrow \mathbf{G_G}$ and the guest labelled $\mathbf{Cl_1} \rightarrow \mathbf{O_{19}}$, while the **Q** unit consists of the host labelled $\mathbf{G_H} \rightarrow \mathbf{G_N}$ and the guest labelled $\mathbf{Cl_{20}} \rightarrow \mathbf{O_{38}}$ (Figure 5.4). The numbering of atoms of a glucopyranose ring then changes accordingly such that the conventional $\mathbf{O_6}$ atom then becomes $\mathbf{O_6A}$ for the glucose residue $\mathbf{G_A}$, $\mathbf{O_6B}$ for the glucose residue $\mathbf{G_B}$ and so on.

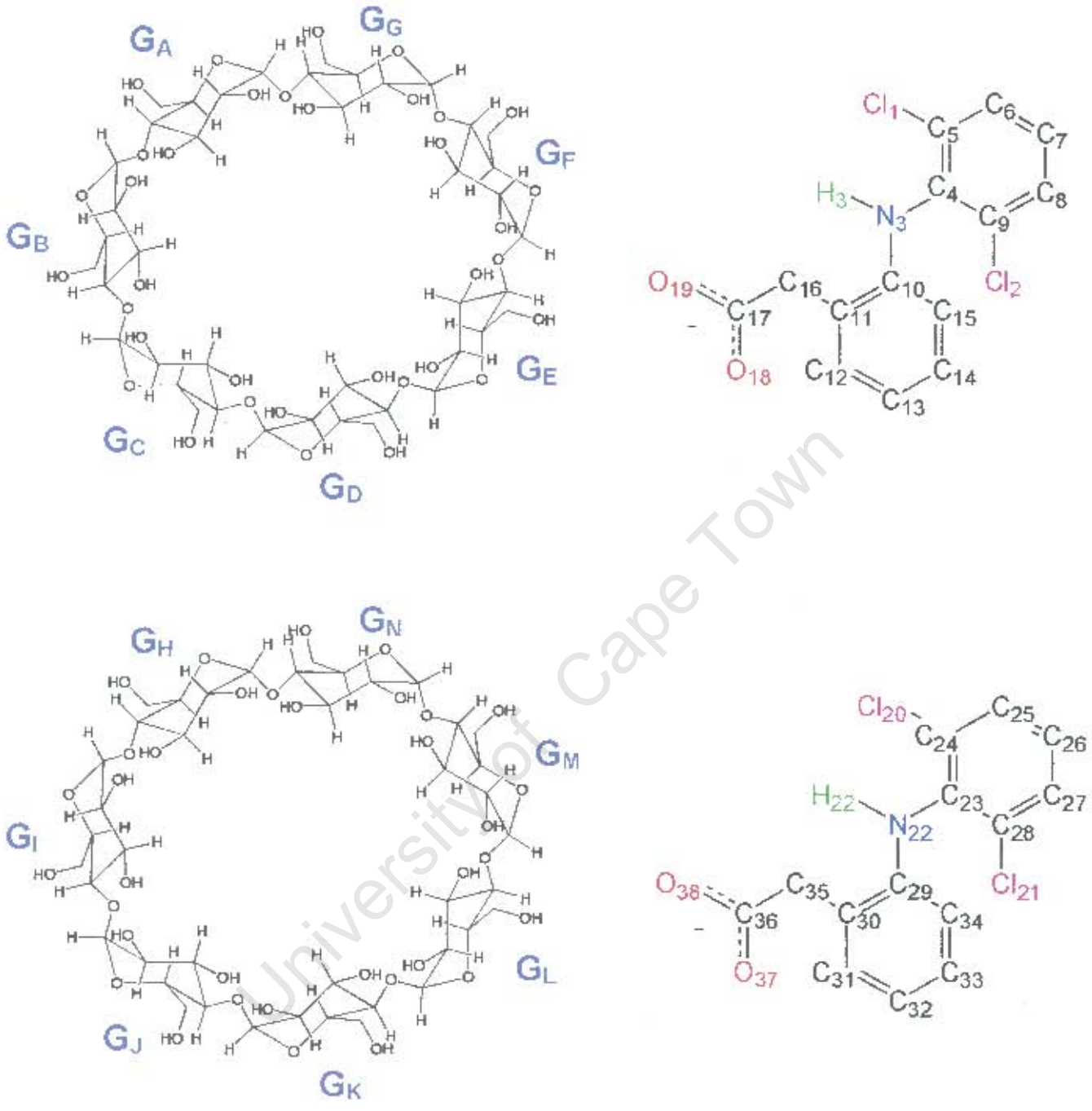

Figure 5.4 – Schematic diagrams showing the host and guest numbering, which is common in both the DKBCD and DCsBCD structures. The top diagrams of both the host and the guest molecules are of a crystallographically independent complex unit (hereinafter the **P** unit) while the bottom diagrams belong to the second crystallographically independent unit (herein after the **Q** unit).

In both the DKBCD and DCsBCD structures, the metal ions and water molecules are on the peripheries of the independent **P** and **Q** complex units and as such cannot be exclusively associated with a unit. Thus for the potassium structure, the two peripheral metal counterions located in the asymmetric unit have been labelled K_1 and K_2 arbitrarily. Since K_1 was later found to be disordered over two sites, the disordered fragments were then labelled K_1A and K_1B (as they appear in Table 5.4). Similarly, the labelling of the disordered fragments of the two caesium ions in the asymmetric unit of the DCsBCD structure is Cs_1A and Cs_1B for one complementary fragment, and Cs_2A and Cs_2B for the other complementary fragment.

All oxygen atoms of water molecules are labelled with a suffix "**W**" (**WA** and **WB** for the disordered water molecules) and are numbered with a subscript (being an integer from one to the maximum number of water molecules located for each structure). Consequently, the twenty water molecules in the asymmetric unit of the potassium complex are labelled $O_1W \rightarrow O_{20}W$, with the disordered O_1W and O_2W labelled O_1WA/O_1WB and O_2WA/O_2WB for the complementing pair of disordered atoms. The same numbering applies for oxygen atoms of water molecules located in the crystal structure of the caesium complex whereby also O_1W and O_2W were found to be disordered and so were labelled O_1WA/O_1WB and O_2WA/O_2WB for the complementary pair. There are eighteen water molecules in the DCsBCD asymmetric unit.

5.4.5 Structure Refinement and Model Optimisation

Both the DKBCD and DCsBCD structures were refined in SHELXL-97 [ref in Chapter 2] by the location of atoms as revealed by difference Fourier syntheses following the least-squares optimisation of the agreement between calculated intensities for the model with those observed from the collected crystal data. The heavy atoms (**K** or **Cs** ions) of each structure were assigned after the first refinement cycle. The assignment of the guest **Cl** and **N** atoms followed. The

cyclodextrin O_2, O_3 and O_6 atoms were then assigned as they appeared on the subsequent difference Fourier maps. All assigned atoms were initially refined isotropically with their thermal parameters being constantly monitored after each cycle. Most of the non-hydrogen atoms were later refined anisotropically, at which point oxygen atoms of the water molecules were assigned.

During refinement of some of the guest non-hydrogen atoms, it became evident that one potassium ion in DKBCD is disordered over two positions, while the second, crystallographically independent potassium ion refined well with a full site-occupancy factor (s.o.f.). The two caesium ions were found to be disordered, each over two positions, in the DCsBCD crystal structure. One O_6 atom in both the DKBCD and DCsBCD structures was also found to be disordered over two sites. The disordered fragments of the O_6 atom occur at identical glucopyranose residues, G_H, in the two structures and with similar s.o.f.'s and fractional coordinates (Table 5.4).

The disordered atoms or ions were modelled by assigning each disordered fragment a fixed U_{iso} value (averaged from ordered atoms of similar type) with variable s.o.f.'s, **x** for one fragment and **1-x** for the other. On settlement of the s.o.f.'s to relatively stable values, the heavy atoms (**K** ions in DKBCD and **Cs** ions in DCsBCD) were allowed to refine anisotropically. With the exception of the disordered atoms/ions and carbon atoms, all the oxygen atoms of the host molecules were refined anisotropically during the late stages of the refinement. For the guest (diclofenac anions), only the carbon atoms of the phenyl rings, and all hydrogen atoms, were refined isotropically in both structures.

Table 5.4 – Refined s.o.f. values and fractional coordinates of disordered atoms in the DKBCD and DCsBCD crystal structures. In parentheses are the estimated standard deviations (e.s.d.'s).

Atom Label	x/a	y/b	z/c	s.o.f.
DKBCD				
K_1A	-0.0813(2)	0.3002(1)	0.57992(6)	0.540
K_1B	0.1673(2)	0.1996(1)	0.59544(7)	0.460
O_6HA	-0.1996(5)	0.6829(3)	0.7385(2)	0.460
O_6HB	-0.1062(6)	0.6997(3)	0.6955(2)	0.540
O_1WA	0.2961(7)	0.1594(4)	0.5739(3)	0.530
O_1WB	0.7752(6)	0.3849(4)	0.3958(3)	0.470
O_2WA	-0.0125(5)	0.6686(2)	0.3811(2)	0.760
O_2WB	-0.051(2)	0.6607(8)	0.4085(7)	0.240
DCsBCD				
Cs_1A	0.31833(5)	0.81077(2)	0.65482(2)	0.780
Cs_1B	0.7410(2)	0.3446(1)	0.40619(7)	0.220
Cs_2A	0.12968(7)	0.89698(4)	0.85765(3)	0.530
Cs_2B	0.69319(8)	0.69366(6	0.67152(3)	0.470
O_6HA	-0.089(1)	0.7005(6)	0.6976(4)	0.557
O_6HB	-0.195(1)	0.6842(7)	0.7372(5)	0.443
O_1WA	-0.2810(8)	0.4298(5)	0.8547(4)	0.470
O_2WA	0.7403(8)	0.5330(4)	0.4028(3)	0.600
O_1WB	-0.3769(8)	0.4263(4)	0.8713(3)	0.530
O_2WB	0.7991(9)	0.5421(6)	0.4240(4)	0.400

Twenty water molecules were located in the asymmetric unit of the DKBCD crystal structure (an equivalent of 10 water molecules per complex formula unit) while eighteen water molecules (an equivalent of 9 water molecules per complex formula unit) could be located in the DCsBCD structure. Two of the located water molecules in each complex crystal structure were disordered, each over two sites, and were modelled as described above.

Except for the hydroxyl hydrogen atoms of the host, hydrogen atoms were generally added in idealised positions using a riding model. The hydroxyl H-atoms of the host were refined using a hydrogen bond searching model. In some

cases in which a clash of H-bonding was identified, one of the involved H-atoms was refined using a maximum electron density searching model. H-atoms were not placed on the disordered components of the host molecule. No disorder was observed in the guest anions. No attempts were made to locate water hydrogen atoms.

The structural models for both complexes fit the collected data as can be seen from the **R** indices, **S** values and other refinement parameters shown in Table 5.3. While deliberate attempts were made to reduce absorption error as far as possible (i.e use of small, equant crystals and empirical absorption corrections applied using program SADABS), some residual error remained. Further difficulties associated with cation disorder rendered the final refinements challenging. Thus residual electron densities above 1 eÅ $^{-3}$ are present in both structures. The maximum residual electron density, 2.55 eÅ $^{-3}$, in the difference Fourier map of the caesium complex could not be eliminated. This peak occurs at a distance of 1.14 Å from a disordered fragment of the caesium ion (**Cs_1B**). Other atoms neighbouring this residual peak, including symmetry equivalents, are **H_6E**, **O_2D** and **O_6E** with respective distances of 2.08, 2.78 and 2.90 Å. Considering that the DCsBCD complex was analysed as having 9.6 water molecules per complex unit (in Tables 5.1 and 5.2) and yet only 9 were found in the crystal structure, it was tempting to assign the peak as a water molecule but again it is too close (1.14 Å) to a caesium fragment (**Cs_1B**) and consequently could not be refined as such. Bearing in mind the large atomic number of the caesium ion (54 electrons) and the problems associated with its disorder, the final residual density of 2.55 e·Å^{-3} was considered tolerable. A relatively large residual electron density of 1.50 e·Å^{-3} was reported for the caesium niflumate•β-CD complex [38].

As seen in Table 5.3, both the DKBCD and DCsBCD complexes crystallize in the same orthorhombic space group, $P2_12_12_1$, with very similar unit cell parameters and with two formula units in their respective asymmetric units. In contrast to this the DNaBCD complex [36] crystallizes in space group $P6_1$ with one complex formula unit of 1:1 host-guest ratio in its crystallographic asymmetric unit. Furthermore, unit cell edges and interaxial ratios of the DNaBCD complex (a = 15.956 Å and c = 50.95 Å) are distinct from those of the K and Cs analogues. Thus the isostructural DKBCD and DCsBCD inclusion complexes are expected to be non-isostructural with the DNaBCD complex. Comparisons between these three diclofenac salt•β-cyclodextrin inclusion complexes will be presented in the subsequent sections.

5.4.6 Description of the Structure and the Mode of Drug Inclusion

The unique unit required to generate the full contents of the unit cell in both DKBCD and DCsBCD crystal structures consists of a pair of crystallographically independent host-guest complex units and associated water molecules. The reader is referred to section *5.4.4* for nomenclature of the two crystallographically independent host-guest complex units. In each structure, the two CD rings of the **P** and **Q** units are held together by metal coordination bonds and by two types of hydrogen bonds. These two types of hydrogen bonds are the direct head-to-tail links ($O_{6(P)}\cdots O_{2(Q)}$ or $O_{6(P)}\cdots O_{3(Q)}$) and the solvent-mediated links ($O_{6(P)}\cdots OW\cdots O_{2(Q)}$ or $O_{6(P)}\cdots OW\cdots O_{3(Q)}$). Metal- and solvent-mediated interactions are discussed in section *5.4.7*, while host-host intermolecular interactions are discussed in section *5.4.8*. Stereoviews of the DKBCD and DCsBCD X-ray structures, with the components of the asymmetric units, are shown in Figure 5.5.

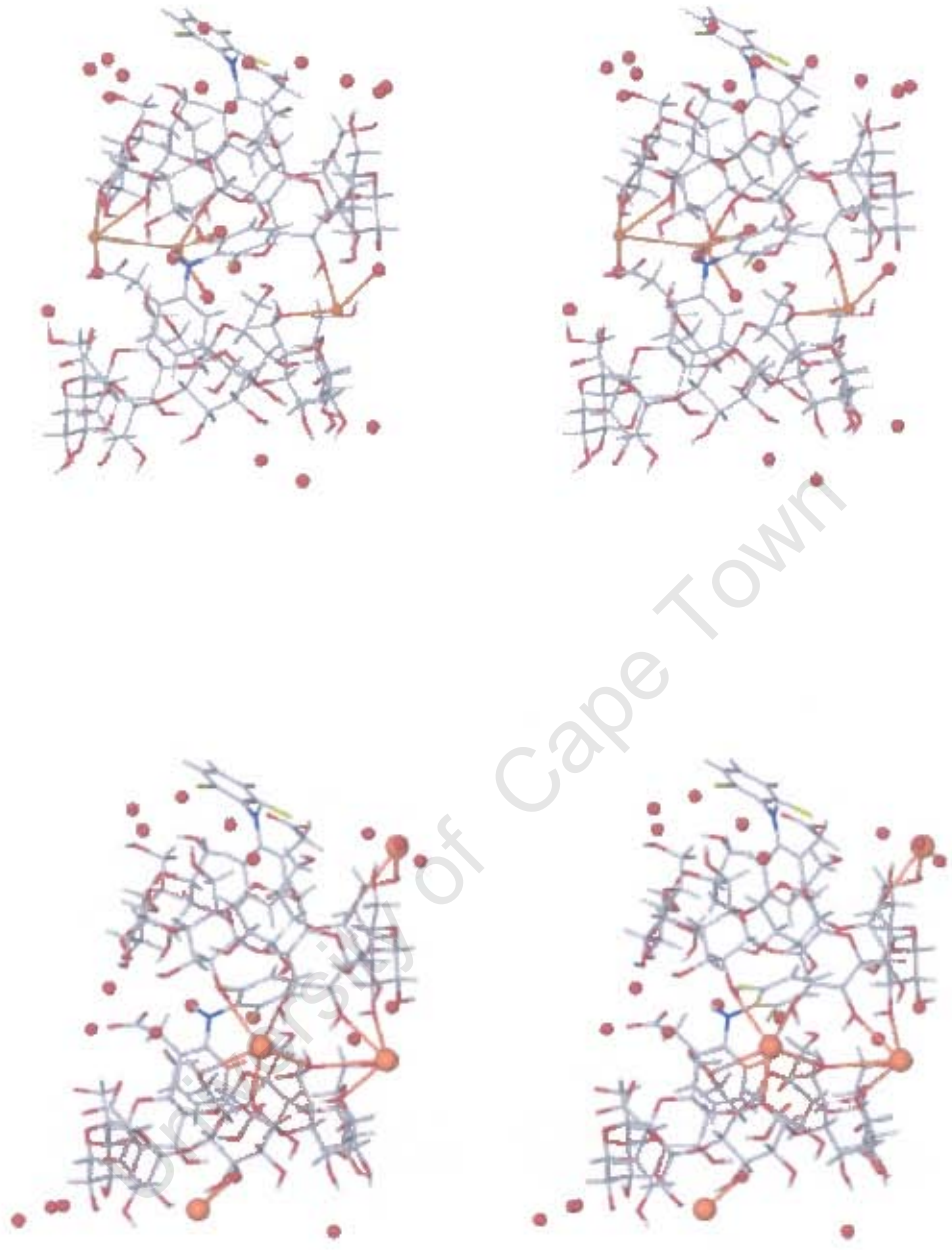

Figure 5.5 – Stereo diagrams showing the asymmetric units of DKBCD (top) and DCsBCD (bottom) complexes as viewed along the crystallographic *b*-axis. Metal cations and water molecules are shown in ball-and-stick mode.

Details of Guest Inclusion Mode

As was the case for the DNaBCD complex [36], the phenyl acetate moiety of the drug in the DKBCD and DCsBCD complexes inserts into the CD cavity via the primary side while the dichlorophenyl residue includes into the secondary side of the neighbouring β-CD molecule (Figures 5.5 and 5.6). The **chlorine, amine, methylene** and **carboxylate** portions of the drug are 'sandwiched' between successive CD molecules.

For the potassium complex, the $C_4 \rightarrow C_9$ phenyl ring is inclined at an angle of 38.3(2)° to the mean $O_4H \rightarrow O_4N$ plane at the symmetry related position 0.5 – x, 1 – y, -0.5 + z. The dichlorophenyl ring $C_{23} \rightarrow C_{28}$ makes the angle 30.0(1)° with the mean $O_4A \rightarrow O_4G$ heptagon. Similar values were observed for the caesium complex (Table 5.5). These inclusion angles are such that the portions C_6–C_7–C_8 and C_{25}–C_{26}–C_{27} are deeper inside the CD cavity and are stabilised by the **phenyl–H** interacting with the host's hydrophobic C_3–H_3's, and by the **phenyl–H···O_4** interactions (Table 5.6). The remaining portions of the dichlorophenyl rings, Cl_1–C_5–C_4–C_9–Cl_2 and Cl_{20}–C_{24}–C_{23}–C_{28}–Cl_{21} are sandwiched between the two CD rings. A shallower angle of inclusion of the dichlorophenyl ring, 26.6°, was observed in the DNaBCD complex [39].

Table 5.5 – Host-guest plane calculations to quantify inclusion mode

Complex	$C_{4\rightarrow9}$ vs O_4(H→N)	$C_{10\rightarrow15}$ vs O_4(A→G)	$C_{23\rightarrow28}$ vs O_4(A→G)	$C_{29\rightarrow34}$ vs O_4(H→N)
DKBCD	38.3(2)°	84.5(2)°	30.0(1)°	77.6(2)°
DCsBCD	37.7(2)°	84.8(2)°	30.6(2)°	76.3(3)°

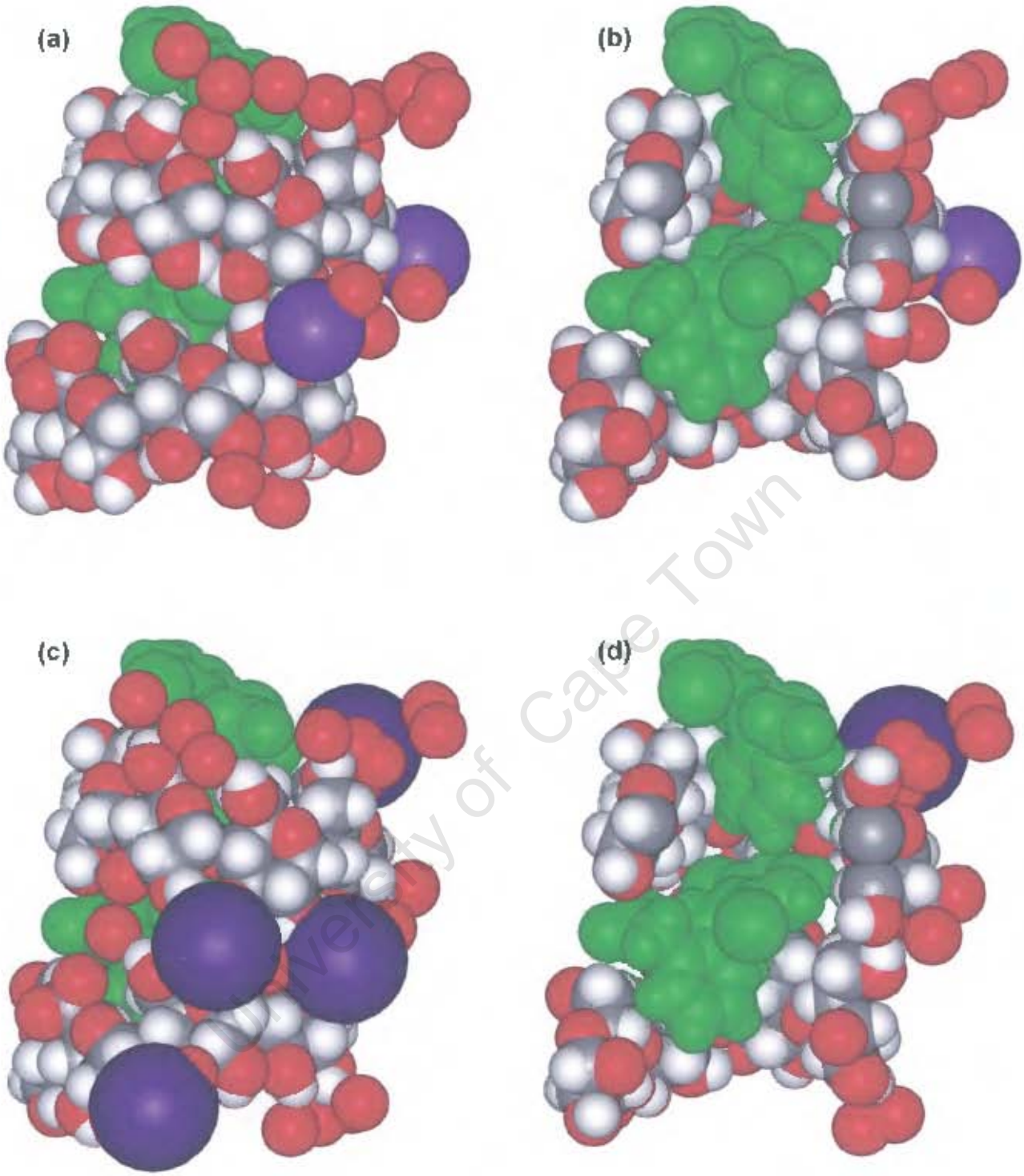

Figure 5.6 – Space-filling diagrams demonstrating the drug inclusion modes in the DKBCD (top diagrams) and DCsBCD (bottom diagrams) complexes as viewed along the *b*-axis. Guest atoms have been coloured green for clarity. Purple spheres represent cations. Diagrams **(a)** and **(c)** show the complete asymmetric unit, while diagrams **(b)** and **(d)**, in which CD rings have been sectioned, show the location and conformation of the drug inside the CD cavities.

Another difference in the inclusion mode of the dichlorophenyl ring in DNaBCD compared to the DKBCD and DCsBCD complexes is that in the latter cases the $C_4 \rightarrow C_9$ ring tilt results in Cl_1 being situated slightly deeper inside the CD cavity of a symmetry related host than Cl_2, whereas the opposite was found in the DNaBCD complex. The dichlorophenyl ring of the guest anion that is sandwiched between the two CD rings comprising an asymmetric unit has a negligible tilt with respect to the Cl atoms, so that Cl_{20} and Cl_{21} are included equally.

The phenyl acetate rings of the two crystallographically independent drug anions comprising an asymmetric unit of the DKBCD and DCsBCD structures also do not enter the primary sides of β-CD molecules perpendicularly, but make oblique angles of 84.5(2)° between the $C_{10} \rightarrow C_{15}$ aromatic ring and the $O_4A \rightarrow O_4G$ CD plane, and 77.6(2)° between the $C_{29} \rightarrow C_{34}$ and the $O_4H \rightarrow O_4N$ planes. A deeper insertion of the phenyl acetate ring was observed in the DNaBCD crystal structure as compared to the other two. The phenylacetate ring in the DKBCD and DCsBCD crystal structures is held in place by the weak hydrophobic interactions of the guest's aromatic hydrogen atoms with the host's C_5–H_5 and C_6–H_6 atoms. Also maintaining the rigidity of the drug inclusion in the CD channels are the guest's intramolecular **COO ···H–N** hydrogen bond and the intermolecular **C–H···π** interaction between the neighbouring guest anions (section ***5.4.9***). The sandwiched portions of the drug molecules also interact with the metal cations and with the water molecules as described in section ***5.4.7***.

Host-Guest interactions

In both the DKBCD and DCsBCD complexes, the drug confinement inside the hydrophobic cavity of the host framework is enhanced by a number of interactions, other than the confinement due to host-host interactions described earlier and in section ***5.4.8***. Other interactions include the intramolecular drug interactions, as well as intermolecular interactions of the drug with the host, with the metal ion and with the water molecules. CD-drug interactions are presented

in Tables 5.6 and 5.7, while interactions of the drug with the metal ions and water molecules appear in section *5.4.7*. Drug intramolecular interactions can be found in section *5.4.9*.

Table 5.6 – Host-guest close contacts between the diclofenac anion and β-cyclodextrin in the DKBCD and DCsBCD crystal structures. The numbering of some hydrogen atoms in DCsBCD is different from that of DKBCD, so the reader is advised that the corresponding interactions such as $H_6\cdots H_3L_1$[a] and $H_6\cdots H_{37}$[a] in this table refer to chemically corresponding atoms.

DKBCD		DCsBCD	
Guest···Host	Contact Distance (Å)[†]	Guest···Host	Contact Distance (Å)[†]
Intra-cavity Interactions			
$H_6\cdots H_3L_1$[a]	2.50	$H_6\cdots H_{37}$[a]	2.55
$H_8\cdots H_3H_1$[a]	2.55	$H_8\cdots H_{23}$[a]	2.56
$H_{12}\cdots H_5G$	2.46	$H_{12}\cdots H_5G$	2.48
$H_{14}\cdots H_5C$	2.63	$H_{14}\cdots H_6C$	2.58
$H_{25}\cdots H_3D_1$	2.72	$H_{28}\cdots H_{11}$	2.68
$H_{27}\cdots H_3G_1$	2.54	$H_{27}\cdots H_{21}$	2.50
$H_{31}\cdots H_5I$	2.45	$H_{31}\cdots H_5I$	2.33
Inter-cavity Interactions			
$H_{15}\cdots H_6C_1$	2.58	$H_{15}\cdots H_6C_1$	2.61
$C_{24}\cdots H_6K_1$	2.73	$C_{24}\cdots H_8K_1$	2.69
$H_{34}\cdots H_6K_2$	2.81	$H_{34}\cdots H_6K_2$	2.92
$O_{18}\cdots O_2J$[a]	2.998		
$O_{37}\cdots O_2B$	3.231	$O_{37}\cdots O_2B$	3.144
$O_{37}\cdots O_2F$[b]	2.700	$O_{37}\cdots O_2F$[b]	2.702

[a] 0.5 – x, 1 – y, – 0.5 + z; [b] x – 1, y, z symmetry related atoms

[‡] Default Contact Radii are those given by [40], or Covalent Radius + 0.8 Å when not given.

[†] Average e.s.d.'s are 0.01 Å for H···H and 0.005 Å for O···O contacts

Isostructurality of the DKBCD and DCsBCD complexes is maintained even at the weak interaction level as the host-guest close contact distances in the two complexes are similar (Table 5.6). Close contact interactions in the two complexes occur both inside the CD cavity and in-between CD cavities as shown in Table 5.6.

A slight difference in the host-guest interactions of the two complexes is that a strong hydrogen bond is established between a secondary hydroxyl group (O_2J–H_2J) of a symmetry related β-CD molecule belonging to the **Q** complex unit and a carboxylate terminal (O_{18}) of the drug anion belonging to the **P** complex unit in DCsBCD (Table 5.7). The same secondary hydroxyl group (O_2J–H_2J) in the DKBCD complex makes a close contact with the carboxylate terminal (O_{18}) (Table 5.6) due to the involvement of the O_2J–H_2J group as a donor in a hydrogen bond with a primary hydroxyl group (O_6N) of a symmetry related CD ring in the DKBCD complex (Table 5.13, section *5.4.8*).

Table 5.7 – A list of host-guest hydrogen bonds in the DKBCD and DCsBCD crystal structures. The numbering of some hydrogen atoms in DCsBCD is different from that of DKBCD, so the reader is advised that the corresponding interactions such as $Cl_1\cdots H_3K_1^{a}$ and $Cl_1\cdots H_{35}^{a}$ in this table refer to chemically corresponding atoms. **D** is the donor atom, **H** is the hydrogen atom and **A** is the acceptor atom (see pages iv and v for abbreviations and symbols).

DKBCD			DCsBCD		
Interaction	D···A (Å)	D–H···A (°)	Interaction	D···A (Å)	D–H···A (°)
Intra-cavity Interactions					
C_3K–$H_3K_1^{a}\cdots Cl_1$	3.774	148	C_3K–$H_{35}^{a}\cdots Cl_1$	3.937	148
C_3H–$H_3H_1^{a}\cdots Cl_2$	3.691	126	C_3H–$H_{23}^{a}\cdots Cl_2$	3.699	131
C_7–$H_7\cdots O_4M^{a}$	3.778	177	C_7–$H_7\cdots O_4M^{a}$	3.692	179
C_3C–$H_3C_1\cdots Cl_{20}$	3.845	150	C_3C–$H_9\cdots Cl_{20}$	3.823	152
C_3G–$H_3G_1\cdots Cl_{21}$	3.599	131	C_3G–$H_{21}\cdots Cl_{21}$	3.575	127
C_{26}–$H_{26}\cdots O_4E$	3.826	174	C_{26}–$H_{26}\cdots O_4E$	3.832	172
Inter-cavity Interactions					
C_6B–$H_6B_1\cdots Cl_1$	3.761	139	C_6B–$H_6B_1\cdots Cl_1$	3.806	137
C_6D–$H_6D_1\cdots Cl_2$	3.604	122	C_6D–$H_6D_1\cdots Cl_2$	3.526	126
C_{16}–$H_{16}A\cdots O_3I^{a}$	3.461	131	C_{16}–$H_{16}A\cdots O_3I^{a}$	3.508	137
C_{16}–$H_{16}B\cdots O_6F$	3.548	171	C_{16}–$H_{16}B\cdots O_6F$	3.627	168
C_6G–$H_6G_1\cdots O_{18}$	3.246	128	C_6G–$H_6G_1\cdots O_{18}$	3.404	128
			O_2J–$H_2J^{a}\cdots O_{18}$	2.977	124
C_6K–$H_6K_1\cdots Cl_{20}$	4.095	152	C_6K–$H_6K_1\cdots Cl_{20}$	4.120	152
C_6M–$H_6M_1\cdots Cl_{21}$	3.534	116	C_6M–$H_6M_1\cdots Cl_{21}$	3.635	120
C_{35}–$H_{35}A\cdots O_2B$	3.363	110	C_{35}–$H_{35}A\cdots O_2B$	3.355	109
C_6I–$H_6I_1\cdots O_{37}$	3.177	128	C_6I–$H_6I_1\cdots O_{37}$	3.177	128
C_2F–$H_2F_1^{b}\cdots O_{37}$	3.156	111	C_2F–$H_{18}^{b}\cdots O_{37}$	3.182	112

Symmetry transformations: [a] 0.5 – x, 1 – y, – 0.5 + z; [b] – 1 + x, y, z

† Average e.s.d. for the D···A distances is 0.005 Å

The host-guest complex in the two structures (DKBCD and DCsBCD) is strengthened by a number of hydrogen bonds operating both inside the CD cavities and in intercavity spaces. The host-guest hydrogen bonding network is also similar in the two complexes (Table 5.7).

The sandwiched guest atoms, in both complexes, are involved in binding the CD molecules of the **P** and **Q** units together (including symmetry related units). Apart from the obvious connection of neighbouring CD molecules due to one portion of the drug interacting with one CD ring while the other portion interacts with the next CD ring, the binding effects due to the sandwiched portions of the guest anions are made possible by the following kinds of host–guest interactions, operating in independent **P** and **Q** CD rings, and in symmetry related CD molecules (Tables 5.6 and 5.7):

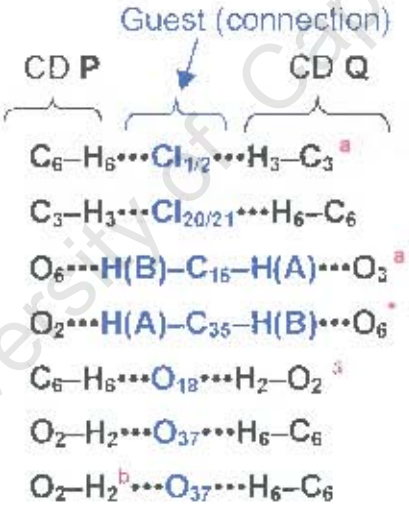

[a] 0.5 – x, 1 – y, z – 0.5; [b] x –1, y, z; * s.o.f. = 0.54 (DKBCD) or 0.56 (DCsBCD)

5.4.7 The Roles of Metal Cations and Water Molecules

The K^+ and Cs^+ ions are situated at the peripheries of the **P** and **Q** complex units (Figures 5.5 and 5.6) and establish the $M^+\cdots O$ coordination bonds shown in Table 5.8 and Figure 5.7. The role of metal cations in connecting successive CD molecules has been highlighted in the preceding section (section *5.4.6*). The metal cations are also found to have a role in a number of other interactions such as holding the water molecules in place (Table 5.8 and Figure 5.7) and thus participate in the hydrogen bonding network. In DCsBCD, a disordered fragment of the caesium ion (Cs_2A with a s.o.f. of 53%) is found to be interacting with the carboxylate end of a symmetry related complex unit (Table 5.8 and Figure 5.7) and therefore holds the drug molecule inside the CD cavities in a fixed conformation.

Table 5.8 – Analysis of the coordination geometry around the metal cations in both DKBCD and DCsBCD crystal structures. Empty rows under the symmetry operator column indicate that the corresponding atoms occupy general x, y, z positions.

DKBCD COMPLEX			DCsBCD COMPLEX		
Atom	Distance From M^+	Symmetry Operator	Atom	Distance From M^+	Symmetry Operator
K_1A (s.o.f. = 54 %)			Cs_1A (s.o.f. = 78 %)		
O_2C	2.845(5)		O_2A	3.717(6)	
O_3C	3.013(5)		O_3G	3.080(5)	
O_5D	2.937(5)	x – 0.5, 0.5 – y, 1 – z	O_2L	3.170(6)	1 – x, 0.5 + y, 1.5 – z
O_6D	2.565(8)	x – 0.5, y – 0.5, 1 – z	O_6M	3.485(8)	
O_2H	2.896(5)	-x, y – 0.5, z – 1.5	O_5N	3.076(5)	
O_9W	2.992(5)	x – 0.5, 0.5 – y, 1 – z	O_8N	3.384(6)	
$O_{11}W$	2.910(6)		O_1WA	3.168	-x, 0.5 + y, 1.5 – z
			O_1WB	3.280	-x, 0.5 + y, 1.5 – z
			O_5W	3.261(6)	x – 0.5, 1.5 – y, 1 – z
			$O_{16}W$	3.15(1)	0.5 + x, 1.5 – y, 1 – z
K_1B (s.o.f. = 46 %)			Cs_1B (s.o.f. = 22 %)		
O_2D	2.664(5)		O_2D	3.088(8)	0.5 + x, 0.5 – y, 1 – z
O_8D	2.728(7)	x – 0.5, 0.5 – y, 1 – z	O_5E	3.260(7)	
O_5E	3.173(5)	x – 0.5, 0.5 – y, 1 – z	O_6E	3.103(9)	
O_3H	2.410(6)	-x, y – 0.5, 1.5 – z	O_3H	3.061(7)	0.5 – x, 1 – y, z – 0.5
O_1WA	2.39(1)		O_2I	3.291(6)	0.5 – x, 1 – y, z – 0.5
O_1WB	2.776	x – 0.5, 0.5 – y, 1 – z	O_9W	3.710	0.5 + x, 0.5 – y, 1 – z

(Table continues on the next page)

$O_{16}W$	2.730(8)		$O_{10}W$	3.60(1)	1.5 – x, 1 – y, z – 0.5
$O_{19}W$	2.606(8)		$O_{13}W$	2.22(1)	0.5 – x, 1 – y, z – 0.5
K_2 (s.o.f. = 100 %)			Cs_2A (s.o.f. = 53 %)		
O_2G	2.651(5)		O_{37}	3.699	-x, 0.5 + y, 1.5 – z
O_2K	2.757(5)	1 – x, 0.5 + y, 1.5 – z	O_{38}	3.270(8)	-x, 0.5 + y, 1.5 – z
O_3K	2.763(5)	1 – x, 0.5 + y, 1.5 – z	O_3E	3.602(6)	1 – x, 0.5 + y, 1.5 – z
O_6M	2.689(5)		O_2F	3.777(6)	1 – x, 0.5 + y, 1.5 – z
$O_{10}W$	2.686(5)		O_6I	3.352(7)	-x, 0.5 + y, 1.5 – z
$O_{20}W$	2.93(1)	0.5 + x, 1.5 – y, 1 – z	O_5J	3.283(6)	-x, 0.5 + y, 1.5 – z
			O_6J	3.188(6)	-x, 0.5 + y, 1.5 – z
			O_3N	3.232(6)	
			O_3W	2.28(2)	
			$O_{15}W$	3.189(5)	-x, 0.5 + y, 1.5 – z
			Cs_2B (s.o.f. = 47 %)		
			O_3F	3.336(5)	
			O_2G	2.965(6)	
			O_6HA	3.507	1 + x, y, z
			O_6HB	2.984	1 + x, y, z
			O_2K	3.077(6)	1 – x, 0.5 + y, 1.5 – z
			O_5M	3.087(6)	
			O_6M	3.525(9)	
			O_4W	2.93(1)	1 + x, y, z
			O_6W	3.781(7)	0.5 + x, 1.5 – y, 1 – z
			O_8W	3.059(8)	0.5 + x, 1.5 – y, 1 – z
			$O_{19}W$	3.43(2)	0.5 + x, 1.5 – y, 1 – z

As shown in Figure 5.7, the ordered K^+ (K_2) has a coordination number of six as was found for Na^+ in the DNaBCD complex [39], but the coordination bonds are longer in DKBCD due to the large size of the potassium ion compared to Na^+. The disordered K^+ fragments, K_1A and K_1B have coordination numbers seven and eight respectively, and their coordination bond lengths vary significantly in each K^+ fragment (Table 5.8).

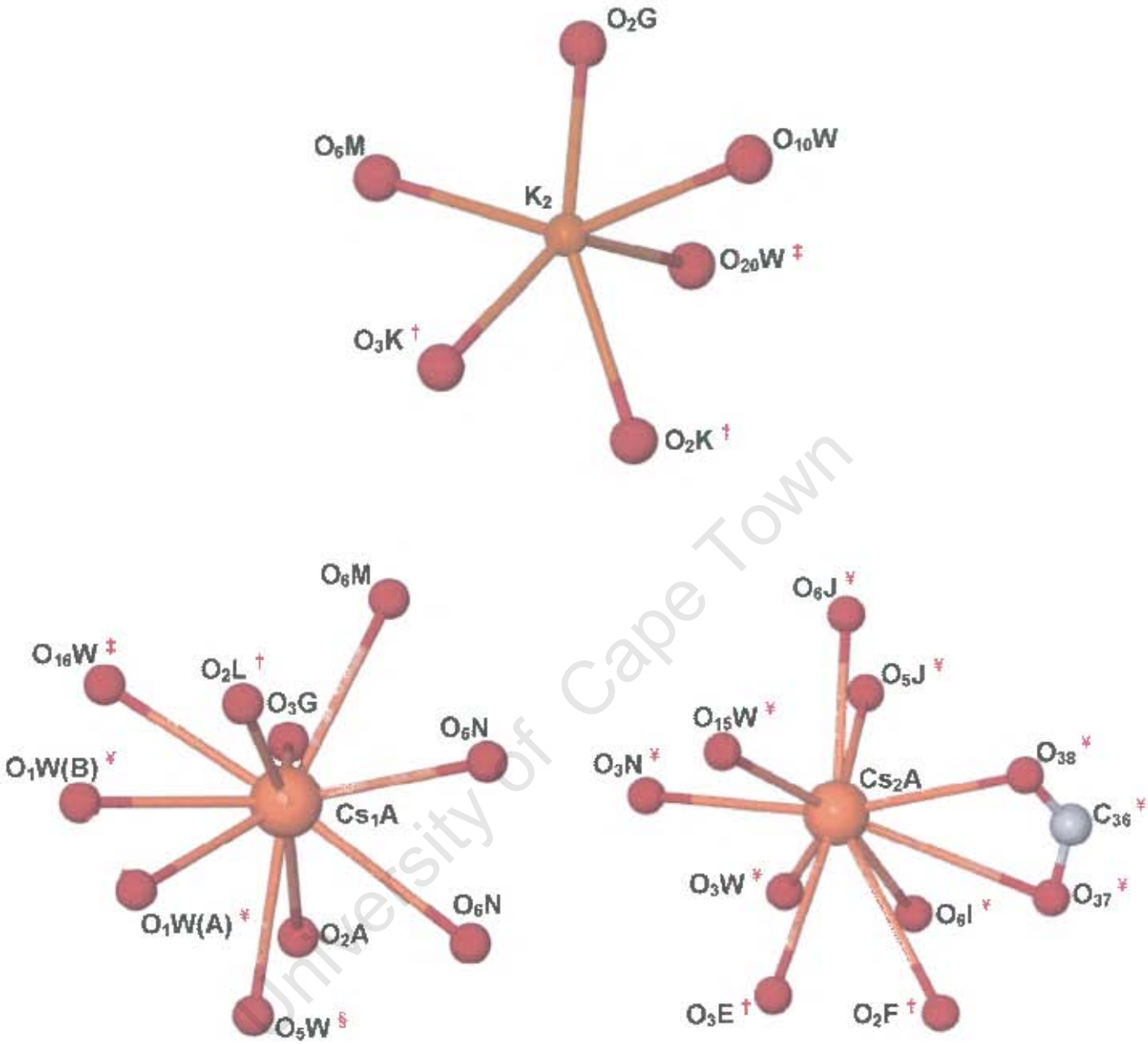

Key: † 1 – x, 0.5 + y, 1.5 – z; ‡ 0.5 + x, 1.5 – y, 1 – z; ¥ -x, 0.5 + y, 1.5 – z; § x – 0.5, 1.5 – y, 1 – z

Figure 5.7 – Diagrammatic representation of the coordination geometry around metal ions. Only the potassium ion with a full site-occupancy is shown for the DKBCD complex. For the DCsBCD complex, only caesium ions with major s.o.f.'s are shown.

The coordination bonds made by the Cs^+ fragments in the DCsBCD complex are the longest in the three complexes. This is not surprising as the caesium ion (r = 1.67 Å) is considerably larger than K^+ (r = 1.38 Å), which is in turn larger than Na^+ (r = 1.02 Å). The caesium ions with the highest s.o.f. values have a coordination number of ten. Other caesium fragments in the DCsBCD crystal structure have coordination numbers eight and eleven for Cs_1B and Cs_2B respectively.

All of the water molecules of crystallization in both the DKBCD and DCsBCD complexes are found to be interacting with both the **P** and **Q** complex units. These solvent molecules are either interacting with each other through hydrogen bonds (e.g. $O_{12}W\cdots O_{16}W$, 2.84 Å in DKBCD and $O_9W\cdots O_7W$, 2.88 Å in DCsBCD), with the metal ions (Table 5.8 and Figure 5.7), or are hydrogen bonded to either (or both) the guest anions and/or the host molecules (Table 5.9).

It is also found, in both structures, that a particular water molecule can be involved in more than one interaction (e.g. $O_{16}W$ coordinated to K_1B and hydrogen bonded to $O_{12}W$ and O_7J in DKBCD). An analogous situation occurs in DCsBCD. This is because a water molecule can utilise its total bonding capabilities by donating both of its hydrogen atoms to suitable H-acceptor atoms and thus leave a partial negative charge on its oxygen terminal. This then attracts positively charged species such as the K_1B ion in the above example.

The difference in the crystal water contents of the complex DKBCD (with 10 water molecules per formula unit) and complex DCsBCD (with 9 water molecules per formula unit) altered the water-mediated hydrogen bonding network in the two complexes (Table 5.9). As a result, the potassium complex has more hydrogen bonds involving water molecules than the caesium complex, although the two complexes differ by only one water molecule per complex unit.

Table 5.9 – Analysis of hydrogen bonds involving crystal water molecules of both DKBCD and DCsBCD complexes. **D** is the donor atom, **H** is the hydrogen atom and **A** is the acceptor atom (see pages iv and v for abbreviations and symbols).

DKBCD [†]			DCsBCD [†]		
Interaction	**D···A (Å)**	**D–H···A (°)**	**Interaction**	**D···A (Å)**	**D–H···A (°)**
Water···Guest interactions					
C_{35}–H_{35B}···O_{18W} [a]	3.34(1)	136			
β-CD C–H···Water interactions					
C_1G–H_1G···O_{14W} [b]	3.412(8)	153	C_1G–H_1G···O_6W [b]	3.53(1)	154
C_4F–H_4F···O_{14W} [b]	3.395(7)	152	C_4F–H_4F···O_6W [b]	3.44(1)	155
C_4H–H_4H···O_{19W} [c]	3.45(1)	149			
Water interactions with β-CD secondary rim					
O_2D–H_2D···O_{12W}	3.315(7)	161	O_2A–H_2A···O_5W [a]	2.644(8)	109
			O_2C–H_2C···O_{15W}	2.798(9)	111
O_2L–H_2L···O_{15W}	2.739(8)	178	O_2M–H_2M···O_{13W} [i]	2.74(2)	136
O_2M–H_2M···O_{17W} [e]	2.754(9)	130	O_3C–H_3C···O_7W	2.88(1)	104
O_3A–H_3A···O_6W [a]	2.812(6)	146			
O_3C–H_3C···O_{16W}	2.993(8)	143	O_3D–H_3D···O_9W	2.837(9)	150
O_3D–H_3D···O_{12W}	2.828(7)	148	O_3E–H_3E···O_{11W}	2.745(9)	148
O_3E–H_3E···O_8W [f]	2.734(6)	149	O_3K–H_3K···O_{19W} [e]	2.61(1)	145
O_3I–H_3I···O_6W [e]	2.901(6)	161	O_3L–H_3L···O_1WB [i]	2.90(1)	120
O_3L–H_3L···O_{17W} [e]	3.046(9)	163	O_3M–H_3M···O_{10W}	2.794(9)	149
O_3M–H_3M···O_7W	2.750(7)	141			
Water interactions with β-CD primary rim					
O_6A–H_6A···O_{10W} [d]	2.713(6)	160	O_6A–H_6A···O_{16W}	2.85(1)	114
O_6B–H_6B···O_4W	2.675(6)	139	O_6A–H_6A···O_{19W}	3.21(1)	139
O_6C–H_6C···O_7W [g]	2.757(7)	168	O_6B–H_6B···O_1WB [j]	2.54(2)	137
O_6E–H_6E···O_1WA [h]	3.06(1)	170	O_6C–H_6C···O_{10W} [g]	2.95(1)	174
O_6F–H_6F···O_3W	2.751(7)	161	O_6D–H_6D···O_{15W} [h]	3.08(1)	164
O_6G–H_6G···O_{14W}	2.766(6)	137	O_6F–H_6F···O_5W	2.731(8)	158
O_6I–H_6I···O_{13W}	2.623(7)	123	O_6G–H_6G···O_6W	2.704(9)	138
O_6J–H_6J···O_{16W}	2.741(9)	131	O_6K–H_6K···O_9W	2.89(1)	170
O_6K–H_6K···O_{12W}	2.795(7)	168	O_6N–H_6N···O_{14W}	2.832(9)	166
O_6N–H_6N···O_6W [a]	2.829(7)	169			

[a] – 0.5 + x, 1.5 – y, 1 – z; [b] 0.5 + x, 1.5 – y, 1 – z; [c] – x, 0.5 + y, 1.5 – z;
[d] – 1 + x, y, z; [e] 0.5 – x, 1 – y, 0.5 + z; [f] 1 – x, – 0.5 + y, 1.5 – z;
[g] 0.5 – x, 1 – y, – 0.5 + z; [h] 0.5 + x, 0.5 – y, 1 – z; [i] 1 + x, y, z;
– 0.5 – x, 1 – y, – 0.5 + z. [†] Average e.s.d. in angle ~ 2°

5.4.8 The Host Framework

CD rings of the neighbouring **P** and **Q** units are inclined with respect to each other by angles of 16.57(2)° and 16.78(3)° between their corresponding O_4 mean planes in the DKBCD and DCsBCD complexes respectively (Figure 5.8 – only the potassium host frame is shown). Geometric parameters that describe structural features of cyclodextrin molecules in the two complexes are shown in Tables 5.10 – 5.12. These geometric parameters have been defined in Chapter 1 (section *1.1.3*).

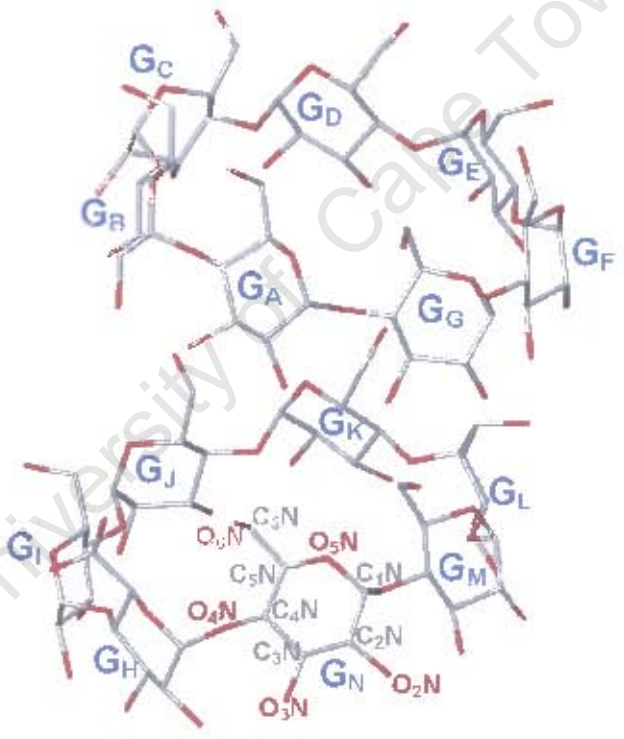

Figure 5.8 – A representative asymmetric unit of the host framework of DKBCD and DCsBCD crystal structures showing the structure and conformation of the host molecules as viewed obliquely from the primary side. The top CD ring with labelling $G_A \rightarrow G_G$ forms part of the **P** unit while the bottom CD ring labelled $G_H \rightarrow G_N$ is part of the **Q** unit.

Inclusion of the diclofenac caesium and potassium salts in β-cyclodextrin has introduced some distortion in the host molecules. As for the principal torsion angles (Table 5.10), two of the C_6–O_6 bonds, **C_6F–O_6F** and **C_6H–O_6H** of a disordered component (the one with a higher site-occupancy factor), are pointing inside the CD cavity while the rest of the C_6–O_6 bonds adopt the usual *(-)-gauche* conformation. The two C_6–O_6 bonds, **C_6F–O_6F** and **C_6H–O_6H** are in the *(+)-gauche* conformation since they interact with the sp^3 carbon atoms of the diclofenac anions in-between CD cavities via weak hydrogen bonds (Table 5.7, section ***5.4.6***).

The secondary face of a β-CD molecule is wider than its primary face and hence the glycosidic torsion angle Φ is smaller than the glycosidic torsion angle ψ (Chapter 1, Table 1.1). This was also the case for the DKBCD and DCsBCD complexes (Table 5.10), the main difference being the deviation of the DKBCD and DCsBCD Φ and ψ values from the average values known for parent β-CD molecules [41].

All glucopyranose units (CD monomers) in both the DKBCD and DCsBCD complexes are in the usual $^4C_1$ chair conformation as evidenced by the plus signs of Θ_1 and the minus signs of Θ_2 values in both diclofenac complexes. Furthermore, the Θ_1 and Θ_2 torsion angles in the two complexes did not deviate significantly from the mean values [41].

Table 5.10 – β-CD principal torsion angles in DKBCD and DCsBCD complex structures. The values have been rounded off to the nearest unit.*

	DKBCD					DCsBCD				
Glucose Unit	ω (°)	Φ (°)	ψ (°)	Θ_1 (°)	Θ_2 (°)	ω (°)	Φ (°)	ψ (°)	Θ_1 (°)	Θ_2 (°)
The P Unit										
G_A	-64	+101	+123	+56	-62	-62	+97	+124	+55	-62
G_B	-72	+112	+133	+58	-58	-66	+111	+131	+58	-58
G_C	-67	+102	+128	+54	-53	-70	+101	+131	+55	-54
G_D	-69	+110	+133	+54	-56	-69	+108	+132	+54	-62
G_E	-70	+107	+124	+58	-59	-67	+107	+120	+54	-57
G_F	+74	+107	+132	+55	-52	+69	+107	+131	+54	-52
G_G	-72	+107	+135	+50	-56	-71	+110	+136	+54	-57
The Q Unit										
G_H*	+48	+107	+131	+50	-52	+47	+106	+129	+49	-51
G_I	-62	+109	+131	+48	-53	-64	+109	+131	+51	-57
G_J	-57	+116	+130	+57	-60	-57	+116	+131	+58	-59
G_K	-61	+103	+122	+56	-53	-60	+104	+120	+53	-52
G_L	-76	+99	+150	+55	-53	-76	+100	+148	+55	-54
G_M	-75	+113	+132	+52	-59	-71	+112	+132	+52	-59
G_N	-60	+102	+108	+56	-58	-58	+104	+109	+54	-57

* O_6 atom with a higher s.o.f. used in ω calculations

*e.s.d.'s ranges are as follows:-

DKBCD: [P Unit] ω (0.6 – 0.7°), Φ (0.5 – 0.6°), ψ (0.5°), Θ_1 (0.6°), Θ_2 (0.5 – 0.6°)

[Q Unit] ω (0.5 – 0.8°), Φ (0.5 – 0.6°), ψ (0.5 – 0.6°), Θ_1 (0.6 – 0.7°), Θ_2 (0.5 – 0.7°)

DCsBCD: [P Unit] ω (0.8 – 1.0°), Φ (0.7 – 0.8°), ψ (0.6 – 0.7°), Θ_1 (0.8 – 1.0°), Θ_2 (0.8 – 0.9°)

[Q Unit] ω (0.7 – 1.1°), Φ (0.6 – 0.8°), ψ (0.6 – 0.7°), Θ_1 (0.8 – 1.0°), Θ_2 (0.7 – 0.9°)

The intersaccharide bond angles φ (Table 5.11) of the DKBCD and DCsBCD complexes do not deviate significantly from the mean value of 118°. The **O_2(n)•••O_3(n-1)** distances are also close to the usual mean value of 2.92 Å for all but one link. This link, **O_2M•••O_3L** (indicated in red in Table 5.11), is broken as a result of the metal ions **K_2** and **Cs_2B** causing the primary side of pyranose ring **G_M** to be tilted to a significant extent towards the inside of the CD cavity.

Table 5.11 – The glucopyranose conformation descriptors in the DKBCD and DCsBCD complexes.

	DKBCD			DCsBCD		
Unit (n-1)	φ (°)	$O_2(n)\cdots O_3(n-1)$ (Å)	τ_2 (°)	φ (°)	$O_2(n)\cdots O_3(n-1)$ (Å)	τ_2 (°)
The P Unit						
G_A	117.9(4)	2.925(6)	22.1(2)	116.4(6)	2.942(8)	23.6(3)
G_B	118.6(5)	2.879(6)	14.0(2)	119.9(6)	2.864(9)	13.9(3)
G_C	118.3(4)	2.983(6)	18.0(3)	117.7(6)	3.10(1)	16.8(4)
G_D	117.3(4)	2.865(7)	10.5(2)	117.6(6)	2.907(9)	13.3(3)
G_E	115.6(5)	2.795(6)	19.2(2)	117.9(6)	2.802(8)	19.0(2)
G_F	117.9(4)	2.911(6)	13.2(1)	119.3(6)	2.922(8)	12.3(1)
G_G	118.6(4)	2.945(7)	12.9(1)	117.7(6)	2.850(9)	11.7(1)
The Q Unit						
G_H	118.5(5)	2.935(7)	7.5(1)	119.4(6)	2.889(9)	8.1(2)
G_I	118.6(5)	2.904(6)	6.4(1)	117.8(6)	2.852(8)	6.2(1)
G_J	117.2(4)	2.755(7)	17.4(2)	117.2(6)	2.778(9)	15.8(3)
G_K	119.5(4)	2.945(6)	24.8(3)	118.5(6)	2.903(8)	24.1(4)
G_L	116.5(5)	3.61	6.8(2)	117.0(6)	3.51	6.3(2)
G_M	116.7(4)	2.813(6)	21.3(2)	115.7(5)	2.834(8)	20.4(2)
G_N	116.7(4)	2.782(7)	33.3(2)	115.4(6)	2.817(9)	31.1(2)

The G_L and G_I glucose residues exhibit the smallest tilt angles (τ_2 in Table 5.11) in both complexes. Also notable in both complexes is the significant difference in the τ_2 values of the **P** and **Q** units. These values are more uniform for the **P** unit but vary considerably in the **Q** units. This can be attributed to the interactions of the metal ions as stated above.

With regard to the O_4 heptagon, a few O_4 atoms exhibited above average [42] deviations from the mean O_4 plane, in particular for the cyclodextrin ring of the **Q** unit (Table 5.12). Consequently, torsion angle values $|t|$ vary from as low as 2.2° to as much as 24.6° in DKBCD and from 2.7° to 22.2° in the DCsBCD complex. Other parameters describing the O_4 heptagon (t, a and r) remained fairly constant and close to the average values known for β-CD compounds [42,43].

Table 5.12 – Geometric parameters describing the O_4 heptagon of β-CD molecules in the DKBCD and DCsBCD complexes.

	DKBCD					DCsBCD				
O_4 atom (n)	l (Å)	a (°)	t (°)	r (Å)	$\|d\|^*$ (Å)	l (Å)	a (°)	t (°)	r (Å)	$\|d\|^*$ (Å)
The P Unit										
O_4A	4.429	131	+5.0	4.905	0.003	4.412	132	+6.9	4.882	0.038
O_4B	4.263	126	-7.2	5.165	0.089	4.283	126	-7.2	5.164	0.088
O_4C	4.391	127	+4.3	5.136	0.107	4.403	126	+3.8	5.159	0.092
O_4D	4.429	131	+2.4	4.896	0.006	4.438	131	+2.7	4.893	0.006
O_4E	4.327	131	-5.2	4.961	0.087	4.351	131	-6.2	4.965	0.080
O_4F	4.315	124	+3.2	5.424	0.061	4.328	123	+5.9	5.275	0.079
O_4G	4.523	129	-2.2	5.032	0.012	4.471	130	-5.7	4.999	0.034
The Q Unit										
O_4H	4.302	123	+5.6	5.256	0.320	4.319	123	+4.8	5.248	0.298
O_4I	4.557	130	+12.5	4.954	0.081	4.551	130	+12.3	4.946	0.095
O_4J	4.325	133	-9.3	4.822	0.353	4.294	132	-8.4	4.852	0.335
O_4K	4.349	124	-13.0	5.243	0.029	4.360	124	-12.7	5.222	0.012
O_4L	4.486	125	+24.6	5.154	0.428	4.488	125	+22.2	5.128	0.409
O_4M	4.399	131	-7.5	4.812	0.327	4.389	131	-4.9	4.854	0.282
O_4N	4.258	130	-11.4	4.962	0.178	4.268	131	-11.8	4.963	0.194

*e.s.d.'s distances involving the O_4 atoms:

DKBCD: 0.003 Å for all atoms of the P unit and 0.003 – 0.004 Å for atoms of the Q unit

DCsBCD: 0.004 – 0.005 Å for atoms of the P unit and 0.004 Å for all atoms of the Q unit

Apart from the $O_2\cdots O_3$ intramolecular CD interactions (Table 5.11) which bind adjacent glucopyranose monomers together and thereby keep CD rings in a defined 'truncated cone'-like shape, a number of intermolecular host-host interactions that are established between the extra-cavity atoms maintain the crystal packing in the DKBCD and DCsBCD complexes. Interactions of the primary and secondary CD rims, which link successive CD layers and adjacent channels together, are presented in Table 5.13. Although only the hydroxyl **O–H···O** interactions are shown in Table 5.13, other interactions like **C–H···O** exist in the DKBCD and DCsBCD structures.

Table 5.13 – O···O hydrogen bond distances for the intermolecular host-host interactions established by the primary and secondary hydroxyl groups in the DKBCD and DCsBCD crystal structures.

DKBCD		DCsBCD	
Interaction	Contact Distance (Å)	Interaction	Contact Distance (Å)
$O_2G\cdots O_6M$	3.112(6)	$O_2G\cdots O_6M$	2.832(9)
$O_2H\cdots O_6D$ [d]	2.833(8)	$O_3H\cdots O_6D$ [d]	2.88(1)
$O_2K\cdots O_6H$ [e] [A]	2.812(9)	$O_2K\cdots O_6H$ [e] [A]	2.70(2)
$O_6L\cdots O_3F$	2.871(6)	$O_6L\cdots O_3F$	2.872(8)
$O_6M\cdots O_3G$	2.869(6)	$O_6M\cdots O_3G$	3.153(9)
$O_3A\cdots O_6G$ [a]	2.730(6)	$O_3A\cdots O_6G$ [a]	2.750(8)
$O_3C\cdots O_6D$ [b]	3.065(8)	$O_3C\cdots O_6D$ [b]	3.18(1)
$O_6I\cdots O_6L$ [c]	2.734(7)	$O_6I\cdots O_6L$ [c]	2.78(1)
$O_6D\cdots O_3H$	2.886(8)	$O_6D\cdots O_2H$	2.81(1)
$O_2J\cdots O_6N$ [f]	3.033(7)	$O_2J\cdots O_6N$ [f]	3.127(8)
		$O_6L\cdots O_2F$	3.234(8)

[a] –0.5 + x, 1.5 – y, 1 – z; [b] –0.5 + x, 0.5 – y, 1 – z; [c] –1 + x, y, z;

[f] 0.5 – x, 1 – y, 0.5 + z; [e] – x, – 0.5 + y, 1.5 – z;

[A] The disordered atom fragment is the one with a low s o f and with the $C_5\cdots O_5$ bond pointing away from the CD cavity (i.e. in the *(-)-gauche orientation)* in both complexes.

The host-host hydrogen bonding networks in the DKBCD and DCsBCD complexes differ to some extent. This is to be expected as these are extra-cavity interactions and the extra-cavity environments in the two complexes differ due to the difference in the water content and the nature of the metal ions that participate in interactions outside CD cavities in the two complexes.

In a few instances, from O···O distances in the range 2.6 – 3.0 Å, a host O–H group appears to engage as a donor in more than one hydrogen bond to oxygen acceptor atoms. This may be due to bifurcation, trifurcation and/or the known dynamic nature of H-bonding in CD hosts. Earlier difficulties (section ***5.4.5***) encountered with modelling H atoms on hydroxyl groups were mentioned.

Unlike the DNaBCD complex, which packs in parallel head-to-tail screw channels modulated by a crystallographic 6_1-axis along *c*, the DKBCD and DCsBCD complexes pack in antiparallel head-to-tail screw channels along *c* (Figure 5.9). In the latter complexes, a pseudo 3-fold axis seems to relate the host molecules in an asymmetric unit. In addition, the CD molecules in layers parallel to the *ab* plane are linearly aligned in DNaBCD while these molecules are tilted with respect to each other in the DKBCD and DCsBCD complexes (Figure 5.9).

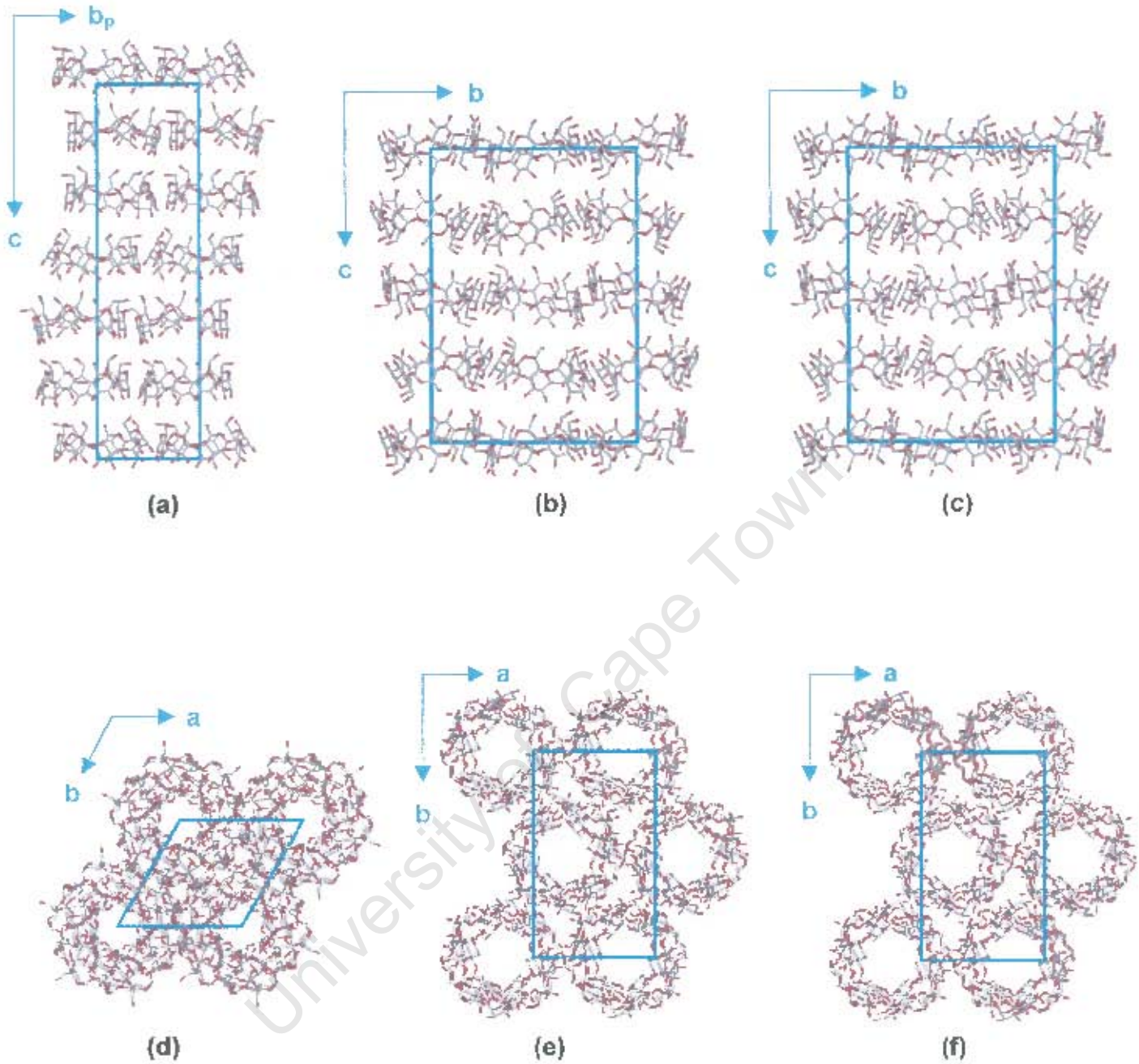

Figure 5.9 – Filled unit cells of DNaBCD, DKBCD and DCsBCD complexes showing packing of β-CD molecules in the crystal structures of the three complexes. The packings are viewed down the *a*-axis (top three diagrams) and down the *c*-axis (bottom three diagrams) for each structure. Diagrams **(a)** and **(d)** are for the sodium complex, **(b)** and **(e)** are for the potassium complex, while **(c)** and **(f)** are for the caesium complex.

5.4.9 Guest Conformation, Interactions and Packing

Drug complexation within the cyclodextrin molecule may change or distort the conformation of the included drug molecule compared to its uncomplexed counterpart, or to its conformation in another CD complex. This was monitored for the studied diclofenac drug. An intramolecular **N–H•••O** hydrogen bond exists in both **P** and **Q** units of the DKBCD and DCsBCD complexes (Figure 5.10 and Table 5.14). This has also been observed in DNaBCD [36,39] and in uncomplexed diclofenac free acid polymorphs [44].

Because of its charge, a single oxygen atom of a carboxylate group of the included drug anion can act as a hydrogen bond acceptor in more than one instance. Thus O_{37} in the DCsBCD and DKBCD complexes is accepting both hydrogen atoms donated by the C_6I and C_2F methyl groups (Table 5.7, section *5.4.6*), while at the same time being possibly hydrogen bonded to O_2F (Table 5.6, section *5.4.6*) and to a disordered Cs^+ fragment (Cs_2A with s.o.f. = 53%) in the DCsBCD complex (Table 5.8 and Figure 5.7). The O_{18} carboxylate terminal is also held in place by a similar network of hydrogen bonds involving $C_6G–H_5G_1$, in both complexes, and a symmetry related $O_2J–H_2J$ in DCsBCD, as hydrogen bond donors (Table 5.7, section *5.4.6*).

The roles of the guest anions in linking neighbouring CD molecules together have been highlighted in section *5.4.6*. The sandwiched chlorine atoms, for example, connect the C_3 methyl groups of one CD ring with the C_6 methyl groups of the next CD ring by acting as a 'linking' hydrogen bond acceptor (Table 5.7). In both the DKBCD and DCsBCD complexes, all chlorine atoms of the included guest anions (Cl_1, Cl_2, Cl_{20}, Cl_{21}) are found to participate in these links, although, however, Cl_{20} establishes weak hydrogen bonds with C_6K (with donor to acceptor distances of 4.1 Å in both complexes).

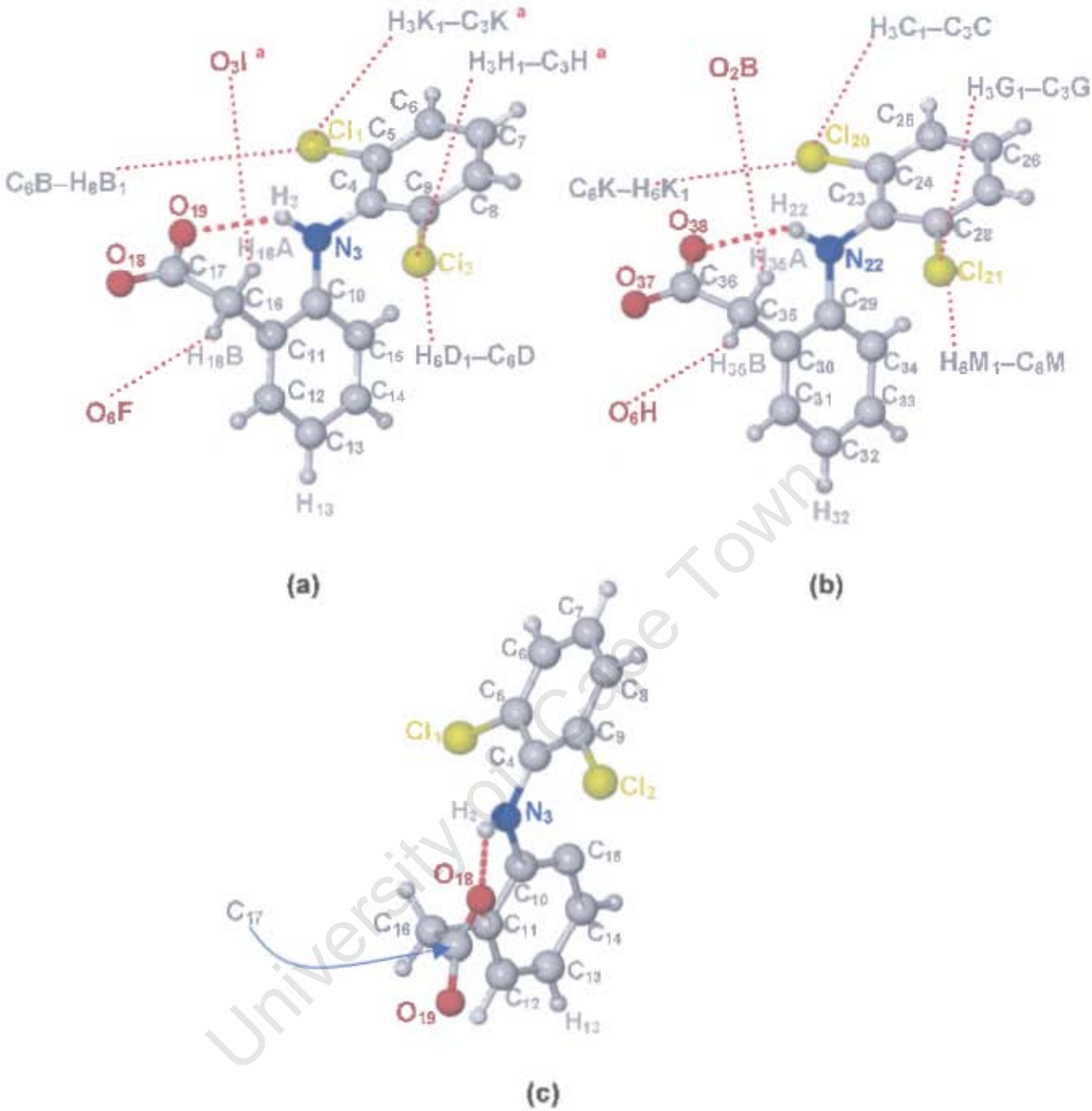

* Symmetry transformation 0.5 – x, 1 – y, – 0.5 + z

Figure 5.10 – Conformation and hydrogen bonding of the guest molecules of the **P** and **Q** complex units, **(a)** and **(b)** respectively, which are similar in both the DKBCD and DCsBCD inclusion complexes. Hydrogen bond distances and angles are not drawn to scale. The guest for the DNaBCD complex **(c)**, in which only the intramolecular hydrogen bond appears, is shown for comparison of the guest conformation with that of the other two complexes.

Also notable is the hydrogen bonding network established between the sp^3 carbon atoms of the guests (C_{16} and C_{35}) and the hydroxyl host atoms (Figure 5.10, values in Table 5.7).

Possible rotations around the C_4–N_3 (or C_{23}–N_{22}) bond gives freedom of orientation of the dichlorophenyl ring with respect to the phenyl acetate ring. This can be described (Table 5.14) by the torsion angle Υ_1 (C_9–C_4–N_3–C_{10} (**P** unit), C_{28}–C_{23}–N_{22}–C_{29} (**Q** unit)). Similarly, the swing of the phenyl acetate ring around the C_{10}–N_3 (or C_{29}–N_{22}) bond can be described by the torsion angle Υ_2 (C_4–N_3–C_{10}–C_{11} (**P** unit), C_{23}–N_{22}–C_{29}–C_{30} (**Q** unit)).

Table 5.14 – Guest conformational descriptors as well as guest-guest inter- and intramolecular interactions in DNaBCD, DKBCD and DCsBCD inclusion compounds.

Intramolecular Guest-Guest Interactions			
Complex Unit	**Interaction**	**D···A (Å)**	**D–H···A (°)**
DKBCD, Unit P	N_3–H_3···O_{19}	2.909(7)	139
DKBCD, Unit Q	N_{22}–H_{22}···O_{38}	2.965(7)	134
DCsBCD, Unit P	N_3–H_3···O_{19}	2.913(7)	138
DCsBCD, Unit Q	N_{22}–H_{22}···O_{38}	2.95(1)	136
DNaBCD	N_3–H_3···O_{19}	2.820(7)	143
Intermolecular Guest-Guest Interactions			
Complex Unit	**Interaction**	**D···A (Å)**	**D–H···A (°)**
DKBCD, Unit P	C_{13}–H_{13}···π	3.965	156
DKBCD, Unit Q	C_{32}–H_{32}···π [#]	4.180	135
DCsBCD, Unit P	C_{13}–H_{13}···π	4.024	157
DCsBCD, Unit Q	C_{32}–H_{32}···π [£]	4.237	132
DNaBCD	C_{13}–H_{13}···π	3.542	135
Torsion Angles Describing the Guest Conformation			
Complex Unit	**Υ_1 (°)**	**Υ_2 (°)**	**Υ_3 (°)**
DKBCD, Unit P	-59.5(9)	153.2(6)	82.3(7)
DKBCD, Unit Q	-59.9(8)	159.0(6)	84.4(8)
DCsBCD, Unit P	-62(1)	157.7(8)	84(1)
DCsBCD, Unit Q	-57(1)	158.9(9)	86(1)
DNaBCD	-113.6	-173.6	-81.0

[#] A **0.5 - x, 1 - y, 0.5 + z** symmetry transformed C_4→C_9 π ring
[£] A $P6_1$ symmetry related C_4→C_9 π ring

Rotation around the C_4–N_3 (C_{23}–N_{22}) bond resulted in Cl_2 (and Cl_{21}) being close to the phenyl acetate ring in the case of the DKBCD and DCsBCD complexes, while Cl_1 was found to be closer to the phenyl acetate ring in the DNaBCD complex (Γ_1, Table 5.14). The phenyl acetate ring in DNaBCD was found to be almost coplanar with the C_4–N_3–C_{10} (C_{23}–N_{22}–C_{29}) link (Γ_2, Table 5.14). This extent of co-planarity was not evident in the DKBCD and DCsBCD complexes.

Another interesting difference in the guest conformation in the DNaBCD complex versus the other two complexes is an approximate 180° swing of the carboxylate group around the C_{11}–C_{16} (C_{30}–C_{35}) bond so that the **N–H···O** hydrogen bond (described earlier) is established on the opposite side of the phenyl acetate ring in the DKBCD and DCsBCD complexes compared to the DNaBCD complex. This is also evident from the Γ_3 values, which are defined by the torsion angles C_{17}–C_{16}–C_{11}–C_{10} and C_{36}–C_{35}–C_{30}–C_{29} for the **P** and **Q** complex units respectively.

In all three complexes, the guest packing down the CD channels is strengthened by **C–H**···π interactions between neighbouring guest anions within a channel (Table 5.14 and Figure 5.11). In the asymmetric unit of the DKBCD and DCsBCD complexes, the two guest anions are related to each other by an approximate 120° rotation around the z-axis and are displaced ~ $^{c}/_{4}$ (9.2 Å) away from each other. The 2_1-screw-axis necessitates a 180°, 0.5 + z orientation of the **P** or **Q** unit relative to its next counterpart. Consequently, the spiralling of the guest anions along the *c* channels of a unit cell is effectively of the geometry 120°, 60°, 120°, 60° (with corresponding translations: ~ ¼, ½, ~ ¾ and 1 along *c*) so that every fifth guest anion has the same orientation as the first. In contrast, the DNaBCD complex has a strict 60° ($^{1}/_{6}$ + z), 60° ($^{1}/_{3}$ + z), 60° ($^{1}/_{2}$ + z), 60° ($^{2}/_{3}$ + z), 60° ($^{5}/_{6}$ + z), 60° (1 + z) packing arrangement of the unit cell contents modulated by the crystallographic 6_1-axis.

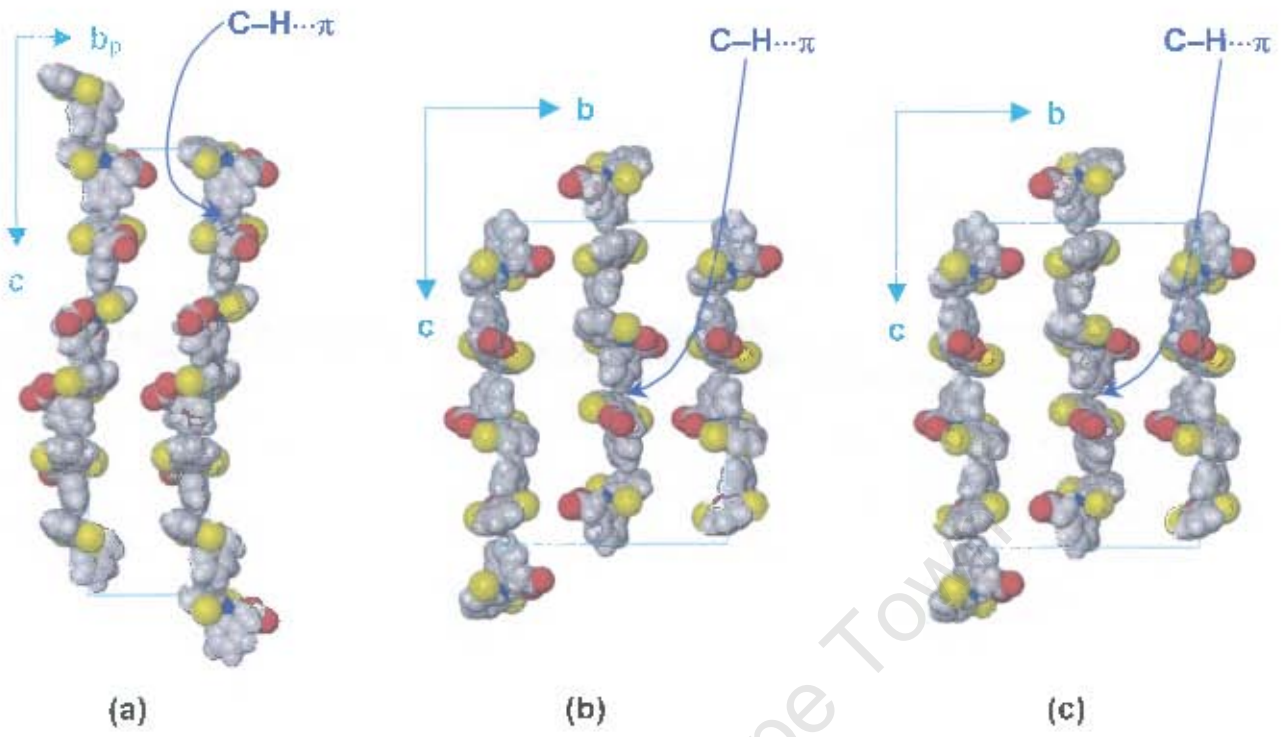

Figure 5.11 – (100) projections of DNaBCD **(a)**, DKBCD **(b)** and DCsBCD **(c)** complexes showing the guest packing and the C–H···π interactions in the crystal structures of the three complexes.

5.4.10 Emphasis on the Isostructurality of Diclofenac Salt Structures

As shown above and in the preceding sections, the two structures, DKBCD and DCsBCD, are highly isostructural with respect to both their cyclodextrin molecules and the included drug molecules. Their isostructural behaviour is shown quantitatively in Table 5.16 and can be seen in Figures 5.5, 5.6, 5.9 and 5.11. Calculations of isostructural indices in Table 5.16 were performed over the entire unit cell with both the host and the guest anions present. Metal cations and water solvent molecules were excluded from these calculations as they occupy

different positions in the two structures. Indices for the DNaBCD complex versus the two (DKBCD and DCsBCD) are shown for comparison. I_v values of 13.3 % (Table 5.16) emphasise the distinctly different structure of DNaBCD from the other two.

Table 5.16 – Isostructural indices for DKBCD, BCsBCD and DNaBCD complexes as compared against each other

Complex	Π	ε	A	εA	I_v (%)	I_{max} (%)
DKBCD – DCsBCD	0.001	0.001	0.748	0.000	96.1	99.9
DKBCD – DNaBCD	0.045	0.096	2.79	0.267	13.3	85.9
DCsBCD – DNaBCD	0.045	0.096	2.78	0.268	13.3	86.0

Shown in Figure 5.12 are the X-ray powder diffractograms of the DKBCD and DCsBCD complexes, which are superimposable on each other. Thus, the computed traces of these complexes were averaged and constitute an isostructural class, series **B10**, as discussed in Chapter 3.

Good matches between the experimental PXRD patterns and those computed from the structural models for the DKBCD and DCsBCD complexes imply that the refined models best represent the structures of these complexes in their solid states. The slight differences in the fine structures between the computed and the experimental traces of both complexes can be attributed to differences in the resolutions, with step values of 0.025° θ and 0.005° θ for the computed and experimental patterns respectively. Slight angular shifts for peaks in computed and experimental traces result from the fact that the former refer to a temperature of 113 K while the latter were recorded at 294 K.

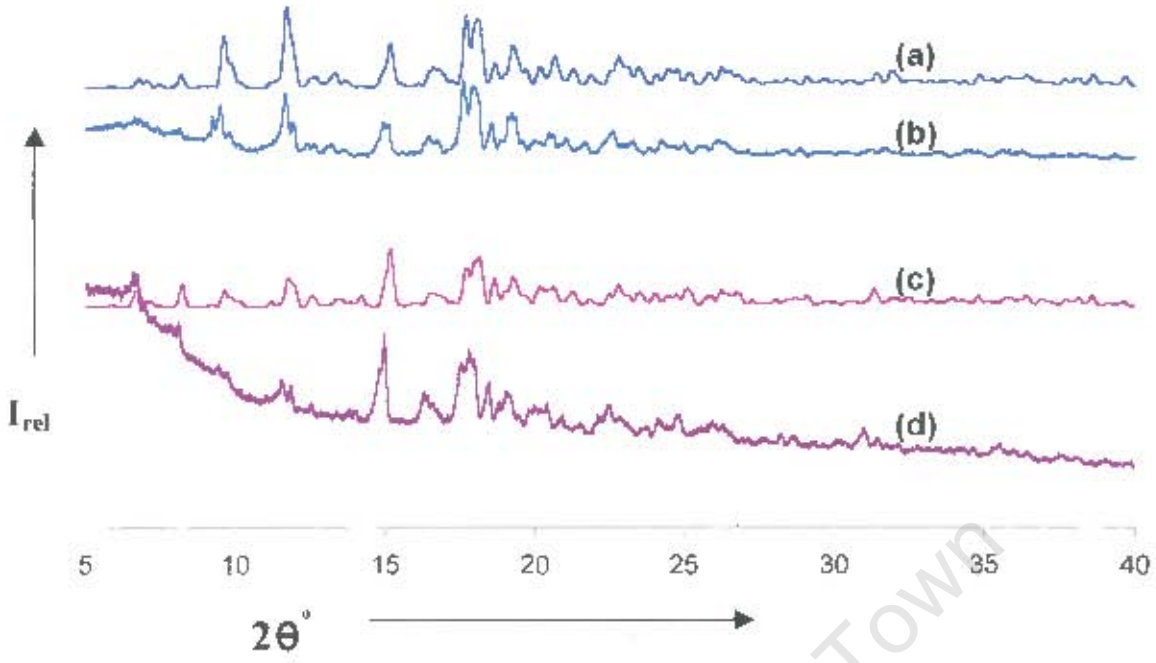

Legend: **(a)** = Computed PXRD trace for the DKBCD complex

(b) = Experimental PXRD trace for the DKBCD complex

(c) = Computed PXRD trace for the DCsBCD complex

(d) = Experimental PXRD trace for the DCsBCD complex

Figure 5.12 – Computed and experimental PXRD patterns for the DKBCD and DCsBCD complexes.

5.5 References

1. P. A. Todd and E. M. Sorkin, *Drugs*, 1988, **35**, 244 – 285.
2. A. Fini, V. Zecchi and A. Tartarini, *Pharm. Acta Helv.*, 1985, **60**, 58 – 62.
3. V. Zecchi, L. Rodriguez, A. Tartarini and A Fini, *Arch. Pharm.*, 1984, **317**, 897 – 905.
4. P. E. Ebong, E. U. Eyong and E. O. Udosen, *Afr. J. Med. Med. Sci.*, 1998, **27**, 243 – 246.
5. E. C. Ku, J. M. Wasvary and W. D. Cash, *Biochem. Pharmacol.*, 1975, **24**, 641 – 643.
6. S. N. Ciccolunghi, B. Levi and H. A. Chaudri, *Wien. Med. Wochenschr.*, 1975, **125**, 66 – 70.
7. B. J. R. Whittle, *Fundam. Clin. Pharm.*, 2003, **17**, 301 – 313.
8. J. Carson, W. M. Notis and E. S. Orris, *New Engl. J. Med.*, 1990, **323**, 135.
9. R. Benoit, O. Grobost and T. Crepeau, *Presse Med.*, 2001, **30**, 1102 – 1104.
10. E. E. Gabison, P Chastang, S. Menashi, S. Mourah, S. Doan, M. Oster, A. Mauviel and T. Hoang-Xuan, *Ophthalmology*, 2003, **110**, 1626 – 1631.
11. J. K. W. Hsu, W. T. Johnston, R. W. Read, P. J. MacDonnell, R. Pangalinan, N. Rao and R. E. Smith, *J. Cataract Refr. Surg.*, 2003, **29**, 250 – 256.
12. S. M. Helfgott, J. Sandberg-Cook, D. Zakim and J. Nestler, *J. Am. Med. Assoc.*, 1990, **264**, 2660 – 2662.
13. M. R. Kramer, C. Levene and C. Hershko, *Scand. J. Haematol.*, 1986, **36**, 118 – 120.
14. N. M. Agrawal, H. E. van Kerckhove, L. J. Erhardt and G. S. Geis, *Digest. Dis. Sci.*, 1995, **40**, 1125 – 1131.
15. E. H. Choy and D. L. Scott, *Drugs*, 1997, **53**, 337 – 348.
16. A. Fini, G. Fazio and I. Rapaport, *Drug. Exp. Clin. Res.*, 1993, **19**, 81 – 88.
17. T. Khazaeinia and F. Jamali, *J. Pharm. Pharm. Sci.*, 2003, **6**, 352 – 259.

18. J. L. Goldstein, F. E. Silverstein, N. M. Agrawal, M. Naurang, R. C. Hubbard, J. Kaiser, C. J. Maurath, M. K. Verburg and G. S. Geis, *Am. J. Gastroenterol.,* 2000, **95**, 1681 – 1690.
19. T. M. Borg, M. H. El-Shaboury and H. Mohamed, *Mansoura Journal of Pharmacutical Sciences,* 2000, **16**, 82 – 97.
20. K. Uegama, F. Hirayama and K. Minami, *Pat. Appl.* A2 19990119, 1999.
21. K. D. Rainsford, W. E. Perkins, P .I Stetsko, *Digest. Dis. Sci.*, 1995, **40**, 1435 – 1444.
22. P. He, H. Lu, and Y. Guo, *Anal. Lett.,* 2003, **36**, 493 – 510.
23. J. A. Arancibia, M. A. Boldrini, G. M. Escandar, *Talanta*, 2000, **52**, 261 – 268.
24. G. L. Kis, A. Fetz and C. Schoch, *PCT Int. Appl.*, WO 9710805, 1997.
25. F. Barbato, B. Cappello, M. I. La Rotonda, A. Miro and F. Quaglia, *J. Incl. Phenom. Macro.*, 2003, **46**, 179 – 185.
26. T. Iliescu, M. Baia and V. Miclaus, *Eur. J. Pharm. Sci.,* 2004, **22**, 487 – 495.
27. B. Pose-Vilarnovo, L. Santana-Penin, M. Echezarreta-Lopez, M. B. Perez-Marcos, J. L. Vila-Jato, and J. J. Torres-Labandeira, *S.T.P. Pharma Sci.,* 1999, **9**, 231 – 236.
28. Y. Zhang, X. Wu and Q. Zhao, *Zhongguo Yaoxue Zazhi (Beijing)*, 1999, **34**, 165 – 167.
29. D. V. Whittaker, L. J. Penkler, L. A. Glintenkamp, M. C. B. Van Oudtshoorn and P. L. Wessels, *J. Inclus. Phenom. Mol.*, 1996, **25**, 177 – 180.
30. S. Astilean, C. Ionescu, G. Cristea, S. I. Fărcaş, I. Bratu and R. Vitoc, *Biospectroscopy*, 1997, **3**, 233 – 239.
31. A. Mucci, L. Schenetti, M. A. Vandelli, B. Ruozi and F. Forni, *J. Chem. Res.*, 1999, **M**, 1761 – 1795.
32. J. A. Arancibia and G. M. Escandar, *Analyst*, 1999, **124**, 1833 – 1838.
33. M. Bogdan, M. R. Caira, D. Bogdan, C. Morari and S. I. Fărcaş, *J. Incl. Phenom. Macro.*, 2004, **49**, 225 – 229.

34. M. R. Caira, V. J. Griffith and L. R. Nassimbeni, *J. Therm. Anal.*, 1998, **51**, 981 – 991.
35. B. Cwiertnia, T. Hladon and M. Stobiecki, *J. Pharm. Pharmacol.*,1999, **51**, 1213 – 1218.
36. M. R. Caira, V. J. Griffith, L. R. Nassimbeni and B. van Oudtshoorn, *J. Chem. Soc. (Chem. Comm.)*, 1994, **9**, 1061 – 1062.
37. S. Budavari, M. J. O'Neil, A. Smith and P. E. Heckelman, *The Merck Index,* 11th Edition, Merck & Co. Inc., Rahway, 1989.
38. M. Bogdan, M. R. Caira and S. I. Fărcaş, *Supramol. Chem.*, 2002, **14**, 427 – 435.
39. V. J. Griffith, *PhD Thesis, Physicochemical Characterisation of Cyclodextrin-Drug Complexes*, University of Cape Town, South Africa, 1996.
40. A.Bondi, *J. Phys. Chem.*, 1964, **68**, 441 – 451.
41. F. W. Lichtenthaler and S. Immel, *Liebigs Ann.*, 1996, **1**, 27 – 37.
42. K. B. Lipkowitz, K. Green, and J. Yang, *Chirality*, 1992, **4**, 205 – 215.
43. K. Harata, in *Inclusion Compounds*, ed. J. L. Atwood, J. E. D. Davies, and D. D. MacNicol, Oxford University Press, London, 1984, **Vol. 5**, Chapter 9.
44. P. Moser, A. Sallmann and I. Wiesenberg, *J. Med. Chem.*, 1990, **33**, 2358 – 2368.

CHAPTER 6: CONCLUSIONS, COMMENTS AND RECOMMENDATIONS

6.1 Isostructurality of Cyclodextrin Inclusion Compounds

An up-to-date version of the IsoPXRD method applied to cyclodextrin inclusion compounds is given in chapter 3 of this dissertation. A number of CD compounds, not reported previously, are documented in this survey. In updating the IsoPXRD method, we noticed some interesting isostructural phenomena in some CD compounds, as summarised below. As for natural CD inclusion complexes containing organic guest molecules, a number of reported crystal structures, as found in the Cambridge Structural Database, were found to be isostructural with known isostructural series.

6.1.1 Isostructurality in Parent CD Compounds

Appearing in this report are a number of parent CD compounds, some of which are found to be isostructural to some extent, both among α- and β-CD compounds. The PXRD traces of the nearly isostructural parent CDs, although having close resemblance within a restricted θ-range, are however distinguishable from each other. Thus their limited isostructural behaviour does not restrict the use of the IsoPXRD method. Also highlighted here, are two isostructural trimethylated β-CD parent compounds whose structures have recently been published [1].

6.1.2 Isostructurality in α-CD Inclusion Complexes and in Complexes of the Methylated α-CD Derivatives

One isostructural class, not reported previously [2], was identified on updating inclusion complexes of α-CD species. This new series (**A5**) comprises an α-CD organic inclusion complex with *n*-butylisothiocyanate as a guest [3] (which appeared in the literature after the last IsoPXRD update [2]) and a known α-CD

complex with acetone as a guest molecule [4]. Of the natural α-CD complexes that have been grouped into isostructural series previously, the generated series is the only one in which α-CD molecules form dimers. No new isostructural series were identified for inclusion complexes of the derivatised α-CDs. Of the isostructural series documented for complexes of the α-CD species thus far, there is no ambiguity in matching of their PXRD traces, thus making the referencing of the PXRD patterns in the use of the IsoPXRD method easier.

Two sets of α-CD complexes with matching X-ray powder diffractograms, but not satisfying all the conditions for isostructural compounds, were identified. In one set, the complexes have identical space groups and similar unit cell parameters, except for a major difference in the *c*-axes (in which one axis is almost double the other) and the β-angle (difference of 11.9°). Their crystal packing diagrams are almost indistinguishable from each, being just distinguishable only on their (001) projections. In the other set, the complexes differ only in their space groups (one being $P2_12_12_1$ and the other $C222_1$), with all other isostructural conditions satisfied.

6.1.3 Isostructurality in Complexes of β-CD Species

Turning to the organic inclusion complexes of natural β-cyclodextrin, two new series were generated. One is a variant of the **CH** packing arrangement of β-CD dimers in the triclinic space group P1 and the other comprises two organic salt inclusion complexes with β-CD molecules packing in antiparallel head-to-tail screw channels along *c*. More variants of the **CH** packing mode in both space groups P1 and C2, series **B4** and **B6** respectively, are foreseen in future updates of the IsoPXRD method, as some compounds found in the current update have unit cell parameters which differ slightly from these series. This is explained in chapter 3 of this dissertation.

As has been noted before [5], variations in the monoclinic **SC** packing mode of complexes of series **B9**, whereby the β-CD dimers in consecutive layers can be displaced while the unit cell parameters are retained, resulting in closely matching PXRD traces of non-isostructural compounds, are highlighted in this update. Users of the IsoPXRD method are also cautioned regarding the two coincidental matches of PXRD patterns noted here (series **B4** with **B6** and **B8** with **B9**) that could result in misclassification of newly prepared complexes. Series **B4** and **B6** have the **CH**-type packing arrangement but possess different space groups and different unit cell parameters. The dimeric **SC** packing arrangement of complexes of series **B9** can be altered so as to approximate the **CB** packing mode found in series **B8**.

A number of isostructural series of derivatised β-CDs, that were not captured previously, are reported in the current update. The new series are due to several methylated β-CD parent compounds that are found to be isostructural with their inclusion complexes of small organic guest molecules, and derivatised β-CDs in which an organic substituent (or more than one) has been attached to one or more of the primary hydroxyl groups of a cyclodextrin. Subtle relationships in unit cell parameters and/or packing diagrams also exist in both methylated and unusually derivatised β-CD compounds, such that closely matching PXRD patterns for complexes that are not completely isostructural exist.

Encountered also were the two distinct sets of TRIMEB organic inclusion complexes. In each set, complexes have closely matching unit cell parameters and a common space group, but differences in their packing arrangements result in different PXRD traces (matching only in restricted regions). The complexes comprising a set are therefore isostructural to a limited extent only, and as such cannot comprise a series. Complexes in each set can be distinguished on paying close attention to their PXRD patterns.

6.1.4 Conclusions on the IsoPXRD Method

We conclude that the IsoPXRD method, based on crystal isostructurality of cyclodextrin organic inclusion complexes and X-ray powder diffraction, is a quick and easy tool to use for structural characterisation of crystalline organic-CD inclusion compounds at a detailed level. Apart from our own routine use of the technique, we have also noted from the recent literature that other researchers are beginning to employ this method [6-7]. This method has an added advantage of requiring reduced sample size and labour (in sample preparation and PXRD recording) compared to the conventional use of X-ray powder diffraction in the identification of CD-drug inclusion complexes. However, great care is needed in both 'matching' and interpretation of the respective PXRD patterns so as to avoid misclassification of a newly prepared complex, as we have encountered some non-isostructural complexes and series with closely matching PXRD patterns. For future development of the IsoPXRD method, it may be worth monitoring the frequency with which PXRD traces of non-isostructural CD compounds resemble each other.

Although the computation of PXRD traces and inspection of crystal packing arrangements of a large number of existing CD inclusion complexes in order to examine their isostructurality is a tedious and time-consuming exercise, the author considers it worthwhile in view of its subsequent utility once the reference patterns have been grouped into isostructural classes. Although also tedious, since only pairwise comparisons can be made, the volumetric measure of isostructurality is also considered an ideal complement to the IsoPXRD method as it provides a quantitative measure of isostructurality.

6.2 Use of the IsoPXRD Method

We were further able to use the IsoPXRD method to demonstrate the relative reactivities of two tautomeric forms of sulfasalazine with β-cyclodextrin. Thus we were able to show that the imide tautomer (crystallizing in the monoclinic system) of sulfasalazine has a high tendency to form inclusion complexes with β- and γ-CDs while the amide tautomer (crystallizing in the triclinic system) could not be included in any of the natural cyclodextrins by kneading. The experiments involving sulfasalazine thus yielded an interesting, novel result, namely preferential inclusion of one of the two tautomers of the drug in the natural cyclodextrins. As shown in Chapter 4, the difference between these forms is manifested as an apparently minor proton shift, but this is evidently sufficient to enable their discrimination by the host CD molecules.

Also identified using the IsoPXRD method is an inclusion complex of salicylamide with β-cyclodextrin whose PXRD trace closely matched the reference pattern for isostructural series **B6**.

Encountered also in our application of the IsoPXRD method is an inclusion complex of aspirin with β-CD which has a unique PXRD trace, different from that of a reported quaternary aspirin•salicylic acid•β-CD hydrate complex [8], implying different packing arrangements in the two aspirin•β-CD inclusion complexes. However, attempts to recrystallize the new aspirin•β-CD complexes failed, and since no further analysis was performed on the kneaded aspirin•β-CD material, it is not known to what extent it may have contained salicylic acid as a decomposition product of aspirin.

6.3 Inclusion of Diclofenac Salts in β-Cyclodextrin

Although crystallization experiments to isolate single crystals from the kneaded sample materials that were characterised by the IsoPXRD method failed, we were successful in preparing crystals of two β-CD inclusion complexes of an ionic organic guest (the diclofenac anion) differing only in the nature of the counterions, which were alkali metals of different sizes.

Metal counterions in organic salt inclusion complexes of cyclodextrins are generally found to link adjacent CD rings (by co-ordination to oxygen atoms on CD rims) and thus contribute significantly to the channel packing arrangements of CD molecules usually observed in such complexes. The nature of these channels may differ, and we have found in the prepared complexes that the potassium and the caesium salt inclusion complexes are isostructural but non-isostructural with the sodium analogue. The author is aware of the effective ionic radii of metal cations and the effect of coordination numbers on them [9]. However, the potassium and caesium ions were found to occupy different positions in the prepared DKBCD and DCsBCD complexes and the only complex components occupying similar positions in the two complexes, and therefore rendering these complexes isostructural, are the host β-CD and the guest diclofenac anion. An extensive hydrogen bonding network (Chapter 5) which involved diclofenac anion, β-cyclodextrin and water molecules, was observed in both the DKBCD and DCsBCD complexes and this can thus be taken as having a dominant role in maintaining the favoured channel packing arrangement, different from that of DNaBCD, in these complexes.

An important outcome of the X-ray analyses of DKBCD and DCsBCD was the establishment of a new isostructural series for β-CD inclusion complexes. As part of the continuation of this study, it would be interesting to investigate isostructurality of lithium-, rubidium- and francium-diclofenac•β-CD complexes so

as to note the extent to which isostructurality can be maintained in CD-drug inclusion complexes of alkali metals.

Complexation of diclofenac sodium with β-CD considerably improved the solubility of this drug [10]. It would be interesting to know if the solubilities of the potassium and the caesium salts of diclofenac have been improved by their respective complexation with β-cyclodextrin and, if so, whether or not to the same extent, as the two complexes were found to be isostructural. This could be the subject of a future study.

6.3 References

1. M. R. Caira, S. A. Bourne, W. T. Mhlongo and P. M. Dean, *Chem. Commun.*, 2004, **19**, 2216 – 2217.
2. M. R. Caira, *Rev. Roum. Chim.*, 2001, **46**, 371 – 386.
3. C. Sicard-Roselli, B. Perly and G. Le Bas, *J. Incl. Phenom. Macro.*, 2001, **39**, 333 – 337.
4. I. Nicolis, F. Villain, A. W. Coleman and C. De Rango, *Supramol. Chem.*, 1994, **3**, 251 – 259.
5. M. R. Caira, E. De Vries, L. R. Nassimbeni and V. W. Jacewicz, *J. Incl. Phenom. Macro.*, 2003, **46**, 37 – 42.
6. S. S. Braga, P. Ribeiro-Claro, M. Pillinger, I. S. Gonçalves, F. Pereira, A. C. Fernandes, C. C. Romão, P. B. Correia and J. J. C. Teixeira-Dias, *Org. Biomol. Chem.*, 2003, **1**, 873 – 878.
7. L. Cunha-Silva and J. J. C. Teixeira-Dias, *New J. Chem.*, 2004, **28**, 200 – 206.
8. F. Nishioka, I. Nakanishi, T. Fujiwara, K. Tomita, *J. Inclusion Phenom.*, 1984, **2**, 701 – 714.
9. R. D. Shannon, *Acta Crystallogr.*, 1976, **A32**, 751 – 767.
10. V. J. Griffith, L. R. Nassimbeni, D. G. Nicholson, M. D. Bodley, M. R. Caira, L. Glintenkamp, L. Penkler and M. C. van Oudtshoorn, *Eur. Pat. Appl.*, **647451**, 1995.

APPENDICES

The following supplementary material can be found on the compact disc attached to the inside back cover of this dissertation:

A folder named "APPENDIX A" contains the Legacy CSD Crystallographic format (FDAT) files. The files can be opened with the **X-Seed** interface program system (see Chapter 2 for a reference to this program). The file types and the information that they contain are listed in Table 2.1 (Chapter 2).

A folder named "APPENDIX B" contains the crystallographic information files for each of the solved structures (reported in Chapter 5) of this dissertation. There are eight files for each crystal structure presented in chapter 5. The reader is again referred to Table 2.1 (in Chapter 2) for the file types and the information that they contain. The files can be accessed in sub-folders "K-structure" (for the diclofenac-potassium•β-CD complex) and "Cs-structure" (for the diclofenac-caesium•β-CD complex). Except for the *.htm* files, which can be opened with a web browser like 'Internet Explorer' or 'Netscape', the files are readable with a text editor such as WORDPAD in Windows98 or any later version thereof.